1-1-2013

Bridging The Gap: Defining the Molecular Mechanisms of Cep290 Disease Pathogenesis

Theodore George Drivas
University of Pennsylvania, theodore.drivas@gmail.com

Bridging The Gap: Defining the Molecular Mechanisms of Cep290 Disease Pathogenesis

Abstract
Mutations in the gene CEP290 cause an array of debilitating and phenotypically distinct human diseases, ranging in severity from the devastating blinding disease Leber congenital amaurosis (LCA) to Senior LÃ¸ken Syndrome, Joubert syndrome, and the embryonically lethal Meckel-GrÃ¼ber syndrome. The pathology observed in these diseases is thought to be due to CEP290's essential role in the development and maintenance of the primary cilium, but despite its critical role in biology and disease we know only little about CEP290's function. Here we identify four novel functional domains of the protein, showing that CEP290 directly binds to cellular membranes through an N-terminal domain that includes a highly conserved amphipathic helix motif, and to microtubules through a domain located within its myosin-tail homology domain. Furthermore, CEP290 activity was found to be regulated by two novel autoinhibitory domains within its N- and C-termini, both of which were also found to play critical roles in regulating ciliogenesis. Disruption of the microtubule-binding domain in the rd16 mouse LCA model was found to be sufficient to induce significant deficits in cilium formation leading to retinal degeneration. Taking these findings into account, we developed a novel model that accurately predicts patient CEP290 protein levels in a mutation-specific fashion. Predicted CEP290 protein levels were found to robustly correlate with disease severity for all reported CEP290 patients. All these data implicate CEP290 as an integral structural and regulatory component of the primary cilium and provide insight into the pathological mechanisms of LCA and related ciliopathies. Our findings also suggest novel strategies for therapeutic intervention in the treatment of CEP290-based disease that, if fully realized, would be the first treatment available for the many patients suffering the devastating effects of CEP290 dysfunction.

Degree Type
Dissertation

Degree Name
Doctor of Philosophy (PhD)

Graduate Group
Cell & Molecular Biology

First Advisor
Jean Bennett

Keywords
CEP290, Ciliopathy, Cilium, Leber Congenital Amaurosis

Subject Categories
Cell Biology

BRIDGING THE GAP:

DEFINING THE MOLECULAR MECHANISMS OF CEP290 DISEASE PATHOGENESIS

Theodore G. Drivas

A DISSERTATION

in

Cell and Molecular Biology

Presented to the Faculties of the University of Pennsylvania

in

Partial Fulfillment of the Requirements for the

Degree of Doctor of Philosophy

2013

Supervisor of Dissertation

Signature: _____

Dr. Jean Bennett
F.M. Kirby Professor of Ophthalmology, Perelman School of Medicine

Graduate Group Chairperson

Signature: _____

Dr. Daniel Kessler
Associate Professor of Cell and Developmental Biology, Perelman School of Medicine

Dissertation Committee

Dr. James M. Wilson
Professor of Pathology and Laboratory Medicine, Perelman School of Medicine

Dr. Joshua L. Dunaief
Associate Professor of Ophthalmology Perelman School of Medicine

Dr. Erika L.F. Holzbaur
Professor of Physiology, Perelman School of Medicine

Dr. Aimee S. Payne
Albert M. Klingman Assistant Professor of Dermatology, Perelman School of Medicine

BRIDGING THE GAP:

DEFINING THE MOLECULAR MECHANISMS OF CEP290 DISEASE PATHOGENESIS

Για τους γονείς μου,

Γιώργο κ Ελένη

και για τους παππούδες μου,

Θοδωρή, Ιφιγένεια, Παναγιώτη, κ Σταματία

οι οποίοι με εκπαίδευσαν, με διασκέδασαν, με μεγάλωσαν, με ενεπνευσαν, μου έδωσαν κουράγιο, με υποστήριξαν, και θυσίασαν τόσα πολλά για να μπορέσουν τα παιδιά τους κ τα εγγόνια τους να κάνουν κάτι καλύτερο στην ζωή τους.

Αν αυτό σημαίνει κάτι, τότε ας είναι η διαθήκη για όλα όσα έχετε κάνει.

ACKNOWLEDGMENTS

The greatest difficulties sometimes spring forth from the simplest of tasks. I've certainly learned this lesson in the lab where the well-intentioned promise of "it'll be done in a week" can sometimes take more than a month to fulfill. I've discovered this aphorism to hold true in the writing of my dissertation as well. This section of my thesis, seemingly the simplest, has been perhaps the most challenging to write – not because it is terribly long (I have surely forgotten to thank many people), nor because it required any amount of hard work (in fact I should have worked harder to thank, in person, the many people listed here), but because it is impossible to fully express the gratitude one feels for all the mentors, supporters, and friends that one gains along the journey from science-obsessed child to fledgling scientist.

However, in the lab I also learned that the most difficult of problems are often the most rewarding to resolve. This maxim holds true here too – reflecting back on the many dozens of people who encouraged, supported, and challenged me throughout my life has been orders of magnitude more rewarding and gratifying than any number of picture-perfect western blots or journal acceptances. Each of these people shares a part in the work I present here for shaping me into the person I have become and the scientist I will grow up to be.

Innumerable lab and life lessons have been imparted to me by many people, but a few mentors stand out as the ones who truly inspired me and introduced me to science and the beauty of the natural world. I have been extremely lucky to have had many such mentors during every stage of my life, beginning at day one with my father. Not every child is given a microscope and chemistry set in elementary school, nor does every father take his infant son on hour-long walks through the salt marshes and natural forests of northern Manhattan, pointing out trees by name and imparting those pieces of knowledge that impressionable young children never forget – the five needle cluster of the white pine; the fresh lemony scent of a sassafras leaf rubbed between one's hands; the cat-faced leaves and long, straight trunk of the tulip tree, used by native Americans to make dugout canoes. These walks grew longer as I grew old enough to walk, stopping every few feet to collect insects and plants. It's a true testament to my mother's patience that she allowed so many collected creatures into her home.

Eventually I graduated from my father's classroom and was enrolled in New York City's public school system. Here I was introduced to a number of people to whom I am forever indebted for their encouragement and support. Each of these individuals went above and beyond any expectations of what a teacher is expected to do. Every single teacher I met along the way deserves a full page to acknowledge all that they've done for me, but in particular I must name Ms. White, Ms. Alister, Ms. Shapiro, and Ms. Williams (as they will always be known to me, no matter how often they now tell me to use their first names) for helping me grow so much as both a student and as a person.

In New York's public schools I was also introduced to two scientific mentors who left indelible marks on my personality and ambitions. These mentors were Mr. Peter Hannon in elementary school and Dr. John Utting in high school, both of whom picked up where my father left off in fostering my interest in science. I was exceptionally lucky to have Mr. Hannon as a dedicated science teacher with a dedicated science lab – even in 1st and 2nd grade the time I looked forward to most was the time spent in Mr. Hannon's classroom dissecting owl pellets (my mother still has a reconstructed vole skeleton hanging somewhere in the house), building electromagnets, and growing plants in the back garden of the school. It was probably in Mr. Hannon's class that I first seriously considered "doing science" as a career.

If there was any question about my future ambitions, however, my mind was firmly made up after meeting Dr. John Utting at Stuyvesant High School. Dr. Utting was a fantastic teacher, both in the numerous courses he taught me during the school day throughout my four years at Stuy and after school when he spent multiple hours each week teaching me and a handful of other classmates a college level cell biology course. I am, however, most indebted to Dr. Utting for the time, energy, and emotion he put into helping me complete an independent research project at the Rockefeller University, taking extra time out of his day to review the scientific literature with me, plan experiments, and review my writing. I will never forget how genuinely passionate Dr. Utting was for the subject that he taught and for the students that he cared for so deeply.

While I was incredibly lucky to have had so many fantastic people push me into the sciences, I was equally lucky to have been given hands-on lab experience from a very young age. Again, my father began this task, bringing me to the lab as a child while he was a graduate student and post-doctoral fellow. He then passed the torch on to Dr. Elias Coutavas, a graduate

school classmate of his, a close friend of our family, and an incredibly passionate, patient, and giving mentor. Elias took me into the lab as a high school student with no experience and only a tenuous grasp of the real-world applications of the scientific method (I still don't know how he ever put up with a kid who took four pages of notes – I actually went back and counted – on how to run a precast SDS-PAGE gel). After multiple high school semesters and college summers with me at his side, he left me with an exciting project, newfound skills, and, most importantly, a whetted appetite for scientific pursuit. I probably have Elias to thank, more than anyone, for launching my scientific career.

In addition to the fantastic scientific mentors I have had along the way, I have also been fortunate to have had so many cheering fans and supporters. Support comes in all forms and from people too numerous to thank, sometimes too numerous to remember, but there are certain people who have supported me in ways that I can never repay them for.

In the lab, I don't know what I would have done without Dr. Jeannette Bennicelli. Jeannette has spent so much of her time over the past few years fielding my questions, finding me reagents, and helping me plan my experiments. I don't know if any part of my thesis would have been possible without her help and support. I also have to thank Adam Wojno, a fellow graduate student, Drs. Ed Stone and Budd Tucker, our collaborators at the University of Iowa, and Drs. Erika Holzbaur and Jake Lazarus, collaborators here at Penn, for helping me to get so many aspects of my dissertation work done, for teaching me so many invaluable techniques, and for reading my papers and helping me develop experimental plans and hypotheses.

All of my work was performed with the enthusiastic support and under the watchful eyes of my thesis committee, Drs. James Wilson, Erika Holzbaur, Aimee Payne, and Josh Dunaief, all of whom have been an absolute pleasure to work with. I may be one of the few people who actually looked forward to committee meetings and have to thank my committee members for their guidance in so many aspects of my work and career.

Of course, I wouldn't even be at the University of Pennsylvania without the support of the MD-PhD program. Maureen Kirsch, Drs. Skip Brass, Aimee Payne, Gary Koretzky, and Mitch Weiss have all been so helpful and generous with their time and support. The word *generous*, however, doesn't even begin to describe Maggie Krall and all that she does. I don't know if the

MSTP program would be lost without Maggie, but I know that I certainly would be. Maggie has gotten me through every single important decision I have made since starting at Penn, from choosing rotations, to picking a thesis committee, and even to getting a dog. I have gone to Maggie before anyone else with half-formed ideas and panicked questions at every turn in the MD-PhD road. Of the many things that make Penn great, these people are some of the greatest.

Any discussion of the support I've received would be embarrassingly incomplete without mention of the two strongest pillars of support I have: my friends and family. I am indebted to so many of my friends – from Stuyvesant, the Hopkins crew team, SigEp, and now here at Penn – for their camaraderie and encouragement. I must particularly thank Ting Yang and Nick Kreston for being unbelievably supportive, undeniably fun, and absolute pleasures to know. I feel bad for all those people out there who don't get to count you two among their friends, but am absolutely so pleased that this means that I get more of your time to myself.

I have already mentioned how influential my father has been on my career but I don't think I can overstate how thankful I am for both of my parents' unyielding (overbearing, if you will) support. My mother, Helen, and my father, George, have more than supported me in everything that I have done throughout my entire life. Their unconditional love is certainly just that - I know from having tested it at certain points in my younger years. Many parents provide their children with financial, emotional, and mental support throughout their lives, but I doubt as many parents also insist on reading every grant proposal and paper prepared for submission (with extensive critique) or eagerly make monthly trips to their son's home to provide a full-service, top-to-bottom house cleaning. I often pretend to be embarrassed by their constant interest in my life and seemingly uncontainable desire to help me and my brother along the road to success (apparently success is in part mediated by the number of dish towels and pairs of socks that one owns). In truth, however, I am embarrassed only by how poor of a job I have done at thanking them over the years for all of the many, many selfless things that they have done and all that they have sacrificed so that I might succeed. Μαμα and μπαμπα, thank you so much for everything.

My parents' fantastic qualities come at least in part from good rearing – whatever my parents sacrificed for my success, my grandparents sacrificed ten-fold. It's still hard for me to

believe that only 60 years ago two Greek immigrants escaping a war-ravaged country met each other in America, married, and with less than $200 between the two of them and through nothing but back-breaking hard work and sheer determination sent both of their children to prestigious universities and carved out comfortable lives for their children and grandchildren. Each of my grandparents has played such a crucial role in my upbringing and education – their love and support are the true foundations of everything I have done. I aspire to be even half as admirable, loving, and virtuous as each of them - Pete, Tia, Jean, and Teddy - and hope that I continue to make them proud in whatever I go on to do.

Perhaps not surprisingly for a Greek American I have many more relatives to thank. I have to start by thanking my brother Peter (although I'll never admit to committing that statement to writing). People often confuse our constant arguing and prodding for something akin to loathing, but in reality it belies a deep mutual respect for each other and profound need to win each other's approval in everything that we do and say. I have probably learned as much from my brother as I have from all of my dissertation work. Opinionated and loud as we may be, we each stand up for what we believe in, including each other, and I'm very thankful for that. God help the poor person who happens to vocalize a thought that we both disagree with.

In fact, arguments and stories seem to be the currency of my entire family – a good one of either can settle any debate and is looked forward to at every family gathering. Through these verbal charades we propagate our family's mythology and, likewise, bond over our past and relish the present. These stories have been told by many – my cousins Kosta, Kevi, Ali, Theo, Catherine, Ianni, and Peter; my aunts and uncles Soula, Yianni, Dimitri, Rena, Nick, and Karen. I was lucky to be so close to all of these people throughout my life, and I am certain that this closeness played no small role in getting me to where I am today. Thank you all so much for supporting me in so many ways, both tangible and intangible, throughout my life.

To the new additions to our family, John Michael and Panayiota, I look forward to watching you grow and to pushing you forcibly into scientific careers. Hector, my rambunctious and loving dog, I don't think I'll have as much success pushing you into the sciences, but I am forever indebted to you for sitting through so many of my practice presentations. I do wish you had provided more feedback, though.

Finally, regarding family, there's one person who's still missing. If my parents were lukewarm about me welcoming Hector into the family, they were thrilled when they met Mike.

Mike Hart has been with me every step of the way during my dissertation work, has suffered through numerous lengthy tirades about failed experiments, and has read through so many drafts of my papers and grant proposals that he probably knows more about CEP290 than I do. He has also been the most supportive, helpful, and encouraging person I know and has the amazing ability to talk me down and put everything in perspective when things go wrong (except where broken egg yolks and wrinkled fondant are concerned). Thank you, Mike, and I love you.

I have, however, saved the most important acknowledgment for last. As is often the case with Jean Bennett, she defies categorization – more than a scientific mentor, the most enthusiastic and exuberant Teddy supporter there is, and as important to me as family, Jean is in a class of her own. My parents will tell you that they knew I wanted to work with Jean before I knew so myself and before, even, I had enrolled at Penn. I was scheduled by the MSTP program to meet with her during Penn preview weekend as a chance for the university to showcase its outstanding faculty and their exemplary research. For months after this meeting when I was asked which school I had decided to attend, I would say, "UPenn. And let me tell you about an amazing woman I met there!" It wasn't just the groundbreaking science (although Jean has some of the most moving and scientifically astounding PowerPoint slides I have ever seen) or even the pervasive feeling throughout her lab that big discoveries are imminent, but her scintillating personality, warmth, and enthusiasm that gripped me. Who was this woman, I asked myself, and how can I be more like her?

I can say with 100% certainty that I have never before met, nor will I ever again meet, anyone as supportive, cheerful, enthusiastic, clever, unconventional, passionate, productive, brilliant, upbeat, or caring as Jean Bennett. Jean, I cannot thank you enough for giving me the opportunity to work with you in your lab and for being so supportive and encouraging at every step along the way. If I can be even a fraction of the mentor you have been for me I will consider my career to have been a success.

My training was supported in part by an NIH/NEI T32 Training Grant (EY007035-34) and an NIH/NIA Ruth L. Kirschstein NRSA predoctoral fellowship (1F30AG044078)

ABSTRACT

BRIDGING THE GAP:

DEFINING THE MOLECULAR MECHANISMS OF CEP290 DISEASE PATHOGENESIS

Theodore George Drivas

Dr. Jean Bennett

Mutations in the gene *CEP290* cause an array of debilitating and phenotypically distinct human diseases, ranging in severity from the devastating blinding disease Leber congenital amaurosis (LCA) to Senior Løken Syndrome, Joubert syndrome, and the embryonically lethal Meckel-Grüber syndrome. The pathology observed in these diseases is thought to be due to CEP290's essential role in the development and maintenance of the primary cilium, but despite its critical role in biology and disease we know only little about CEP290's function. Here we identify four novel functional domains of the protein, showing that CEP290 directly binds to cellular membranes through an N-terminal domain that includes a highly conserved amphipathic helix motif, and to microtubules through a domain located within its myosin-tail homology domain. Furthermore, CEP290 activity was found to be regulated by two novel autoinhibitory domains within its N- and C-termini, both of which were also found to play critical roles in regulating ciliogenesis. Disruption of the microtubule-binding domain in the rd16 mouse LCA model was found to be sufficient to induce significant deficits in cilium formation leading to retinal degeneration. Taking these findings into account, we developed a novel model that

accurately predicts patient CEP290 protein levels in a mutation-specific fashion. Predicted CEP290 protein levels were found to robustly correlate with disease severity for all reported *CEP290* patients. All these data implicate CEP290 as an integral structural and regulatory component of the primary cilium and provide insight into the pathological mechanisms of LCA and related ciliopathies. Our findings also suggest novel strategies for therapeutic intervention in the treatment of *CEP290*-based disease that, if fully realized, would be the first treatment available for the many patients suffering the devastating effects of CEP290 dysfunction.

TABLE OF CONTENTS

LIST OF TABLES

LIST OF FIGURES

CHAPTER 1:

CHAPTER 2:

CHAPTER 3:

CHAPTER 4:

CHAPTER 5:

PREFACE

This dissertation presents a work of molecular biology, cell biology, biochemistry, and bioinformatics that attempts to address multiple fundamental questions regarding Centrosomal protein of 290 kDa, or CEP290, and its role in the function of the primary cilium and in human disease. It is my hope that the work laid out within these pages should not only contribute to our understanding of the basic biology of the primary cilium, but that it may someday aid in the development of novel therapeutic interventions for patients suffering the devastating effects of CEP290 related disorders.

I began this project by asking a simple question – can I break CEP290 down into individual units of discrete functionality? This simple question spawned multiple lines of investigation that resulted in a new understanding of CEP290's role in the primary cilium. Like the LEGO-obsessed child I have always been, digging through the LEGO bin for the perfect piece for the project at hand, I was fascinated by the unique properties of each piece of the protein I had created – a microtubule binding domain here, a membrane binding domain there. Starting with a protein broken into five pieces, I had soon generated twelve, then eighteen, and finally thirty-two CEP290 fragments. The smaller and smaller the pieces got the more I discovered – novel regulatory domains, new interacting partners, and, of course, more questions.

With my lab notebook overflowing with CEP290 pieces, I began to wonder whether I'd ever be able to fit any of them together. I began assembling them, like LEGO bricks, and as I assembled I began to see how different pieces might connect. The pieces began to suggest a critical role for

CEP290 in maintaining the structural integrity of the cilium. Through a little bit of hard work (and at least as much dumb luck) I demonstrated how the breakdown of this structural integrity can result in severe retinal degeneration in a mouse model of human disease. With this newfound knowledge, and in collaboration with fantastic researchers both at UPenn and the University of Iowa, I formulated and validated a novel model for *CEP290* disease pathogenesis that explains, for the first time, how different mutations in the same gene can result in such drastically different diseases. More recently my childhood instinct to push the directions aside and dive straight for the LEGOs took over again as I attempted to assemble all of my CEP290 pieces into a finished product without a complete instruction manual. Even as I write this I find it hard to exchange the pipette for the pen, and have begun experiments to see how much the *miniCEP290* I pieced together looks like the picture on the box.

What follows is a discussion of much of the work that I have done on *CEP290*. I begin with a comprehensive introduction that lays out our understanding of the primary cilium and *CEP290* up to the point of the publication of this work. The introduction, divided into three parts, covers the history, structure, and function of the primary cilium, diseases arising from ciliary dysfunction, and, finally, the structure, function, regulation, and clinical importance of CEP290. Following the introduction is a presentation, in three chapters, of the body of work that comprises this thesis. The first and most substantial chapter describes the discovery of four novel functional domains within the CEP290 protein and the role that these domains play in CEP290 function, regulation, and disease. The subsequent chapter details the formulation and validation of a novel model for *CEP290* disease pathogenesis. The third chapter deals with my recent work in the application of my findings towards the development of a *miniCEP290*

therapeutic. Finally, in the last chapter, the broad implications and future directions of my findings are discussed.

As a child I used to save my LEGO creations for as long as possible, until necessity or my mother dictated that I put them back into the LEGO bin. But inevitably a chunk of bricks would survive as it was tossed back in and would find itself serving as the foundation for the next bigger, more ambitious project. I can only humbly hope that some small piece of this work will ultimately find its way into such a project and help make a difference in the lives of those *CEP290* patients and supporters who have already made a difference in mine.

-Theodore G. Drivas

CHAPTER 1: INTRODUCTION

Theodore G. Drivas[1]

1. Cell and Molecular Biology Graduate Group and the F.M. Kirby Center for Molecular Ophthalmology, Perelman School of Medicine, University of Pennsylvania, Philadelphia, PA 19104, USA

The primary cilium

A brief history

The primary cilium of the mammalian cell was first described by Zimmerman more than 100 years ago (Zimmermann, 1898), but it has taken the scientific community nearly as long to appreciate its importance. This lone, immotile projection of the apical membrane found on nearly every vertebrate cell (Mahjoub, 2013) took a back seat to its more attention-grabbing cousin, the motile cilium, as biologists honed in on this organelle as the true mover and shaker of the microscopic world. Research quickly progressed in the characterization of motile cilia and the cells they ornamented while the primary cilium remained largely ignored.

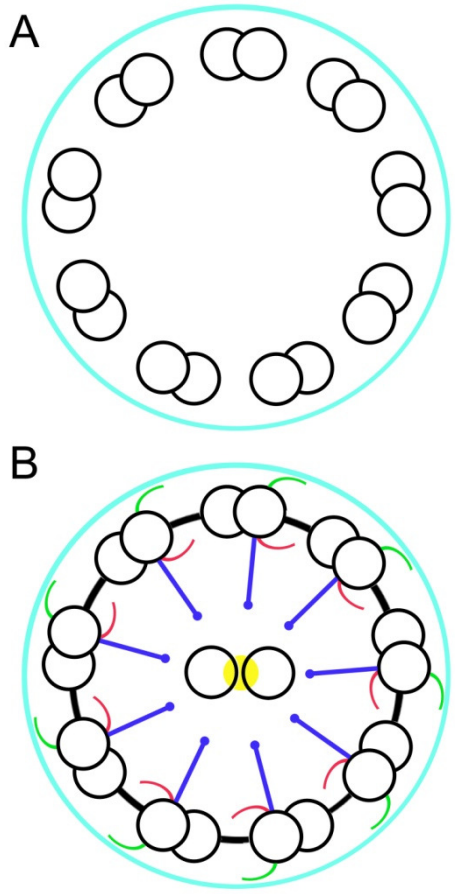

Figure 1.1 Schematic representation of primary and motile cilia in cross section
A. Representation of a primary cilium in cross section illustrating the 9+0 arrangement of microtubule doublets within the ciliary membrane (teal).
B. Representation of a motile cilium in cross section illustrating the 9+2 arrangement of microtubule doublets, inner (red) and outer (blue) dynein arms, nexin connections (black), and radial spokes (blue), all of which are required for motility.

With the advent of electron microscopy, however, the similarity between motile and primary cilia became sharply apparent when both were discovered to be membrane-surrounded organelles built around a ring of microtubule doublets. In 1952

Fawcett and Porter famously described the 9+2 arrangement of the motile cilium's microtubule axoneme (Figure 1.1B; Fawcett and Porter, 1954), and just a few years later De Robertis, perhaps less famously, described the 9+0 arrangement of the axoneme of the primary cilium. (Figure 1.1A; De Robertis, 1956). It soon became apparent that primary cilia were nearly ubiquitous – Barnes, Dahl, Grillo, Palay, Sorokin and others began publishing report after report of primary cilia in cell types and tissues as diverse as fibroblasts, neurons, the pituitary gland, and muscle (Barnes, 1961; Dahl, 1963; Grillo and Palay, 1963; Sorokin, 1962).

However, even with the realization that the primary cilium appeared to be a component of nearly every cell of the human body, scientists continued to shy away from intense study of the organelle as the consensus at the time was that it was merely vestigial, a lonely reminder of our evolutionary past. A few outspoken ciliary biologists, however, began to advocate for a different hypothesis – perhaps the primary cilium, an outgrowth of the centriole, is formed by dividing cells to arrest cell division, sequester the centrosome, and enter quiescence (Dingemans, 1969; Fonte et al., 1971). A number of lines of research seemed to support this presumption and to this day this is still considered an important aspect of the primary cilium's function. The vast importance of the organelle was about to become much more apparent, however, with the publication of Poole, Flint, and Beaumont's work on primary cilia in chondrocytes.

In 1985 Poole and colleagues were the first to clearly, if perhaps speculatively, label the primary cilium a sensory organelle; or, to use their own words, a "cellular cybernetic probe" (Poole et al., 1985). It was at this point that the field of ciliary biology truly took off. With the realization that the primary cilium was critical to the cell's ability to interact with its environment, biologists

finally began to treat the organelle with the respect it currently commands. It soon became clear that deficits in cilium formation and function were at the root of a number of human disease syndromes (Pazour et al., 2000, 2002; Praetorius and Spring, 2001). The more the scientific community began to learn about these diseases, the ciliopathies, the more they learned about the essential basic biology of the organelle.

In the past ten years the number of papers published in the field of ciliary biology has exploded and we are finally beginning to understand the pathways, mechanisms, and components required by the cell for building and operating the organelle. The pathways involved in ciliogenesis are remarkably conserved, and thoroughly understanding them will help illuminate both the role of the cilium in human disease and the role of particular ciliary proteins, such as CEP290, in human health and pathology.

Ciliogenesis

Ciliogenesis is the name given to the highly orchestrated sequence of events that together give rise to the primary cilium. Ciliogenesis requires the temporal and spacial coordination of a number of proteins and subcellular machines, but can be divided into a number of distinct steps (Sorokin, 1968). While we tend to discuss each of these steps as discrete events, it is almost certain that many of these steps occur concurrently, at least to a degree, with checkpoints along the way to ensure proper cilium formation (Miyamoto et al., 2011).

To understand ciliogenesis, however, we must first understand the organelle from which the cilium is derived. The cilium is, at its most basic level, a membrane-enclosed extension of the

centriole (Bornens, 2012). Each centriole is composed of a ring of nine microtubule triplets, at 40° angles to each other, that come together to form a short cylinder roughly 0.25 µm in diameter and a little less than 1 µm long (Gönczy, 2012). Two centrioles, a mother and daughter (the daughter being built using the mother as a template upon completion of the cell cycle), come together at a 90° angle within a cloud of dense pericentriolar material to form the centrosome (Bettencourt-Dias and Glover, 2007). The centrosome is the organelle familiar to even middle school biology students (I still remember using pieces of Twizzlers to represent the centrosome for a 6^{th} grade "edible cell" project) as the site of spindle body formation during mitosis. Spindle formation is a critical step along the way to cell division wherein the chromosomes, attached to microtubule projections emanating from the centrosome, are induced to line up along the midline of the cell before being pulled apart to opposite cellular poles upon the completion of anaphase (Bettencourt-Dias and Glover, 2007).

As important as spindle formation is, the cell spends only a fraction of its time in mitosis. During the rest of the cell cycle the centrosome is repurposed for the equally important job of acting as the cell's microtubule organizing center. It is in this capacity that the centrosome helps to define cell polarity, position cellular organelles, and pave the roadways that make up the intracellular highway in the form of the microtubule network (Bettencourt-Dias and Glover, 2007).

But just as the cell spends only a small portion of the cell cycle in mitosis, most cells in the human body spend only a small fraction of their time in the cell cycle (Vermeulen et al., 2003). Upon terminal differentiation, cells can choose to exit the cell cycle and enter a phase of their lives known as G_0. It is during G_0 that we return to the story of ciliogenesis (Goto et al., 2013).

While we can never know the motivation behind any evolutionary "decision," it has been proposed that the primordial differentiated cell choose to sequester its centriole at the cell surface to guard against aberrant reentry into the cell cycle. Perhaps this was the case, or perhaps the evolutionary drive for a highly specialized cellular antenna was the motivating factor (Cavalier-Smith, 2010; Satir et al., 2008), but regardless of etiology evolution dictated that, upon entry into G_0, the vertebrate cell sequester its centrosome in the structure we know as the primary cilium (Kobayashi and Dynlacht, 2011).

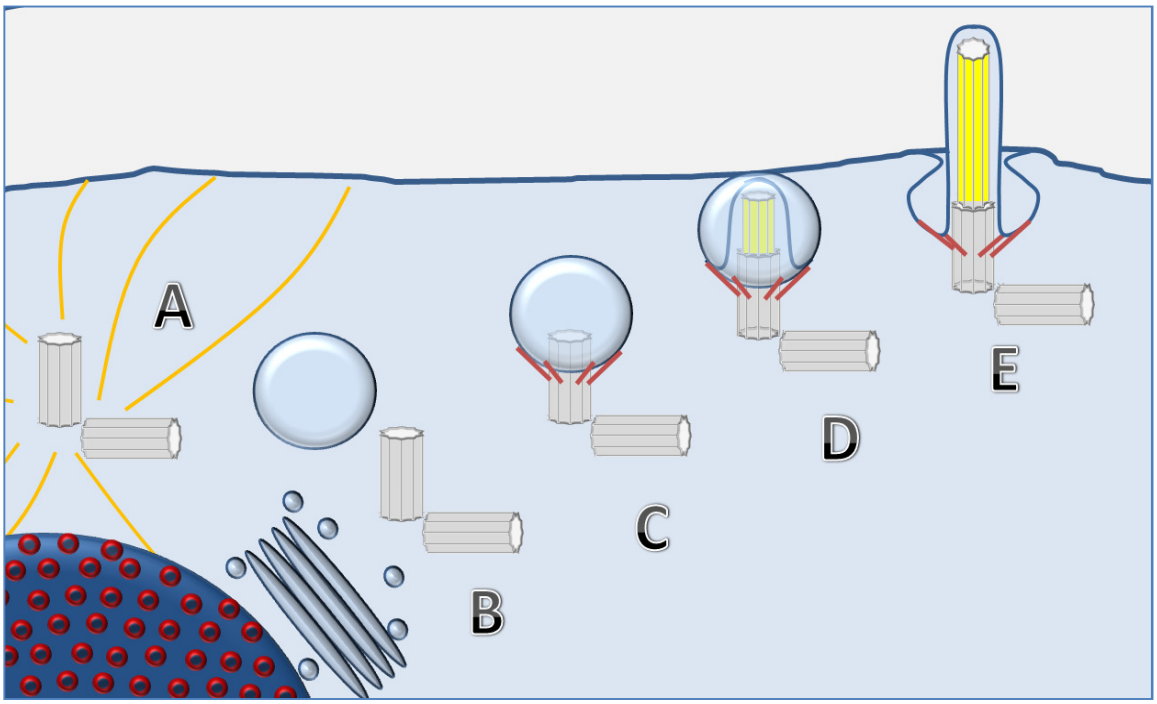

Figure 1.2. A schematic diagram of the events involved in ciliogenesis.
(A) The centrosome acts as the microtubule organizing center of the cell during the cell cycle, helping to position the nucleus and other organelles. (B) As the cell enters $G_{1/0}$ the centrosome begins to migrate towards the cell surface. (C) The mother centriole docks with a Golgi-derived ciliary vesicle by means of the ciliary transition fibers. (D) Axoneme extension begins into an invagination in the ciliary vesicle while the whole complex docks at the apical cellular membrane (E) The ciliary vesicle fuses with the plasma membrane, the axoneme completes extension, and ciliogenesis is complete.

Ciliogenesis, then, begins at G_0 (it is worth mentioning that eukaryotic cells sometimes also produce cilia during the G_1 phase of the cell cycle through the same process discussed below) when a signal, which has not yet been fully elucidated, induces the centrosome to begin migrating towards the apical surface of the cell (Figure 1.2A; Kobayashi and Dynlacht, 2011). During this journey the mother centriole encounters and docks with a Golgi-derived ciliary vesicle (Figure 1.2B; Sorokin, 1962, 1968). Dense, proteinaceous transition fibers begin to extend from the mother centriole, anchoring the centrosome (now referred to as a basal body) to the ciliary vesicle that will ultimately give rise to the ciliary membrane (Figure 1.2C; Anderson, 1972; Deane et al., 2001). It is at this point that two critical steps occur: the basal body must nucleate the outgrowth of the microtubules that will go on to make up the core of the primary cilium (Figure 1.2D; Sorokin, 1962), and the ciliary vesicle must dock at and fuse with the plasma membrane (Figure 1.2E; Sorokin, 1962, 1968).

Once each of these critical steps is accomplished, ciliogenesis is complete. The ciliary axoneme will continue to elongate until it reaches a stable length of about 3-8 μm (Besschetnova et al., 2010), driven by the trafficking of axonemal components to the ciliary compartment and by the opposing inward and outward forces of intraflagellar transport (Ishikawa and Marshall, 2011; Rosenbaum and Child, 1967).

The structure of the cilium

The fully-formed primary cilium can be divided into a number of distinct domains. Below is a discussion of each region of the cilium, moving from proximal to distal, along with a brief description of the structure, components, and hypothesized roles of each. Figure 1.3 serves to

illustrate many of these same points and, while it will be specifically referenced at different points in the following text, it also provides a good stand-alone summary of ciliary structure.

Basal body

During the process of ciliogenesis the centrosome migrates to the cell surface where it matures into the basal body of the nascent primary cilium. While the basal body consists of both the mother and daughter centriole of the centrosome, it is only the mother centriole that acts in the attachment to the cell cortex and the nucleation of the microtubules that will ultimately make up the core of the ciliary axoneme (Beisson and Jerka-Dziadosz, 1999).

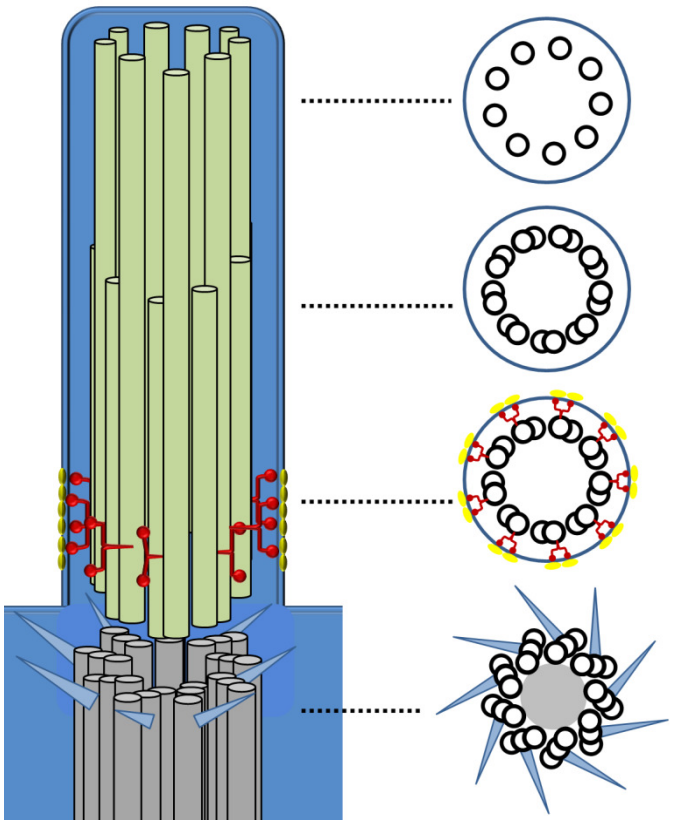

Figure 1.3. A diagram of the structure of the primary cilium

An illustration of the different domains of the cilium in profile and in cross section. The microtubules of the basal body are indicated by grey cylinders. The microtubules of the axoneme are indicated by green cylinders. The distal appendages are indicated by blue wedges. The ciliary Y-links are depicted in red while the ciliary necklace is depicted by yellow dots. At each distinct level of the cilium a cross section of the organelle is provided.

The basal body is, not surprisingly, nearly identical in structure to the centriole. It is characterized by a ring of 9 microtubule triplets, each containing a fully formed A microtubule and two incomplete microtubules, the B and C tubules (Figure 1.3, Basal Body; Avidor-Reiss and Gopalakrishnan, 2012; Azimzadeh and Marshall, 2010). The mother centriole of the basal body is distinguished from the daughter by the presence of the distal appendages, ancillary structures found at the distal end of the mother centriole (Paintrand et al., 1992). In the basal body, these distal appendages are extended and elaborated to form the dense propeller-like array of transition fibers, the strong physical connectors between the basal body and the cell cortex (Ringo, 1967; Sorokin, 1968).

Although often considered a more-or-less static structure, important more for the structural stability of the cilium than anything else, the basal body also serves as a waypoint for ciliary transport, acting as a loading dock for ciliary cargo (Deane et al., 2001; Hsiao et al., 2009). The basal body, even while attached to the cilium, also continues to act as the major microtubule organizing center for the cell (Basten and Giles, 2013). Thus, cilium-directed trafficking of proteins and vesicles is accomplished by means of dynein-mediated transit along the microtubule network towards the microtubule minus ends and the basal body. Cargos then accumulate at the basal body before being transported into the cilium and across the diffusion barrier at the ciliary transition zone (Cole et al., 1998; Stephan et al., 2007).

Transition zone

Just past the basal body lies the transition zone of the cilium. Here the A and B microtubules of the nine basal body microtubule triplets elongate, giving rise to the 9+0 arrangement of

microtubule doublets characteristic of the transition zone and ciliary axoneme (Czarnecki and Shah, 2012; Reiter et al., 2012). The aptly named transition zone is the point of transition from basal body to true axoneme. As such, it contains a number of important protein complexes that both define its structure and play critical roles in the regulation of cilium formation and function (Szymanska and Johnson, 2012).

Perhaps the most striking feature of the transition zone, when compared to the rest of the ciliary axoneme, is the presence of the dense, proteinaceous ciliary Y-links and the punctate ciliary necklace (Figure 1.3, Transition Zone). The Y-links span the distance between the microtubule core of the transition zone and the overlying membrane (Craige et al., 2010). Immediately abutting the ciliary Y-links is the ciliary necklace, a circumferential collection of several parallel strands of intramembranous particles that stud the ciliary membrane (Gilula and Satir, 1972; Torikata, 1988). These two structures contain dozens of proteins that appear critical for ciliary function. It is thought that these two structures act together to form a ciliary pore and diffusion barrier, both of which are responsible for maintaining the ciliary milieu (Kee et al., 2012; Ounjai et al., 2013). In fact, when either of these structures is disrupted, protein trafficking into the cilium becomes highly dysregulated with non-ciliary proteins gaining access to the organelle and ciliary proteins unable to enter (Craige et al., 2010).

As one might imagine, mutations in many of the protein components of the ciliary transition zone can result in severe human disease. This is thought to be due to the critical nature of the transition zone in establishing and supporting intraflagellar transport (IFT), the highly regulated process whereby ciliary proteins are transported into and along the axoneme (Hsiao et al.,

2012). Even small defects in the transition zone can have deleterious effects further down the axoneme since transition zone dysfunction can lead to the detainment or complete exclusion of protein components destined for the ciliary compartment.

The ciliary pocket

Immediately adjacent to the transition zone is a structure known as the ciliary pocket. This region of the organelle, found in most, but not all, vertebrate cilia, consists of a depression in the plasma membrane in a ring immediately surrounding the ciliary axoneme at the point where the regular plasma membrane transitions to the well-defined ciliary membrane (this structure is not shown in Figure 1.3 but is present in Figure 1.2E; (Benmerah, 2013; Molla-Herman et al., 2010)). The ciliary pocket is thought to be critical in the trafficking of ciliary membrane proteins into the organelle for axonemal extension and ciliary function (Molla-Herman et al., 2010). In some cilia, such as those of endothelial cells, the ciliary pocket can be as deep as the axoneme is long, such that the axoneme barely projects past the surface of the cell (Geerts et al., 2011). In other cells, such as the epithelial cells of the renal tubules, the ciliary pocket is so small it is barely noticeable (Geerts et al., 2011).

Ciliary axoneme

The ciliary axoneme begins where the transition zone leaves off. The microtubule doublets of the transition zone continue to extend distally, past the Y-links and ciliary necklace, to produce the canonical membrane-enveloped 9+0 organization of the primary cilium (Figure 1.3, Proximal Axoneme; De Robertis, 1956). The organelle continues to extend in this fashion, projecting outward and into the environment surrounding the cell. In the very distal region of the organelle

the B tubule of the microtubule doublet ceases to elongate, leading to a short stretch of 9 single microtubule extensions that finally end, a few micrometers away from the basal body, at the terminus of the organelle (Figure 1.3, Distal Axoneme; Sorokin, 1968).

One might say that the ultimate goal of ciliogenesis is the formation of the ciliary axoneme. As important as the basal body and transition zone are, both to ciliary function and in human disease, the function of the cilium is truly accomplished distally to both these regions. Intraflagellar transport (IFT) drives the accumulation of innumerable signaling molecules, G protein-coupled receptors, and downstream effector molecules within the axonemal lumen and membrane, and it is the high concentration of these molecules that allows the cilium to perform its function as the cell's antenna (Boekhoff et al., 1990; Elias et al., 2004; Jenkins et al., 2006). But exactly how do these molecules make their way into the cilium and along the axoneme?

Trafficking to the cilium

Proteins cannot be synthesized within the ciliary lumen and thus all the components of the cilium must be specifically shuttled into the organelle from the cytosol (Rosenbaum and Child, 1967). Both soluble and membrane-associated proteins accumulate at the base of the cilium by means of the network of microtubules that emanates from the ciliary basal body, the primary microtubule organizing center for ciliated cells (Guo et al., 2006). Proteins can also reach the base of the cilium by diffusion, both through the cytosol for soluble proteins and laterally across the plasma membrane for transmembrane proteins, but recent evidence suggests that active trafficking along microtubules plays a much more prominent role in ciliary trafficking (Dammermann and Merdes, 2002; Quintyne and Schroer, 2002; Wright et al., 2011).

Having completed their journey towards the ciliary base, proteins and vesicles accumulate around the basal body awaiting the next step in their journey (Dammermann and Merdes, 2002; Kubo et al., 1999). From here, soluble proteins must transit across the ciliary basal body and transition zone to enter the organelle. The entry of proteins into the cilium is an active process, the tight regulation of which is accomplished by a ciliary diffusion barrier that excludes all proteins larger than 10kD and allows only the specific translocation of cilium-destined cargo in a highly selective fashion (Calvert et al., 2010; Hu and Nelson, 2011; Kee et al., 2012; Najafi et al., 2012). Recent evidence suggests that this is accomplished by a pore-like complex at the transition zone of the cilium (Kee et al., 2012; Ounjai et al., 2013). This pore appears to share much in common with the nuclear pore complex and, as with nuclear transport, ciliary transport has recently been demonstrated to be dependent on a gradient of RanGTP/RanGDP, importin and exportin proteins that act as shuttling chaperones, and even nuclear pore protein components themselves (Dishinger et al., 2010; Kee et al., 2012). Just as nucleus-destined proteins contain specific nuclear localization signals, proteins destined for the cilium appear to contain some kind of ciliary localization signal (CLS) that mediates their entry into the organelle. A number of CLSs have been identified, but no single canonical CLS sequence has yet been defined (Berbari et al., 2008a; Dishinger et al., 2010).

These same CLSs also appear to serve in the targeting of membrane proteins to the ciliary compartment (Geng et al., 2006; Ward et al., 2011). The specifics of membrane protein translocation through the ciliary diffusion barrier are still debated, but it has been convincingly demonstrated that Golgi-derived vesicles containing proteins destined for the cilium are

recognized by means of their CLSs (Geng et al., 2006; Jenkins et al., 2006; Ward et al., 2011) and chaperoned to the base of the cilium by the exocyst and BBSome, two complexes of proteins critical in ciliary membrane trafficking (He and Guo, 2009; Mazelova et al., 2009). Ciliary membrane transport is aided by a number of additional vesicular trafficking proteins such as Clathrin, Rab8, Rab11, and the SNARE family of proteins (Kaplan et al., 2010; Mazelova et al., 2009; Westlake et al., 2011). Once at the base of the cilium it is thought that these vesicles fuse with the periciliary membrane and the transmembrane protein cargo then transits the ciliary diffusion barrier by mechanisms not yet completely elucidated (Hu et al., 2010; Ou et al., 2007).

Intraflagellar transport

After successfully navigating the ciliary pore and diffusion barrier, proteins are transported along the length of the cilium by means of a highly regulated process known as intraflagellar transport (IFT). IFT was first observed by differential interference light microscopy in the *Chlamydomonas* flagellum, the algal ortholog of the mammalian cilium (Kozminski et al., 1993). Here small particles could be seen moving along the flagellar axoneme in opposite directions, both towards and away from the tip of the organelle (Pedersen and Rosenbaum, 2008). The IFT particles were noted to be closely associated with both the microtubules of the flagellar axoneme and with the flagellar membrane and it wasn't long before it was discovered that the movement of these IFT particles was coordinated by a set of dynein and kinesin microtubule motor proteins (Kozminski et al., 1995; Pazour et al., 1998). The microtubules of the cilium are always organized with their plus ends projecting from the cell towards the tip of the organelle (Binder et al., 1975), and thus it quickly became apparent that the anterograde motion of IFT particles is driven by the kinesin class of microtubule motor proteins in association with

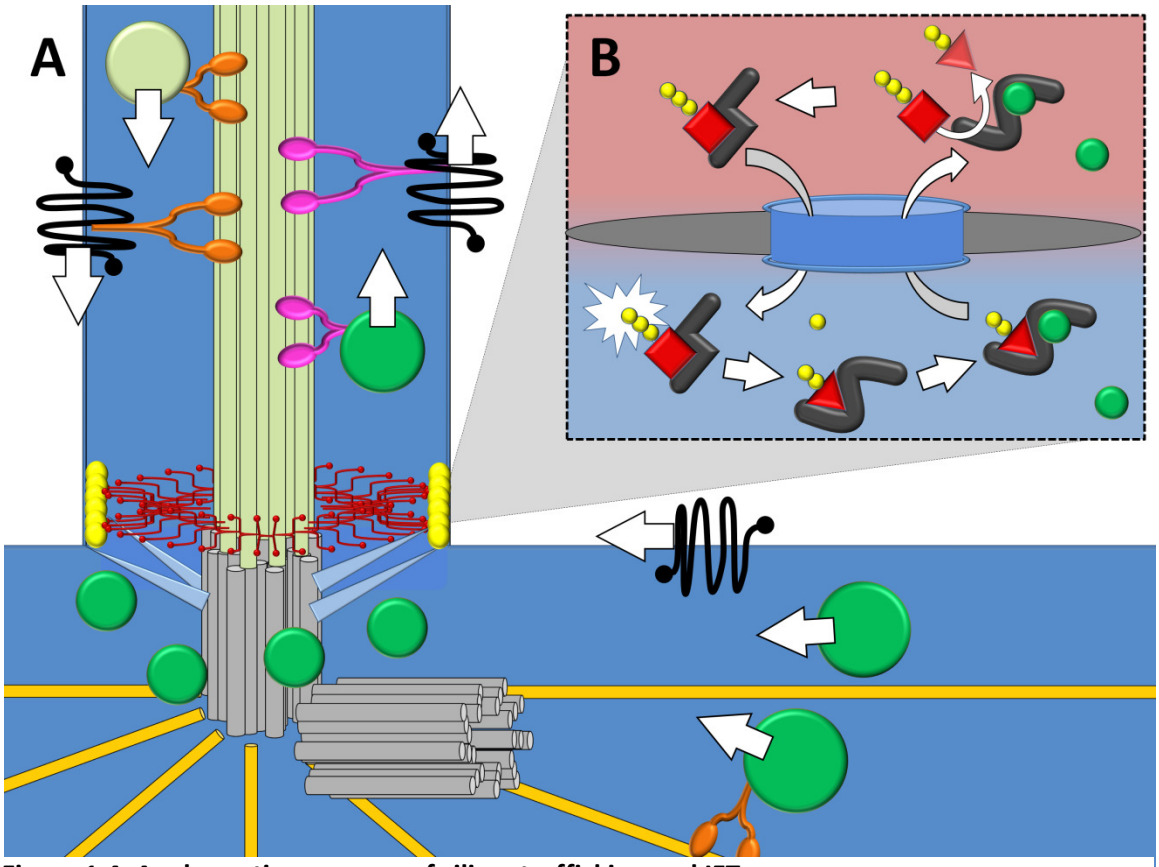

Figure 1.4. A schematic summary of ciliary trafficking and IFT

(A) Cargos destined for the cilium (green) transit towards the basal body either by diffusion or by means of the microtubule network, driven by cytoplasmic dynein (orange). Membrane proteins destined for the cilium (black) can be transported in the same fashion, packaged in golgi-derived vesicles, or can diffuse laterally along the plasma membrane towards the cilium. Cargos then accumulate at the ciliary base before translocating through the ciliary pore at the transition zone (red and yellow). Once within the cilium, ciliary components are shuttled along the length of the axoneme by the process of IFT. Anterograde transport is accomplished by the microtubule motor protein kinesin (pink), while retrograde transport is accomplished by the axonemal dynein motor proteins (orange)

(B) While the specifics of ciliary pore translocation have not yet been fully worked out, the import of many proteins has been shown to be dependent on the same class of importin proteins (dark grey) that shuttle cargos into the nucleus. A gradient of RanGTP(red background) and RanGDP (blue background) is established across the ciliary pore and this gradient helps drive directional ciliary transport. An importin molecule, bound to RanGDP (red triangle, phosphates in yellow) on the cytoplasmic side of the ciliary pore binds to a cilium-destined cargo (green) by recognizing a ciliary localization signal contained within the protein's amino acid sequence. This complex then navigates the ciliary pore, exchanges RanGDP for RanGTP (red square, phosphates in yellow) within the ciliary lumen, causing a conformation change in the importin freeing the cargo protein. RanGTP-bound importin then exits the cilium, hydrolyzing RanGTP to RanGDP within the cytoplasm to free inorganic phosphate (yellow) and affect a comformational change returning the importin to its original state for the next round of import.

the IFT-B subcomplex (Kozminski et al., 1995), while the retrograde movement of IFT particles is driven by dynein family members in association with the IFT-A subcomplex of proteins (Pazour et al., 1998; Pedersen and Rosenbaum, 2008).

IFT particles are loaded onto the IFT highway by a vast array of proteins, many of which are certainly still unknown, but a key player in this process is the protein machine known as the BBSome. The BBSome is a complex of a number of ciliary proteins that aid in the ciliary targeting of membrane-associated proteins, the loading of cargo into IFT particles, and the recycling of particles at the ciliary tip (Wei et al., 2012; Zhang et al., 2013). IFT particles, loaded onto the IFT highway by the BBSome at the basal body, appear to move in a continuous loop – particles make their way to the tip of the cilium, unload their cargo, begin retrograde transport, and are finally recycled at the base for another round of transport (Wei et al., 2012). These cycles of IFT accomplish multiple purposes. First, anterograde transport accomplishes the delivery of retrograde transport machinery to the ciliary tip (Piperno et al., 1996), while retrograde transport accomplishes the recycling of anterograde transport machinery to the ciliary base (Pazour et al., 1999; Signor et al., 1999). Defects in transport in either direction will ultimately lead to a breakdown in ciliary structure, either through the inability to initiate anterograde transport and axoneme extension or by the depletion and accumulation of anterograde transport machinery at the tip of the cilium with no means of recycling it (Engel et al., 2012).

Perhaps even more importantly, IFT is completely responsible for the shuttling of axonemal subunits, signaling molecules, and all the components required for ciliary function to different locations along the length of the organelle (Zhao and Malicki, 2011). Without IFT the growth and

maintenance of the ciliary axoneme would be impossible, and the specialized signaling environment of the cilium would not exist. All of the many transmembrane receptors, effector proteins, and downstream signaling molecules that are critical to the cilium's function as a sensory organelle must be specifically trafficked into and along the cilium by IFT. In fact, failure of important components of the IFT machinery can, as will become apparent, result in significant human disease (Blacque et al., 2008).

Ciliary function

The principle that structure follows function (while obviously not adhered to in the organization of the sections of this introduction) is certainly a truism for most biological systems. The cilium is no exception – the great lengths that the cell goes to to produce and maintain such a highly structured organelle is not without explanation. Much as the antennas we use to receive and transmit electromagnetic waves have evolved over time to produce a shape most conducive to this activity, the primary cilium has evolved into a highly specialized, highly efficient cellular antenna. The unique signaling environment afforded by the cilium's rigorously maintained structure is critical to its function and allows for its participation in the coordination of numerous cellular activities.

The cilium is critical in development, repair, homeostasis, and growth. These activities are all triggered or inhibited by extracellular stimuli that the cilium senses and transduces to the rest of the cell. It accomplishes this both by means of the large concentration of signaling molecules within its membrane and lumen and by means of its strategic location on the apical surface of the cell, the side most often in contact with the cellular environments critical for cellular

function (Basten and Giles, 2013; Oh and Katsanis, 2012). The epithelial cells of the kidney project cilia into the lumen of the renal tubules to detect and respond to fluid flow (McAteer et al., 1986). Acinar cells of secretory organs project cilia into the acinar lumen where they are critical in the development of the glandular structure and in maintaining and regulating secretion (van Asselt et al., 2013). The endothelial cells of the circulatory system produce cilia, submerged deep within profound ciliary pockets, which are thought to be essential in detecting and responding to blood flow and serum composition (Geerts et al., 2011). Perhaps most intriguingly, recent evidence has begun to suggest that the immune synapse that forms between circulating T-cells and antigen presenting cells is driven by IFT machinery in a process that shares much in common with ciliogenesis (Finetti et al., 2011).

While it is clear that primary cilia are present in and essential to nearly every organ system of the human body, some signaling pathways and organ systems are more dependent on ciliary function than others. Below is a discussion of some of the specialized functions that primary cilia play in these diverse pathways and tissues.

Hedgehog signaling

The Hedgehog signaling pathway is critical during embryogenesis and plays an essential role in the homeostasis of many adult tissues. Hedgehog signaling is mediated by the membrane receptor Patched that actively inhibits the transmembrane protein Smoothened, resulting in the proteolytic processing of the Gli family of transcription factors (Lum and Beachy, 2004). In the processed state, the Gli proteins act to inhibit transcription at a number of genomic loci. When the Patched receptor is bound by its ligand, Shh, inhibition of Smoothened is relieved – the Gli

family proteins thus remain unprocessed, actively *promoting* transcription at the same genomic loci (Lum and Beachy, 2004).

The proper function of the primary cilium is critical in each of these steps. The Gli proteins are specifically trafficked to the tip of the cilium where they are processed and released to act as transcriptional repressors in the nucleus (Haycraft et al., 2005). In the absence of Shh ligand, Patched is confined to the ciliary membrane (Rohatgi et al., 2007), actively excluding Smoothened from the ciliary compartment. The binding of Patched to Shh ligand results in its exit from the cilium and the concurrent entry of the Smoothened effector molecule (Corbit et al., 2005). Once inside the cilium Smoothened gains access to the Gli proteins at the ciliary tip, arresting their proteolytic processing and releasing them to the nucleus in their transcription-promoting forms (Haycraft et al., 2005).

Defects in cilium formation have a catastrophic effect on embryogenesis and development, and much of this is thought to be due to deficiencies in Hedgehog pathway regulation (Fliegauf et al., 2007; Wang et al., 2007). Neural tube closure defects, abnormal brain morphology, and limb patterning defects, all hallmarks of deficiencies in Shh signaling, are also seen in human ciliopathy patients and mouse models of ciliary disease (Huangfu et al., 2003). The precise role that the Hedgehog pathway plays in the maintenance and function of adult tissues is still being worked out, but it is clear that it is essential in the proliferation of adult hematopoietic and neural stem cells and in the processes of growth and regeneration in general (Bhardwaj et al., 2001; Han et al., 2008; Ruiz i Altaba et al., 2002). It will be interesting to see the role the primary cilium plays in regulating these processes as we continue to learn more about the organelle.

Wnt signaling

While the exact role that the primary cilium plays in Shh signaling has been more or less resolved, the organelle's role in Wnt signaling is still being debated. The Wnt family of ligands represents a class of secreted lipid-modified proteins that affect numerous critical processes within the cell. This is accomplished by the interaction of Wnt ligands with the Frizzled class of receptor proteins that, in the canonical Wnt pathway, results in activation of the cytoplasmic pool of the protein Disheveled, ultimately acting to inhibit the protein Axin. (Komiya and Habas, 2008). Axin normally localizes to the destruction complex where it works to target the transcription factor β-Catenin for degradation, but with Axin's inhibition β-Catenin accumulates and enters the nucleus, affecting numerous changes in the transcriptional regulation of the cell (MacDonald et al., 2009; Rao and Kühl, 2010). In the noncanonical Wnt signaling pathway, activated Frizzled receptor binds directly to cytoplasmic Disheveled, resulting in its activation and accumulation at the plasma membrane. Here Disheveled initiates a β-Catenin-independent signaling cascade that ultimately results in major cytoskeletal changes (Gordon and Nusse, 2006).

A number of different lines of evidence have begun to implicate the primary cilium as critical in the regulation of both of these pathways. Numerous studies have suggested that the primary cilium acts to restrain canonical Wnt signaling through the sequestration of β-Catenin and Disheveled at the ciliary basal body (Gerdes et al., 2007). In support of this model, knock down of a number of proteins essential for ciliogenesis results in increased nuclear β-Catenin (Basten and Giles, 2013; Corbit et al., 2008; Kishimoto et al., 2008). At the same time, however, many groups have begun publishing reports of the primary cilium mediating both activation and

repression of the non-canonical Wnt signaling pathway (Gerdes et al., 2007; Leitch et al., 2008; Ross et al., 2005). While the details of the cilium's role in Wnt signaling are not yet settled, it seems that the organelle may be playing a role in the switch between the canonical and non-canonical pathways (Simons et al., 2005). Regardless of the specific mechanisms involved, it is clear that the cilium has strong input on Wnt pathway regulation.

Fluid flow

One of the more interesting roles that the cilium plays is in the sensing of fluid flow in the renal tubules. The renal tubules connect the glomeruli (the sites of blood filtration) to the collecting ducts (the sites of urine collection) of the kidney. It is in the renal tubules that components of the filtrate, including water, sugar, salt, and amino acids, are reabsorbed by the body and the urine is concentrated (Torres and Harris, 2006).

While the importance of the renal tubule epithelial cells' ability to sense fluid flow for the proper function of the kidney seems apparent, what is less obvious is how this ability is essential for renal development and growth. Many ciliopathies result in the development of renal cysts that, in some cases, are severe enough to result in embryonic lethality (Torres and Harris, 2006). These cysts are a direct result of the renal epithelial cells' inability to sense fluid flow during kidney development. Normally these cells divide in a coordinated fashion along the same plane as fluid motion, working to elongate the renal tubules (Fischer et al., 2006). When ciliary mechanotransduction is impaired, these cells are no longer able to coordinate their division in the direction of fluid flow and begin dividing in a haphazard fashion, resulting in the formation

of cystic structures that continue to enlarge over time and with repeated cell divisions (Luyten et al., 2010).

Deficits in many different ciliary proteins can result in such a phenotype – as one might imagine, any mutation that blocks ciliogenesis has a good chance of eliciting renal cyst formation (Lancaster and Gleeson, 2009; Nishio et al., 2010). Such deficits are often also accompanied by extrarenal disease manifestations, as a properly functioning cilium is critical to many different tissues (Lancaster and Gleeson, 2009). The specific dysfunction of ciliary components essential only to mechanosensation, however, can result in an isolated renal phenotype. Two examples of such components are the polycystic kidney disease proteins Polycystin-1 and Polycystin-2. Deflection of the cilium by fluid flow stresses the ciliary membrane and causes a conformational change in these membrane proteins creating a pore for the influx of calcium ions (Nauli et al., 2003). This is an essential step in the detection of fluid flow and the key underlying deficit in polycystic kidney disease and related disorders.

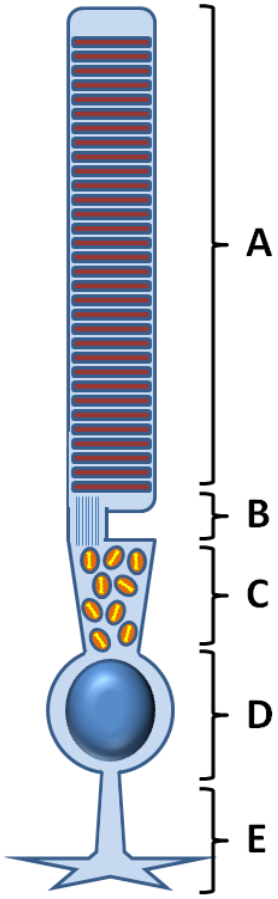

Figure 1.5. Schematic representation of a rod photoreceptor
A. Rod outer segment
B. Connecting cilium
C. Rod inner segment
D. Nucleus
E. Synaptic body

Phototransduction

Just as the renal tubule epithelial cells produce cilia highly specialized for mechanotransduction, the photoreceptor cells of the retina are characterized by a cilium highly specialized for phototransduction. The main function of the photoreceptor is to

transform incident light energy into an electrical impulse to be transmitted to the brain. This is accomplished through a complicated system of photopigments and enzymes, all of which must be strictly compartmentalized for phototransduction to occur (Deretic et al., 1995). The process of phototransduction is also highly energetically demanding. As such, the photoreceptor is a very rigorously structured cell with different compartments dedicated to different activities (Masland, 2001).

The photoreceptor cell can be divided into many different segments (Figure 1.5). The inner segment of the cell serves as the cell's powerhouse. Overflowing with mitochondria, this segment is dedicated to the production of energy to make phototransduction possible (Mustafi et al., 2009). The outer segment of the cell, on the other hand, is dedicated to light capture. Here stacks of membranous disks full of photopigment sit, ready to capture incident photons (Mustafi et al., 2009). These two compartments are separated by a structure known as the connecting cilium. This structure, a derivative of the primary cilium, serves as the only passage from the inner to outer segment (Röhlich, 1975). In fact, the entire outer segment can be thought of as a highly elaborated primary cilium specialized for the process of phototransduction (Louvi and Grove, 2011). As no protein production takes place within the outer segment, all of its many components must transit through the connecting cilium to assume functional positions within the outer segment disks – no small feat when one considers that the entire outer segment is recycled every 10 days (Kevany and Palczewski, 2010). It is precisely because of this high turnover rate and their complete dependence on the connecting cilium and IFT that photoreceptors are so often affected by mutations in ciliary disease genes.

Ciliary dysfunction

As one might suspect having read through the long list of cell types and cellular processes that cilia are so intimately involved in, dysfunction of the primary cilium can lead to a whole host of human diseases. These diseases are collectively known as ciliopathies and the organ systems that they affect and the symptoms that they produce are as varied as the many different genes involved in their pathogenesis.

Below is a discussion of the ciliopathies. I have divided this discussion into two main headings – dysfunction of motile cilia and dysfunction of primary cilia. While the dysfunction of motile cilia is clinically an important topic, the mutations that affect only motile cilia are less relevant to the work presented in this thesis. For this reason I will spend less time discussing this class of diseases.

Dysfunction of the primary cilium, on the other hand, receives much more attention in this chapter. In addition to a general discussion of primary cilium dysfunction I have included individual sections describing the details of many of the specific, diagnosable ciliopathies, such as Joubert syndrome and Meckel-Gruber syndrome. Included at the end of the discussion on primary cilium dysfunction is a section on the emerging evidence for the cilium's involvement in common chronic diseases, such as insulin resistance, type 2 diabetes, and obesity (Berbari et al., 2008b; Girard and Petrovsky, 2011; Guo and Rahmouni, 2011). In explaining how defects in ciliary function result in human disease, I hope to also illustrate some of the basic underlying aspects of ciliary biology.

Motile cilium dysfunction

Disorders of the motile cilia go by many names. A disease triad – situs inversus, chronic sinusitis, and bronchiectasis – was first defined by Kartagener in 1933, giving rise to the term Kartagener's syndrome as a diagnosis for patients suffering from these symptoms (Kartagener, 1933). With the realization that the major deficits in these patients stemmed from an inability of their cilia to beat in an organized fashion, the term Kartagener's syndrome was replaced with either immotile ciliary syndrome (ICS) or primary ciliary dyskinesia (PCD), both referring to the same condition (Afzelius, 1976; Eliasson et al., 1977).

As a ciliopathy, PCD is unique in that ciliogenesis and primary cilium structure are not perturbed – PCD is, instead, purely a disease of the machinery of ciliary motion (Sturgess et al., 1979). Mutations in genes affecting the dynein arms, radial spokes, and central doublet of the motile cilium (Figure 1.1) have all been identified in PCD patients (Bartoloni et al., 2002; Olbrich et al., 2002; Pennarun et al., 1999). While each of these components is critical to the motile cilium, they are each dispensable for primary cilium formation and function.

The symptoms of PCD, then, are not surprising. Issues with mucociliary clearance, the result of dysfunctional motile cilia of the airway epithelia, give rise to chronic sinus infections, pneumonia, rhinitis, and otitis media (Carlén and Stenram, 2005). The same mutations that affect the normal rhythmic beating of motile cilia also affect the motion of the sperm flagellum, resulting in significant infertility in male PCD patients (Carlén and Stenram, 2005). Perhaps most interestingly, situs inversus, or a complete reversal of the normal left-right axis of the body, occurs in 50% of PCD patients. The left-right body axis is defined early in development by the

coordinated beating of cilia in the developing embryo. Without ciliary movement, the layout of the left-right axis is left completely to chance (Carlén and Stenram, 2005).

While not particularly common, with an incidence of no more than 1 in 16,000 (Kuehni et al., 2010), PCD has made for an interesting study in the importance of ciliary motion to mammalian health. It is also a compelling reminder of the fact that sometimes the best studied scientific questions turn out to be of only minimal biologic importance – the motile cilium, which received so much attention in the early days of cell and molecular biology, is involved in only a few mild human diseases. The primary cilium, on the other hand, mostly ignored for more than a century, has proven to be involved in various and devastating human disease syndromes and may even play an important role in the pathogenesis of diseases of great public health concern, such as diabetes and obesity (Berbari et al., 2008b; Girard and Petrovsky, 2011; Guo and Rahmouni, 2011).

Sensory cilium dysfunction

While disorders of ciliary motility result in only relatively few symptoms, disorders of ciliary structure and sensory function can lead to a plethora of human disorders, many of which are still being characterized and many of which are certainly still unknown. The list of ciliopathies is long, and while each syndrome is characterized by a unique set of signs and symptoms there are certain characteristics that all or most of the ciliopathies have in common.

First, and this likely goes without saying, all ciliopathies result from dysfunction of the primary cilium (retinitis pigmentosa, discussed later in this chapter, can be caused by mutations in either

ciliary genes or genes important for the visual cycle. It is considered a ciliopathy only if due to ciliary dysfunction (Adams et al., 2007)).

Second, because each cell type of the body depends on the primary cilium to a different extent, certain organ systems are more commonly affected by ciliary diseases than others. In reviewing the list of ciliopathy disease syndromes bellow, it will become apparent that the retina, kidney, and central nervous system (CNS) appear to be the three organ systems most susceptible to ciliary dysfunction (Waters and Beales, 2011).

Third, and perhaps most interesting, ciliary disease seems to exist on a continuous spectrum (Figure 1.6). The clinical cutoffs that separate the ciliopathies into discrete syndromes are useful

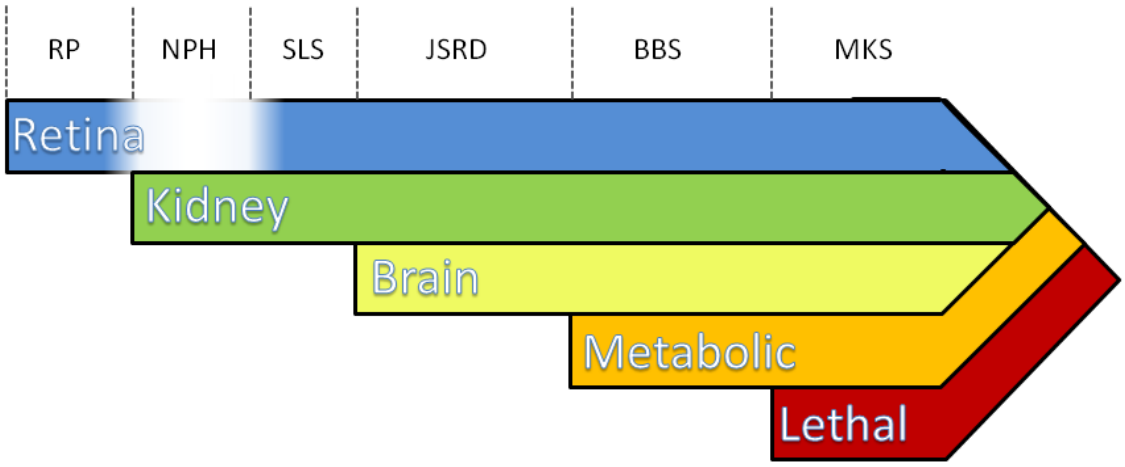

Figure 1.6 The spectrum of ciliopathy disease
The spectrum of affected organ systems and disease symptoms along with the clinical diagnoses applied to patients who fall within each category. RP, retinitis pigmentosa; NPH, nephronophthisis; SLS, Senior Løken syndrome; JSRD, Joubert syndrome and related disorders; MKS, Meckel-Gruber syndrome.

from a diagnostic perspective but can obscure the fact that incremental increases in ciliary dysfunction lead to incremental increases in disease severity with no obvious distinction between different syndromes (van Reeuwijk et al., 2011). This point is hammered home by the fact that different mutations in certain ciliopathy genes, such as CEP290 (Coppieters et al., 2010), can produce phenotypes anywhere along the ciliopathy disease spectrum from isolated retinal degeneration to multi-organ system dysfunction and embryonic lethality. It is clear that ciliary defects do not result in all-or-none ciliopathy disease.

The ciliopathies described below are organized in order of severity, with those diseases affecting only single organ systems described first and with the syndromes affecting multiple organ systems described last. While this list is certainly not exhaustive, it presents a representative

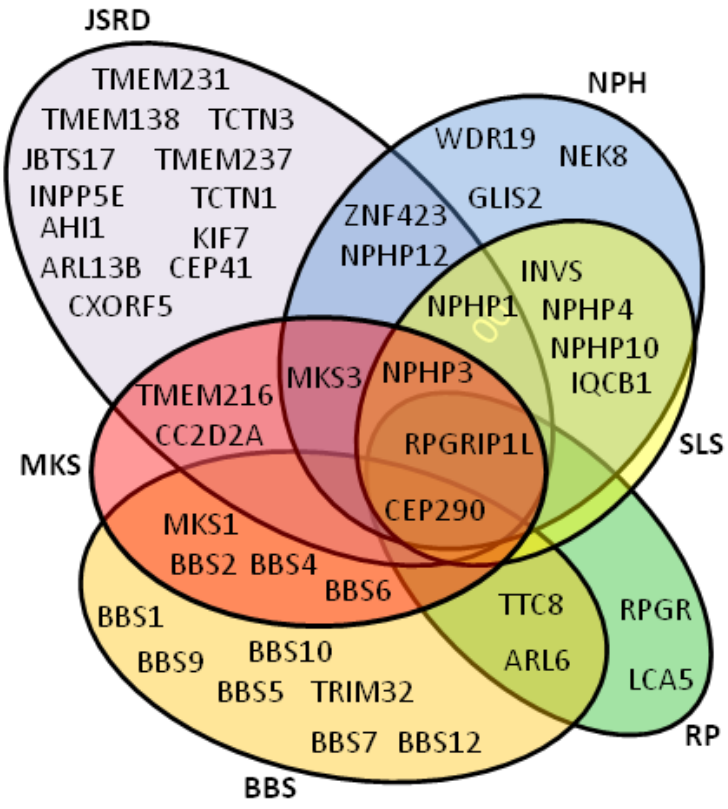

Figure 1.7 Different ciliopathy disease genes cause different overlapping ciliopathy phenotypes
Many ciliopathy disease genes are known causes of multiple clinically distinct ciliopathies. Each ellipse represents a different ciliopathy phenotype. The genes inscribed within each ellipse are known causes of that phenotype. Note that CEP290 has been associated with each of the ciliopathies shown.
NPH, nephronophthisis; SLS, Senior-Loken syndrome; RP. Retinitis pigmentosa; BBS, Bardet Biedl syndrome; MKS, Meckel-Gruber syndrome; JSRD, Joubert syndrome and related disorders

cross-section of ciliary disease and serves to illustrate certain key points regarding the specific pathologic effects of the dysfunction of different ciliary processes. The particular syndromes described were also chosen, in part, because the gene CEP290, the focus of this dissertation, has been implicated in the pathogenesis of each (Figure 1.7; Coppieters et al., 2010).

Nephronophthisis

First described in 1945, nephronophthisis (NPH) is a rare autosomal recessive medullary cystic kidney disease and the most common cause of childhood renal failure (Hildebrandt et al., 2009). Patients typically present with polyuria, polydipsia, secondary eneurisis, and anemia within the first decade of life and progress to end stage renal failure, necessitating dialysis or renal transplant, by the third decade of life. Prevalence is estimated to be about 1 in 1 million in the United States, with the disorder diagnosed in about 1 in 50,000 live births in Canada (Hildebrandt et al., 2009).

The basic pathology of the disease results in the proliferation of multiple renal cysts that ultimately destroy the structure of the kidney. As with polycystic kidney disease (discussed above in the section “fluid flow”), cystic proliferation is due to an inability of the renal epithelial cells to sense the direction of fluid flow within the renal tubules, resulting in uncoordinated cell division and cyst formation instead of renal tubule extension (Fischer et al., 2006). Renal epithelial cells depend on their primary cilia to sense fluid flow and, not surprisingly, mutations in genes involved in ciliary structure and function have been discovered to be at the root of NPH.

To date 14 different genes have been implicated in NPH. They are *NPHP1*, *NPHP2/inversin, NPHP3, NPHP4, NPHP5/IQCB1, NPHP6/CEP290, NPHP7/GLIS2, NPHP8/RPGRIP1L, NPHP9/NEK8, NPHP10/SDCAAG8, NPHP11/TMEM67, NPHP12/TTC21B, NPHP13/WDR19*, and *NPHP14/ZNF423* (Hildebrandt et al., 2009). While the roles than many of these genes play in cilium formation and function remain unclear, it is apparent that they have important jobs in processes as diverse as ciliary structural maintenance, ciliary membrane biogenesis, and ciliary mechanotransduction, implying that deficits in any aspect of primary cilium biology can lead to NPH.

Many of the NPHP disease genes, as will become apparent in the discussion of the other ciliopathies bellow, are also implicated in the ciliary diseases of other organ systems (Figure 1.7). Perhaps not surprisingly, then, more than 10% of NPHP patients are diagnosed with extrarenal disease manifestations such as hepatic fibrosis, CNS malformations, and retinitis pigmentosa (Hildebrandt et al., 2009). Why ciliary dysfunction results only in renal disease in a majority of NPH patients, however, remains unknown.

Retinitis pigmentosa

Retinitis pigmentosa (RP) is a progressive degeneration of the photoreceptors of the retina that can occur either by itself or as a symptom of various syndromic disorders (Ferrari et al., 2011). Unlike all of the other ciliopathies discussed in this thesis, isolated RP is only sometimes the result of the dysfunction of the primary cilium. A number of different mutations affecting cellular processes as diverse as transcription, RNA splicing, and photopigment recycling can all result in RP, and each particular affected gene is associated with a characteristic disease progression and time course (Ferrari et al., 2011). The list of genes associated with non-

syndromic RP is long and rapidly growing, but of the many genes involved only about 10% have been shown to have any role in the function of the primary cilium. Syndromic RP, on the other hand, is almost always caused by mutations in genes affecting ciliary integrity. Mutations in these genes result in photoreceptor degeneration secondary to ciliary dysfunction.

RP affects about 1 in 5,000 people around the world. Of these patients, roughly 20% present with symptoms characteristic of syndromic disorders such as Usher syndrome, Joubert syndrome, and Bardet Biedl syndrome (Ferrari et al., 2011). The pace of retinal degeneration varies with the causative gene – in the most severe cases, retinal degeneration begins before birth and leads to complete blindness within the first two decades of life in a form of congenital RP known as Leber congenital amaurosis (LCA) (Chung and Traboulsi, 2009). Although a distinction is sometimes made between LCA and RP, they are both characterized by very similar signs, symptoms, and clinical time courses, only with different ages of onset.

Regardless of etiology, most RP and LCA patients experience, at some point in the disease process, night blindness, and tunnel vision, and will be found to have retinal atrophy with bone spicule-shaped pigment deposits upon ophthalmoscopy – findings that originally gave RP its name (Chung and Traboulsi, 2009; Ferrari et al., 2011). The disease normally begins with the degeneration of rod photoreceptors within the periphery of the retina. As the disease progresses the retina begins to atrophy from the periphery towards the macula, the area of central vision, until patients are left with only a very narrow cone photoreceptor-dominated visual field. In the end stages of retinal degeneration cone photoreceptors, for reasons that are

not entirely clear, also begin to degenerate, resulting, in some cases, in complete blindness (Chung and Traboulsi, 2009; Ferrari et al., 2011).

The fact that RP can be a symptom of so many different ciliopathies only reinforces the idea that the retina is one of the tissues most susceptible to ciliary dysfunction. This is not altogether surprising since the photoreceptors of the retina are probably the cells in the body most dependent on their cilia for normal function (see the section “phototransduction”, above). It is not difficult to imagine why even small deficits in ciliary function might cause devastating changes in normal photoreceptor function and health.

Senior Løken syndrome

The kidneys and retina being the organs most susceptible to ciliary dysfunction, it is not surprising that pathology of both organ systems can be seen together in a syndrome known as Senior Løken Syndrome (SLS). SLS is diagnosed upon the discovery of nephronophthisis in a patient presenting with Leber congenital amaurosis (Ronquillo et al., 2012). In fact, this is often the way the diagnosis is made – patients or parents notice the retinal deficits first and the renal dysfunction is discovered by a suspicious clinician, aware of the possibility of the two symptoms occurring together, during a renal workup. The natural history and pathophysiology of each of the two aspects of the syndrome (i.e. the retinal and renal degeneration) are identical to the pathophysiology and disease course of LCA and NPH (Ronquillo et al., 2012). Put another way, SLS can truly be thought of as a combined diagnosis of LCA and NPH.

SLS is a rare disease, affecting fewer than 1 in 1 million people, and only very few families with the disease have been described (Ronquillo et al., 2012). To date 6 SLS genes have been identified – NPHP1, NPHP3, NPHP4, NPHP5/IQCB1, NPHP6/CEP290, and NPHP10/SDCAAG8 (Ronquillo et al., 2012). As is apparent from their names, all of the genes responsible for SLS are also associated with other ciliopathies. In fact, all known SLS genes can also cause NPH and all of them are also capable of causing RP, either by itself or in the context of some other ciliopathy syndrome.

Joubert syndrome

The syndrome that we now know as Joubert syndrome (JS) was first described in 1969 by Marie Joubert upon the discovery that the severe ataxia and hyperpnea displayed by four siblings she had been evaluating was due to congenital agenesis of the cerebellar vermis (Brancati et al., 2010). This deficit is the cardinal symptom of Joubert syndrome and is most often detected in imaging studies of the brain where it presents as the "molar tooth sign," an abnormality of the brain stem in transverse section that bears an uncanny resemblance to a molar tooth. JS is diagnosed in about 1 in 90,000 live births, although it is thought that this number is artificially low due to underdiagnosis (Brancati et al., 2010).

Infants with JS most often present, not unlike the siblings studied by Dr. Joubert, with hypotonia, episodic hyperpnea, and abnormal eye movements, all of which are due to the dysfunction of the cerebellum. The hypotonia progresses to ataxia as the patient ages while the hyperpnea tends to improve over time, with resolution generally by six months of age (Brancati et al., 2010). Many JS patients also present with mild to moderate developmental delay,

particularly with regard to language and motor skills, are more prone to seizures, and sometimes present with occipital encephalocele, signs and symptoms thought to be due to the highly irregular structure of the JS brain (Brancati et al., 2010). Most JS patients, however, are capable of attending school, learning specific job skills, and can work in protected environments. It must be noted that developmental delay is not universal and some, although few, JS patients appear completely cognitively normal.

To date, every gene that has been linked to JS (there are already more than 20) has been shown to be critical in primary cilium structure and function. It is thought that these mutations lead to deficiencies in ciliary structure that result in significant deficits in ciliary Hedgehog signaling (see the section “Hedgehog signaling,” above; Brancati et al., 2010). The impairment, in JS patients, of Hedgehog signaling, so critical for neural crest formation, neurodevelopment, and embryonic patterning, results in the various CNS symptoms characteristic of the disease (Aguilar et al., 2012).

A substantial percent of JS patients present with symptoms outside of the CNS. The organ systems that can be affected are many, but the two most commonly hit, not surprisingly, are the retina and kidneys. The same mutations that adversely affect ciliary structure and hedgehog signaling in the CNS are thought to result in deficiencies in the ciliary structure of the photoreceptors and renal epithelial cells, leading to significant pathology in these tissues. Approximately 25% of all JS patients are found to display signs of NPH, with cystic renal degeneration and end stage renal failure early in life (Brancati et al., 2010). Another substantial portion of JS patients present with RP or LCA. In fact, numerous JS patients have been identified

that suffer from SLS, with both retinal and renal degeneration in addition to their cerebellar deficits, truly illustrating how much overlap exists between the different ciliopathies and making even more apparent the continuous spectrum of ciliopathy disease (Brancati et al., 2010).

Because the clinical features of JS are so broad it has become common practice to refer to all patients presenting with agenesis of the cerebellar vermis, regardless of what other symptoms they may manifest, as having one of the Joubert syndrome related disorders (JSRD). The syndromes formally known as cerebello-oculo-renal syndrome, Dekaban-Arima syndrome, COACH syndrome, Varadi-Papp syndrome, and Malta syndrome are now all considered to fall under the JSRD umbrella (Brancati et al., 2010).

Bardet Biedl syndrome

While Joubert syndrome is the result of mild hedgehog signaling impairment, Bardet Biedl syndrome (BBS) is a study in the complete dysfunction of ciliary signaling. The syndrome we know as Bardet Biedl syndrome was first described in 1865 (a full thirty years before the discovery of the primary cilium) as the manifestation of three symptoms: obesity, retinal degeneration, and cognitive deficits (Tobin and Beales, 2007). In the 1920s George Bardet and Artur Biedl independently expanded on this triad, adding polydactyly and hypogonadism to the list of symptoms characteristic of the syndrome that would ultimately bear their names. These five signs and symptoms remain the cardinal features of the syndrome to this day (Tobin and Beales, 2007).

BBS affects roughly 1 in 150,000 Americans and is up to ten times more prevalent in some particular populations in Canada and Kuwait. Not every patient diagnosed with BBS manifests all five of the cardinal symptoms, and the list of BBS associated symptoms is much longer than the cardinal five. Of the cardinal symptoms, 98% of patients present with hypogonadism, 93% with retinal degeneration, 72% with obesity, 69% with polydactyly, and 50% with developmental delays (Tobin and Beales, 2007). Patients diagnosed with BBS also often present with anosmia (60% of patients), speech delay (54%), ataxia (40%), renal anomalies (24%), hearing loss (20%), and diabetes (6%) (Tobin and Beales, 2007).

It is immediately clear that the symptoms of BBS significantly overlap with those of JSRD. What is not readily apparent is that the genes that cause BBS are never responsible for JSRD, and vice versa (Figure 1.7) (with the exception of *CEP290*, and even then only one BBS patient has ever been found to harbor mutations in the *CEP290* gene). All of the 16 identified BBS disease genes (Figure 1.7) are critical to ciliary function, but in ways different from the genes that are responsible for JSRD. Recent scholarship has indicated that most of the genes responsible for BBS cooperate to form a subcellular complex known as the BBSome (Jin et al., 2010). This complex has critical functions in the ciliary transport of membrane proteins such as the Shh receptor/effector proteins Patched and Smoothened. Hence, the major deficits of BBS are primarily due not to deficits in ciliary structural integrity, as is the case with many of the NPH and RP genes, but to deficits in ciliary signaling by transmembrane receptor proteins. Deficits in ciliary leptin signaling within the hypothalamus of BBS patients lead to uncontrollable eating and obesity (Guo and Rahmouni, 2011); abnormalities in the insulin signaling pathway lead to diabetes (Marion et al., 2012); deficits in Shh signaling during development result in polydactyly,

CNS abnormalities, and developmental delays (Zhang et al., 2012). The renal, retinal, and olfactory phenotypes of BBS, on the other hand, are likely secondary to defects in ciliary structure due to inadequate trafficking of structural ciliary membrane proteins due to BBSome dysfunction.

Thus it becomes clear that defects of the cilium can be divided into two broad, phenotypically distinct categories – those that disrupt ciliary receptor trafficking and those that disrupt ciliary structure and IFT. Organs, such as the kidney and retina that depend heavily on the structural integrity of the cilium are more severely affected by deficits in ciliary structure, while organ systems that depend more on ciliary signaling, such as the developing brain, skeletal system, and endocrine system, are more severely affected by deficits in ciliary receptor trafficking.

Meckel-Gruber syndrome

We have so far examined ciliopathies that can be traced back to deficits predominantly in either ciliary structure (RP, LCA, NPH) or ciliary signaling (JSRD, BBS). There do exist, however, human mutations that result in significant deficits in *both* ciliary structure and function, and these almost invariably result in the perinatal lethal condition known as Meckel-Gruber syndrome (MKS). MKS, with an incidence estimated to be somewhere between 1 in 9,000 and 1 in 140,000, depending on the population, was first reported by the German anatomist Friedrich Meckel in 1822 (Chen, 2007). Meckel described a case of two siblings, both of whom died shortly after birth, presenting with severe occipital meningoencephalocele, polycystic kidneys that filled the abdomen, polydactyly, and cleft palette. Similar cases continued to be reported in

the medical literature until Opitz and Howe, in 1969, definitively delineated the clinical features of the syndrome that they named for its discoverer (Chen, 2007).

The cardinal symptoms of MKS are severely dysplastic kidneys, growing to between 10 and 20 times their normal size (present in 95% of patients), occipital encephalocele (60-85%), and postaxial polydactyly (55-96%) (Chen, 2007). MKS patients are also often diagnosed with microcephaly, cerebral and cerebellar hypoplasia, anencephaly, microphthalmia, hepatic fibrosis, cryptorchidism, and shortened limbs (Chen, 2007). Thus, it is apparent that MKS combines the worst features of NPH, BBS and JSRD into one devastating syndrome. It is not surprising, then, that every one of the 10 genes (Figure 1.7) that is known to cause MKS is also capable of causing NPH, JSRD or BBS.

The dysfunction of the primary cilium seen in MKS is likely due to severe deficits that cause catastrophic changes in both ciliary trafficking and structure. It is easy to image how extreme deficiencies in either ciliary structure or trafficking could easily result in deficiencies in the other – without trafficking of ciliary components to the basal body and into the cilium, no axoneme can be extended; without a structurally sound axoneme and ciliary compartment, properly trafficked ciliary proteins have no organelle to populate. MKS, then, can be thought of as the result of complete dysfunction of the cilium, due to debilitating mutations in proteins that play key roles in either ciliary structure or trafficking. The structural deficits in the cilium lead to renal and retinal disease while deficits in Shh and Wnt signaling (Aguilar et al., 2012), secondary to disrupted ciliary trafficking, lead to the dramatic malformations of the brain and limbs

characteristic of MKS. The lethal nature of the syndrome serves to illustrate exactly how important the cilium is to human health and development.

Non-syndromic disorders of the primary cilium

Up until now we have focused on syndromic, clearly heritable disorders of the primary cilium, but recent evidence has also begun to implicate the cilium in the pathogenesis of many much more common diseases. Renal failure, diabetes, obesity, neurologic deficits, and retinal degeneration, all characteristics of multiple ciliopathy disease syndromes, are also aspects of what we consider the common pathology of aging and chronic disease. In the past few years the role of the cilium in the pathogenesis of each of these chronic conditions has begun to be investigated.

The cilium's role in the pathogenesis of obesity in particular has become a significant area of research in the scientific community. Multiple lines of data have implicated ciliary deficits in the hypothalamus as resulting in hyperphagia and increased appetite (Feuillan et al., 2011; Guo and Rahmouni, 2011), and an equal number of studies have also indicated that ciliary signaling plays a critical role in the differentiation and growth of adipocytes (Marion et al., 2009; Romano et al., 2008; Zhu et al., 2009). Insulin sensitivity also appears to be highly regulated by receptors confined to the primary cilium (Hearn et al., 2005; Iwanaga et al., 2011; Romano et al., 2008), an important finding when one considers the huge number of Americans suffering the consequences of insulin resistance and diabetes.

While the relationship of the primary cilium to these common chronic disease is still tenuous, it is tantalizing to think that this organelle might be the key link between so many of the ailments that currently burden our healthcare system. Perhaps a better understanding of this overlooked organelle will help us continue to make strides against these diseases and pave the way for new therapeutics, better patient outcomes, and improved public health.

CEP290

With the conclusion of that wide-ranging discussion of ciliary structure, function, and disease, we can now finally turn to the true subject of this dissertation, centrosomal protein 290 kDa, or CEP290. CEP290 is a key component of the primary cilium and a central player in ciliogenesis and ciliopathy pathogenesis. It has been shown to be critical to the processes of IFT, ciliary signaling, and in the maintenance of ciliary structure (Coppieters et al., 2010). It is the only gene capable of causing NPH, LCA, JSRD, BBS, and MKS, and mutations in the *CEP290* gene are thought to be the most common cause of LCA in North America and Europe (den Hollander et al., 2006). For a protein clearly so important to human disease and ciliary biology we know surprisingly little about what it does and about how mutations in the *CEP290* gene can lead to human disease. Below is an in-depth discussion of all the CEP290 biology that was known up until the point of publication of the work presented in this thesis.

A history of CEP290

The story of the gene that we know today as *CEP290* begins in a human brain cDNA library from Japan. *CEP290* had been completely unknown to the scientific community until the late 1990s when a group of researchers at the Kazusa DNA Research Institute, interested in identifying novel brain-related mRNAs, cloned and described 100 new transcripts of unknown significance. One of these transcripts happened to be *CEP290* (Nagase et al., 1997). They named the *CEP290* transcript they had identified *KIAA0373*, published its sequence, and moved on to other experiments.

Just three years after its discovery in the human brain, another group of researchers independently identified a fragment of the CEP290 protein as the major antigen of the 3H11 antibody (Chen and Shou, 2001), a monoclonal antibody specific for cancerous cells of many different lineages (Shou et al., 1997). Unaware of the *KIAA0373* transcript, they named this protein 3H11Ag and began to characterize its function in the cell. It was noted that the 3H11Ag tumor antigen localized to both the cytoplasm and nucleus, and that its nuclear localization was conferred by the N-terminal region of the protein (Guo et al., 2004). Despite the compelling nature of this study, 3H11Ag's role within the nucleus and in cancer pathogenesis was never actively pursued, and the protein was again shelved, awaiting its third and final renaming.

In 2003 CEP290 was again independently discovered, this time by a group of researchers examining the protein makeup of the centrosome. In one of the first attempts to better define the protein milieu of the organelle, this group subjected purified centrosomal material to analysis by mass spectroscopy in the hopes of discovering novel centrosomal components. Of the many proteins they identified, one of the more common hits was KIAA0373/3H11Ag (Andersen et al., 2003). Following the conventions of the time they renamed this protein centrosomal protein of 290kDa, referencing both its subcellular localization and molecular weight and giving rise to the definitive CEP290 gene name and symbol.

With the discovery that CEP290 was a protein closely associated with the centrosome/basal body, it wasn't long before the gene was discovered to be involved in ciliopathy disease. Interestingly, the discovery that mutations in *CEP290* could result in significant pathology was observed, for the first time, not in a human patient, but in a naturally occurring mouse model of

CEP290 deficiency. In a collaboration between researchers at Jackson Labs and the University of Michigan the genetic deficit responsible for the rapid retinal degeneration of the rd16 mouse was finally identified as a large deletion within the *Cep290* gene (Chang et al., 2006). The mouse mutation was found to result in perturbations of the connecting cilium of the rod photoreceptors causing deficiencies in the ciliary trafficking of proteins critical for phototransduction. This discovery opened the floodgates for research into *CEP290*'s role in human disease – *CEP290* was soon discovered to be the causative gene in a number of cases of Joubert syndrome (Valente et al., 2006) , then Leber congenital amaurosis (den Hollander et al., 2006), and finally even Meckel syndrome (Baala et al., 2007).

Reports of new *CEP290* patients and new *CEP290* disease syndromes continued to pour in, but still no one had any idea of exactly what the protein was doing at the primary cilium or how deficits in protein function might lead to human disease. Hints would occasionally appear – CEP290 seemed important in the regulation of ciliogenesis (Tsang et al., 2008) and appeared to be a component of the numerous protein complexes at the transition zone of the cilium (Gorden et al., 2008; Kim et al., 2008), but it wasn't until Craige et al. published their work on CEP290 in the *Chlamydomonas* model system that CEP290's role in the cell finally began to come into focus.

In an elegant structural study of the flagellum of *Chlamydomonas reinhardtii*, Craige et al. (2010) demonstrated that CEP290 was a critical structural component of the ciliary Y-links. Their data indicated that CEP290 was instrumental in maintaining the physical integrity of these links between the ciliary membrane and microtubule axoneme, and that in the absence of CEP290

these structures were significantly compromised, resulting in the dysregulation of the protein milieu of the ciliary compartment. This was the first direct evidence of the mechanistic underpinnings of CEP290's critical role both in ciliary structure and IFT. In the years since the publication of this work numerous other studies have emerged identifying novel CEP290 interacting partners but no other major insights have been gained into CEP290's function.

CEP290 Structure

CEP290 is a behemoth of a protein, weighing in at 290 kilodaltons, as its name suggests. It is encoded by a 93 kilobase gene on human chromosome 12 containing a roughly 8 kilobase open reading frame composed of 54 exons (Coppieters et al., 2010). From the time of its initial discovery researchers have employed all the bioinformatic tools available to them in an attempt to gain some insight into the structure and function of the gene, searching for predicted structural domains, known protein motifs, and regions of homology to other proteins (Figure 1.9). While this line of investigation has not led to any major discoveries, it has uncovered a number of interesting facts about the gene, some of which may ultimately aid in the identification of domains critical to the protein's function and help complete our understanding of the protein's role in the cell.

Predicted structure

To date no crystal structure has been solved for any piece of the CEP290 protein. What we have to work with, instead, are predicted structural motifs. It is abundantly clear from any number of bioinformatic tools that CEP290 lacks both a signal peptide and any kind of canonical transmembrane domain. This squarely localizes CEP290 to the "regular" pool of non-membrane,

non-luminal proteins that make up about 60% of the protein content of the cell. There is not much else that can be gleaned from bioinformatic structural analysis of the CEP290 amino acid sequence except this: nearly the entire protein is predicted to fold into a coiled coil (Figure 1.8).

Coiled coils are a common motif in biology, utilized by nature to perform many varied processes such as transcriptional regulation, vesicular fusion, and intracellular signaling (Chapman et al., 1994; Chen et al., 1995; Zhang et al., 2000). Regardless of the cellular pathways they are involved in, the mechanism by which coiled-coil domains accomplish their diverse tasks is the same – two or more alpha helices wrap around each other to form a thermodynamically favorable and structurally stable coil (Mason and Arndt, 2004). This bundling action can be used to mediate hetero- or homodimerization and is occasionally employed to achieve intramolecular interactions within a single protein (Hammond et al., 2010). Coiled coil domains aren't only used for mediating protein-protein interactions, however. The motif can also be employed in

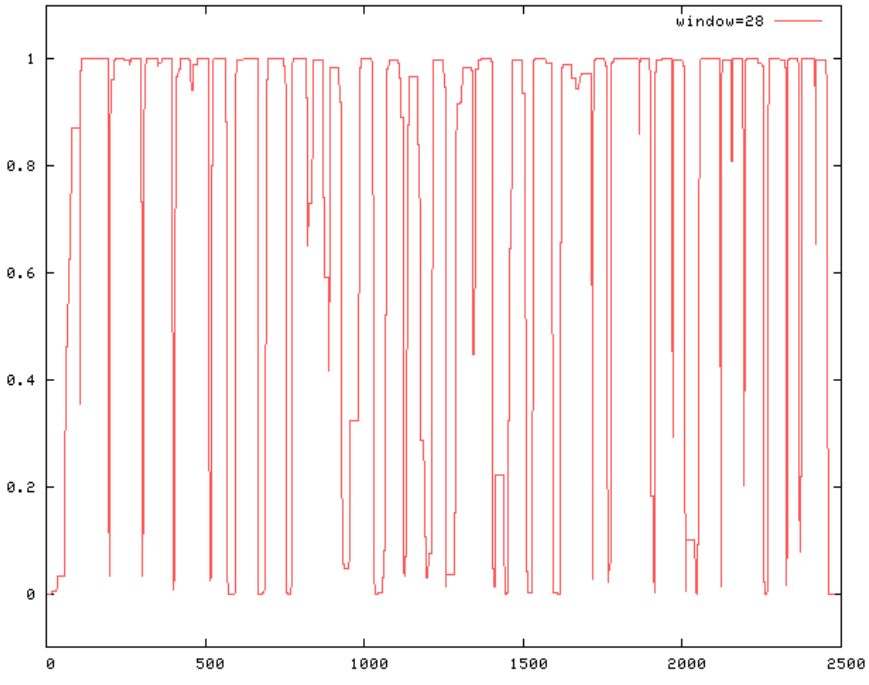

Figure 1.8. More than 80% of CEP290 is predicted to form coiled coils.
The x-axis represents the position along CEP290's amino acid sequence and the y-axis represents the probability that the amino acid sequence analyzed will form a coiled coil. Nearly all of CEP290 is predicted to fold into coiled coils.

Adapted from http://embnet.vital-it.ch/software/COILS_form.html

the creation of rigid, spring-loaded, structurally-stable domains as is the case with the myosin tail (Schwaiger et al., 2002). It is intriguing that CEP290 is, at its most basic structural level, a large coiled coil, but only time and continued research will tell exactly what these coils are doing.

Predicted domains

While the bioinformatic prediction of structural domains within the CEP290 protein yields only few results, the list of predicted functional domains, protein motifs, and regions of homology is long. I have opted not to go through each in detail, especially as most have not been experimentally verified or investigated, but to instead list each of the identified domains, taking time to discuss only those that seem relevant to CEP290 protein function. Let us then begin by discussing regions of homology between CEP290 and other proteins.

Portions of the CEP290 amino acid sequence have been discovered to share significant homology with tropomyosin, structural maintenance of chromosomes (SMC) proteins, and the tail domain of the myosin class of microtubule motors (Chang et al., 2006). These different regions are distributed throughout the protein – the three tropomyosin homology domains are found within CEP290's N-terminus, the SMC homology domain is found near the center of the CEP290 protein, and the myosin tail homology domain comprises most of the C-terminus of the protein. To date no significant function has been ascribed to any of these domains within CEP290, but it is fun to speculate as to what they may be doing. In particular, it is interesting to note that of the 5 homology domains identified 4 are related to proteins involved in generating and maintaining the microtubule organization of the cell. As the cilium is so integrally associated

with the microtubule network, it stands to reason that these domains might allow CEP29 to interact with or modulate the microtubules of the cilium.

The SMC homology domain at first seems a little more perplexing. The SMC proteins are involved in the regulation of mitosis, binding directly to the DNA sequences of different chromosomes during cell division (Carter and Sjögren, 2012). While there is some evidence for CEP290 localization to the nucleus, trying to imagine what a known ciliary protein might be doing binding to DNA is difficult. Consideration of the structure of the SMC proteins, however, provides a hint to the role that the SMC-homology domain might be playing in CEP290 function. The SMCs are composed of two coiled coil arms on either side of a molecular hinge (Melby et al., 1998). The SMC protein's hinge and arms can be selectively swung open or closed (the exact mechanism of how this happens has not yet been completely worked out) to bind to and gather the cell's chromosomes. Perhaps the mechanism of SMC action, but not its teliologic purpose, is conserved in CEP290. The SMC homology domain would then provide a molecular hinge for CEP290, the function of which might be useful in ciliogenesis, the maintenance of ciliary structure, or the regulation of IFT.

In addition to homology domains, CEP290 is predicted to contain a number of known short protein motifs. These include protein kinase inducible domains, ATP/GTP-binding motifs, at least one bipartite nuclear localization signal, and multiple sites predicted to be prime targets for N-glycosylation, tyrosine sulfation, phosphorylation, N-myristoylation, and amidation (Coppieters et al., 2010). It is unclear what any of these motifs may be doing, let alone whether they are true

sites or just artifacts of the prediction algorithms used to detect them. What is clear, however, is that much work remains before we can hope to fully elucidate CEP290's structure and function.

CEP290 Localization

A number of papers have investigated the subcellular localization of CEP290 to varying degrees of specificity and with varying results. The first such paper, published when the gene was still known as 3H11Ag, found that the CEP290 protein localizes to both the cytoplasm and nucleus with the nuclear localization of the protein conferred by a region within its N-terminus (Guo et al., 2004). These findings were later corroborated by Sayer et al. (2006) when they discovered that CEP290 is capable of physically interacting with and activating the transcription factor ATF4. Sayer et al. never explicitly showed that CEP290 was capable of gaining access to the nuclear compartment, but claimed to have evidence for this in unpublished data.

Sayer et al.'s examination of CEP290 localization didn't stop at the nucleus, however. They went on to investigate the localization of the protein during various phases of the cell cycle and found that throughout all of interphase CEP290 clearly localizes to the centrioles. During mitosis, however, the protein appeared to localize more diffusely throughout the cytoplasm until eventually returning to the centrioles upon the completion of cell division. This is in contrast to a study, published at about the same time, that found CEP290 to consistently localize to the centrioles throughout all stages of mitosis (Chang et al., 2006).

No other groups have since investigated the nuclear localization of CEP290, but a number have gone on to more specifically define the localization of CEP290 at the centrioles. Chang et al.

(2006), for instance, provided conclusive proof of CEP290 localization not only to the centrioles but specifically to the primary cilia of cultured cells and to the connecting cilia of mouse photoreceptors. This finding was corroborated by a number of groups, many of whom more finely localized CEP290 to the basal body/transition zone of the cilium (Gorden et al., 2008; Kim et al., 2008).

The definitive study of CEP290 localization, however, was performed by Craige et al. in the *Chlamydomonas* model system (Craige et al., 2010). In a number of elegant ultrastructural studies Craige et al. conclusively demonstrated that CEP290 localizes to the transition zone of the cilium. In particular, they demonstrated that CEP290 localizes to the ciliary Y-links, the structures that link the microtubule axoneme to the ciliary membrane. Using antibodies raised against different regions of the protein they were able to show that the middle portion of CEP290 seems to localize specifically to the ciliary membrane whereas the C-terminal end of CEP290 was found to be more generally localized within the transition zone with perhaps a small preference for the ciliary axoneme. Of course the major caveat of this work is that it was performed in the *Chlamydomonas* model system, but the high degree of similarity between human and *Chlamydomonas* CEP290 and the highly conserved structure of the cilium across all species would seem to indicate that Craige et al.'s findings should apply more generally to all ciliated organisms.

CEP290 interacting partners

While we are limited in our knowledge of CEP290 structure, function, and localization, an abundance of studies have investigated and identified numerous CEP290 interacting partners.

The number of proteins that associate with CEP290, either directly or indirectly, is already more than a dozen and the number continues to grow by the month. The proteins identified vary in function from transcriptional regulation to membrane trafficking and centriolar structure stabilization. Below are listed each of CEP290's known interacting partners along with a brief description of each protein's function (if one is known) and the nature of the interaction with CEP290.

ATF4

ATF4 is a well characterized transcription factor important in modulating the cell stress response (Ye and Koumenis, 2009). Although ATF4 was one of the first CEP290-interacting proteins identified, the importance of the ATF4-CEP290 interaction has not been extensively researched. In 2006 Sayer et al. presented data showing that CEP290 is capable of binding to and activating ATF4, but how this interaction fits into CEP290's greater role in the cell remains completely unknown. Sayer and colleagues demonstrated, both by yeast two-hybrid and coimmunoprecipitation, that the C-terminus of CEP290 is the region of the protein responsible for ATF4 binding and activation and that knockdown of CEP290 results in decreased baseline ATF4 activity. In the 7 years since the publication of these findings no headway has been made in the characterization of CEP290's role in activating ATF4 or its role in the nucleus in general. The presence of multiple bipartite nuclear localization signals within CEP290 make it seem at least feasible that the protein plays an important and potentially completely overlooked role in the nucleus of the cell and it will be interesting to see if and how this story pans out in the coming years.

CC2D2A and NPHP5

It is not surprising that a rigorously structured organelle such as the cilium should be dependent on multiple structural subunits for its assembly. CC2D2A and NPHP5 (IQCB1) both appear to be such structural subunits and each has been shown to interact with CEP290 (Gorden et al., 2008; Schäfer et al., 2008). Why these proteins interact with CEP290 and what these interactions accomplish is not yet known, but understanding how they interact and what happens when these interactions are disrupted may help to provide some insight into CEP290's role in cilium function.

CC2D2A is a protein, like CEP290, composed of numerous coiled coils (Noor et al., 2008). The interaction between CC2D2A and CEP290 has been characterized on many levels – the proteins have been shown to colocalize by confocal microscopy and to directly interact with each other both by yeast two hybrid and in vitro pull down assays (Gorden et al., 2008). It was determined that the domain of CEP290 responsible for this interaction was a region of the protein from amino acids 703-1103. The two proteins were found to interact functionally as well – in zebrafish morpholino experiments knockdown of both proteins was demonstrated to result in a more severe phenotype than would be expected from the additive knockdown of either separately (Gorden et al., 2008).

In many ways the story of NPHP5 is very much like the story of CC2D2A. Like CC2D2A, NPHP5 is a protein composed of a number of coiled coils (Otto et al., 2005) that has been shown to colocalize and coimmunoprecipitate with CEP290 (Schäfer et al., 2008). Like CC2D2A, there is a functional interaction between NPHP5 and CEP290, with knockdown of both synergistically

resulting in a phenotype more severe than would be expected from knockdown of either together (Schäfer et al., 2008).

The ciliary transition zone, the region of the cilium where CC2D2A, NPHP5, and CEP290 are found, is characterized by a dense web of proteinaceous material that serves as a diffusion barrier and ciliary pore (Kee et al., 2012). It is probably not a coincidence that each of these three proteins contains numerous coiled coil domains, motifs often utilized for maintaining structural integrity and strong protein-protein interactions. It is likely that both NPHP5 and CC2D2A cooperate with CEP290 to play important, non-redundant (as evidenced by the phenotypic synergism displayed in zebrafish knockdown experiments) roles in the organization and structure of the transition zone, perhaps serving as key structural components of the ciliary pore and diffusion barrier. It is not surprising, then, that human mutations in both CC2D2A and NPHP5 result in severe human disease (Gorden et al., 2008; Stone et al., 2011). As we continue to learn more about the nature of these proteins and their interactions with CEP290 we may also begin to learn more about the organization and function of the ciliary transition zone.

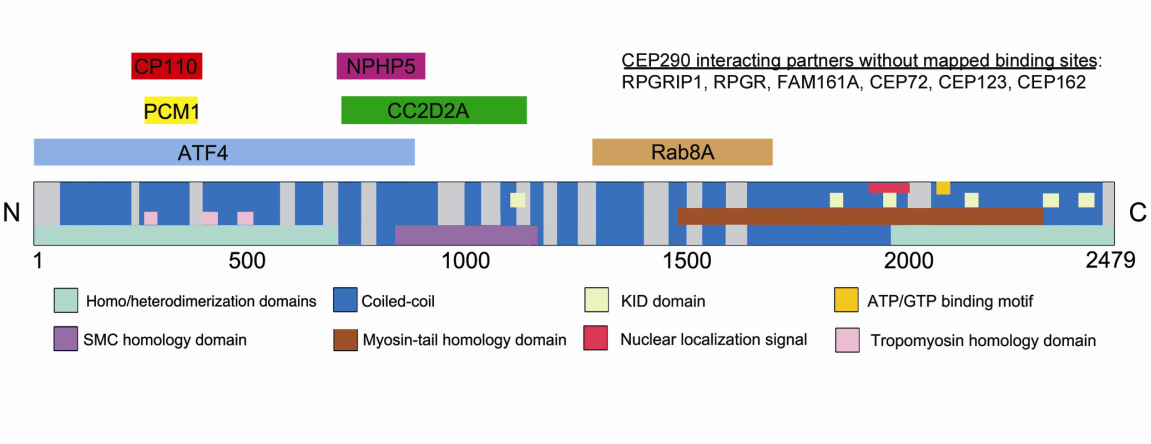

Figure 1.9 Schematic representation of CEP290 homology domains, protein motifs, and interacting partners

RPGRIP1, RPGR, and Rab8a

While RPGRIP1 (RPGR interacting protein 1), RPGR, and Rab8a have all been independently described as interacting partners of CEP290 (Chang et al., 2006; Kim et al., 2008), it is almost certain that they exist as a single complex, collectively recruited to the primary cilium by CEP290. Once properly localized to the ciliary transition zone these proteins can affect their end goal of regulating ciliogenesis and ciliary membrane transport, processes critical to basic ciliary biology and human health (Doherty et al., 2010; Zhao et al., 2003).

Even in the first description of CEP290's involvement in the primary cilium it was noted that the protein exists in a complex with RPGRIP1 and RPGR (Chang et al., 2006). RPGR, in turn, has been shown to directly bind Rab8a – in fact RPGR is critical in the recruitment of Rab8a to the ciliary membrane (Murga-Zamalloa et al., 2010). A more recent study suggests that CEP290 amino acids 1280-1695 serve to recruit Rab8a to the cilium, but no direct interaction between CEP290 and Rab8a was described (Tsang et al., 2008). Regardless, it was noted early on that knockdown of CEP290 results in the drastic mislocalization of RPGRIP1, RPGR, and Rab8a, implying that CEP290 is critical in the ciliary recruitment of each of these proteins.

Taken together these data point towards a model where CEP290, localized to the transition zone of the cilium, binds to and recruits RPGRIP and RPGR. RPGR, in turn, binds to and recruits Rab8a to the ciliary membrane. The ultimate recruitment of Rab8a to the cilium may, in fact, be one of the most important functions of CEP290 – Rab8a is an absolutely critical component of the membrane trafficking machinery of the cell, responsible for the targeting of vesicles from the trans-Golgi network to the cilium and other membranous organelles (Sato et al., 2007). In fact,

ciliogenesis and ciliary function are completely reliant on the delivery of membrane and membrane proteins to the nascent cilium, a process which is regulated by and dependent on Rab8a (Tsang et al., 2008).

FAM161A

FAM161A is one of the newest players in the field of retinal degeneration with the recent discovery that mutations in the *FAM161A* gene can lead to inherited retinitis pigmentosa (Langmann et al., 2010). Even newer, however, is the discovery that FAM161A interacts with a number of ciliary transition zone/basal body components including CEP290 (Di Gioia et al., 2012). The C-terminus of FAM161A was shown to bind directly to CEP290 in both yeast two-hybrid and coimmunoprecipitation experiments, but exactly what this interaction accomplishes remains unknown (Di Gioia et al., 2012). In fact, not much is known about FAM161a in general. In addition to interacting with a number of ciliary disease proteins, FAM161A protein has been shown to localize to the ciliary transition zone where it binds to microtubules, helping to mediate their acetylation (Zach et al., 2012). The large number of high-profile interacting partners that bind to FAM161A hints that the protein may be playing a central role in ciliary biology, but more research is clearly needed to fully understand exactly what it is doing as a component of the ciliary transition zone.

CEP72, CEP123, CEP162, PCM-1

The relationships between these four proteins and CEP290 are probably the most tenuous of those discussed in this chapter. Each of these proteins localizes to the centrosome/basal body and seems to play an important role in the recruitment of ciliary proteins in the initiation of

ciliogenesis (Sillibourne et al., 2013; Stowe et al., 2012; Wang et al., 2013). Each of these proteins has also been shown to associate with CEP290 in coimmunoprecipitation experiments, but whether these associations are indicative of direct or indirect interactions remains to be seen (Kim et al., 2008; Sillibourne et al., 2013; Stowe et al., 2012; Wang et al., 2013). That is not to say that these proteins should be written off as peripheral to the processes of ciliogenesis and ciliary function – in fact each has proven critical to both – but only that whatever interactions they exhibit with CEP290 have not yet been convincingly shown to be critically relevant to CEP290's role in the cilium.

What is known is that CEP162, in particular, appears to be able to mediate the spindle pole microtubule and centriolar satellite localization of CEP290 (Wang et al., 2013). Knockdown of CEP162 results in decreased CEP290 localization to both these areas, although the phenotype was not necessarily clear-cut – for instance, it is difficult to say how much, if any, CEP290 localized to spindle pole microtubules even before CEP162 knockdown (Wang et al., 2013). PCM-1 was similarly shown to be necessary for CEP290 localization to the centriolar satellites, although CEP290 localization to the transition zone of the cilium was not affected by PCM-1 knockdown (Kim et al., 2008). CEP72 was also found to either directly or indirectly associate with CEP290, and in this case this interaction was found to be important in the recruitment of BBSome components to the ciliary transition zone (Stowe et al., 2012). It will be exciting to see what new insights into CEP290 biology can be gained as the interactions between CEP290 and these novel interacting partners are better characterized.

CP110

Up until this point we have focused on CEP290's interactions with proteins that aid in promoting ciliogenesis or maintaining ciliary structure. There is, however, one known CEP290 interacting protein, CP110, that acts to inhibit CEP290 activity and ciliogenesis (Tsang et al., 2008).

CP110 was first discovered as a component of the centriole with important functions in regulating centriolar length and duplication (Chen et al., 2002). It soon became apparent, however, that CP110's functions extended beyond the centriole when it was discovered that the protein plays a critical role in the regulation of ciliogenesis (Spektor et al., 2007). CP110, it turns out, directly binds to the N-terminus of CEP290 and actively inhibits ciliogenesis (Tsang et al., 2008). Overexpression of CP110 prevents cells from forming primary cilia, while knockdown of CP110 results in aberrant cilium formation (Tsang et al., 2008).

It isn't known exactly how CP110 binding to CEP290 inhibits CEP290 function, but the process of CP110 removal from CEP290 is now beginning to be worked out. During the cell cycle CP110 remains bound to CEP290 at both the mother and daughter centrioles, inhibiting axoneme extension and IFT (Tsang et al., 2008). Once the centrosome docks with a ciliary vesicle, however, the processes of axoneme extension and IFT are initiated by the kinase TTBK2. TTBK2 is recruited to the tip of the mother centriole where it specifically affects the removal of CP110 from CEP290 (Goetz et al., 2012). Once this step has occurred, axoneme extension and IFT begin. It seems that the interaction between CP110 and CEP290 is one of the last critical checkpoints in the ciliogenesis pathway. We will need to learn much more about how these

interactions are regulated and how CEP290 is activated, however, before we can begin to understand and manipulate the process of ciliogenesis for potential therapeutic gain.

CEP290

Perhaps the most interesting interacting partner of CEP290 is CEP290 itself. In 2008 researchers investigating CEP290's interaction with NPHP5 made the surprising discovery that purified regions of CEP290 were capable of homodimerization and heterodimerization (Schäfer et al., 2008). In particular, they found that two regions of the protein, one encompassing its N-terminal 695 amino acids and the other spanning a C-terminal portion of the protein from amino acids 1966-2479, were each capable of binding themselves and each other. The researchers didn't investigate this phenomenon any further, but noted in their discussion that such interactions present multiple possibilities for CEP290 tertiary/quaternary structure at the cilium. Numerous models, with CEP290 molecules forming thick bundles, long filaments, or even rings can be supported by these findings. There is even the possibility of intramolecular interactions, with a single CEP290 molecule folding over on itself and binding itself in a head-to-tail fashion.

CEP290's role in ciliogenesis and cilium function

Given its prime location at the transition zone of the primary cilium it is reasonable to assume that CEP290 might play a critical role in mediating ciliogenesis and ciliary function. In fact, we have already discussed some of the ways that CEP290 appears critical to these processes: CP110 inhibits CEP290 as a final checkpoint in the pathway to ciliogenesis, CEP290 binds to numerous ciliary proteins that play critical roles in initiating ciliogenesis and maintaining IFT, and CEP290 is

a critical component of the ciliary-links. But what do we know specifically about CEP290's direct affect on ciliogenesis and cilium function?

A number of labs have looked into this and have discovered that CEP290 is a critical regulator of ciliogenesis and a key player in the maintenance of the ciliary compartment. Knockdown of CEP290 in cultured cells results in dramatic decreases in cell ciliation, implying that CEP290 is absolutely critical for normal ciliogenesis (Tsang et al., 2008). In fact, overexpression of CEP290 alone is enough to induce cells to aberrantly form primary cilia, indicating just how strong a promoter of ciliogenesis CEP290 can be (Tsang et al., 2008). Those cells that do form cilia after CEP290 knockdown are often noted to display significant perturbations of the microtubule network, both within the cell in general and specifically within the ciliary axoneme (Kim et al., 2008; McEwen et al., 2007).

But CEP290's role in ciliogenesis and cilium formation are not limited to structural and regulatory defects. Numerous groups have found that mutation or knockdown of CEP290 results in significant deficiencies in the trafficking or proteins that should normally localize to the cilium. RPGR, PCM-1, Rab8A, and olfactory G-proteins are all mislocalized in the absence of properly functioning CEP290 (Chang et al., 2006; Kim et al., 2008; McEwen et al., 2007). Altogether these data indicate an important structural and regulatory role for CEP290 within the ciliary compartment and illustrate exactly how important the gene is to normal ciliary function.

Animal models of CEP290 disease

Researchers working to elucidate the molecular functionality of CEP290 are lucky to benefit from two naturally occurring models of CEP290 deficiency. The first CEP290 animal model to be identified was the rd16 mouse, a strain characterized by rapid and near-complete photoreceptor degeneration within the first month of life (Chang et al., 2006). This naturally occurring mutant was discovered in 2003 at the Jackson Laboratories and, in a collaboration with researchers at the University of Michigan and elsewhere, the molecular basis for the phenotype was discovered only three years later (Chang et al., 2006). Chang et al. showed that the underlying cause of the retinal degeneration was a deletion of exons 35-39 of the mouse *Cep290* gene, resulting in the in-frame deletion of 897 base pairs of the *Cep290* mRNA and in a Cep290 protein lacking 299 amino acids. They went on to show that the deletion perturbs Cep290's interaction with other ciliary proteins, resulting in paradoxically increased association between Cep290 and RPGR. Subsequent studies by other groups went on to show that the hypomorphic rd16 Cep290 results in the abnormal accumulation of high levels of Raf-1 kinase inhibitory protein in the mouse photoreceptors and in the mistrafficking of ciliary-destined proteins (McEwen et al., 2007; Murga-Zamalloa et al., 2011).

It is interesting that the rd16 mouse phenocopies the retinal pathology of LCA (albeit at a much more rapid pace than in human patients) while producing no pathology in any other organ system. It has been said that engineered mouse strains completely lacking the *Cep290* gene are uniformly embryonic lethal with significant pathology observed in the developing kidneys, liver, and CNS, but no papers on this model have yet been published. This finding may point to the importance of different regions of the protein in the pathology of different organ systems.

In addition to the rd16 mouse, one other animal model of *CEP290* deficiency has been reported. This is the Abyssinian cat rdAc model of late-onset photoreceptor degeneration. In 2007 researchers finally linked the phenotype of this cat model to a mutation in intron 50 of the cat *CEP290* gene (Menotti-Raymond et al., 2007). This mutation creates a strong canonical splice donor resulting in a 4 base pair addition and frame shift in exon 51 of the *CEP290* gene. The more mild phenotype of the rdAc cat (compared to the rd16 mouse) may be a result of the mutation occurring so late in the open reading frame (perhaps enough of the *CEP290* message is translated that the protein maintains some residual function) or perhaps only a small percent of transcripts actually include the additional 4 bases (similar to the most common human CEP290 mutation, where only 50% of transcripts include the cryptic exon (see following section on human CEP290 mutations)), but more work is clearly needed to work out the molecular basis of retinal degeneration in the rdAc cat. Regardless, the existence of a large animal model of CEP290 deficiency can only serve to hasten the path to testing novel CEP290-based therapeutics.

Patient CEP290 mutations

Mutations in *CEP290* have been identified as the molecular cause of each of the ciliopathies described above (see the section titled "Sensory cilium dysfunction"), Leber congenital amaurosis, nephronophthisis, Senior-Loken syndrome, Joubert syndrome, Bardet-Biedl syndrome, and Meckel syndrome (Baala et al., 2007; den Hollander et al., 2006; Valente et al., 2006). In fact, *CEP290* is the only gene that has been implicated in the pathogenesis of so many diverse ciliopathy diseases. The number of *CEP290* patients and novel *CEP290* mutations

continues to grow, but exactly how different *CEP290* mutations lead to such different phenotypes remains to be discovered.

To date over 120 unique mutations have been identified within the *CEP290* gene (Coppieters et al., 2010). None of these mutations seems to cluster to any particular area, but are instead widely distributed anywhere from exon 1 to 54. Interestingly, of the mutations discovered fewer than 10 are missense mutations. The rest are frame shift, splicing, or nonsense mutations predicted to result in severely truncated CEP290 protein or no protein at all through the process of nonsense mediated decay. The significance of the preponderance of pathologic truncating mutations in the *CEP290* gene is still unknown, but it is certainly an interesting aspect of CEP290 disease.

While all the identified mutations are interesting from a scientific perspective, one stands out as both the most common and perhaps the most treatable. This is the c.2991+1655A>G mutation within intron 26 of the *CEP290* gene. Buried deep within the intronic sequence, this mutation creates a strong splice-donor site that results in the inclusion of a cryptic exon between exons 26 and 27 in the fully spliced *CEP290* mRNA (den Hollander et al., 2006). This cryptic exon contains a stop codon that terminates translation just halfway through the *CEP290* mRNA. Interestingly, only 50% of transcripts produced will contain the cryptic exon, resulting in about half-normal levels of full length *CEP290* message (den Hollander et al., 2006). The hypomorphic nature of the c.2991+1655A>G mutation may explain why it has only been identified in LCA patients and never in patients with more severe disease.

The c.2991+1655A>G mutation is widespread, particularly within Europe and the United States, accounting for roughly 20% of all identified pathologic *CEP290* mutations (Perrault et al., 2007). The common nature of this mutation makes it an excellent target for therapeutic intervention – a drug or biologic that successfully corrects even only the c.2991+1655A>G mutation could stand to significantly alleviate the burden of *CEP290*-based disease.

CEP290 as a target for therapeutic intervention

The end goal of much of biomedical science is the development of treatments for human disease. Unfortunately the development of therapeutic interventions for *CEP290*-based disease has not yet reached even the early stages of animal testing. This is in part due to the large size of the *CEP290* gene. With a nearly 8 kilobase open reading frame the *CEP290* cDNA is much too large to package in traditional adeno-associated virus (AAV) vectors (Tal, 2000), the current darlings of the gene therapy field and the only viral vectors proven safe and effective in the treatment of retinal diseases (Maguire et al., 2009). A considerable amount of effort in the gene therapy community has been spent trying to package larger-than-normal genomes within AAV, and any developments in this field would be a major breakthrough for *CEP290* patients. In fact, it was reported in 2008 that packaging of full length *CEP290* cDNA had been achieved in AAV serotype 5 (Allocca et al., 2008), but to date no one has been able to replicate these results and *CEP290* patients remain without any effective treatments.

In the absence of a catch-all treatment for *CEP290* disease a number of researchers have been investigating strategies to correct at least the most common *CEP290* mutation, the c.2991+1655A>G cryptic splicing event (Collin et al., 2012; Gerard et al., 2012). All of these

approaches revolve around the vectored delivery of a small antisense oligonucleotide (AON) complementary to the cryptic exon splice site. The hope is that the AON might bind to and mask the cryptic splice site, skewing the ratio of mutant to normal transcript more in the favor of normal and potentially ameliorating the retinal degenerative phenotype of *CEP290* LCA patients. This strategy is still being actively pursued, but no results in animal models have yet been published.

Finally, a third approach to the treatment *CEP290*-based disease is also in the works. This approach relies on the vectored delivery of a tuncated version of the *CEP290* gene small enough to fit within AAV vectors but still large enough to maintain some or all of the full-length gene's function. This is not a completley novel idea – a mini-gene approach has met some success in the treatment of muscular dystrophy. The functionality of dystrophin, a large structural protein that is at the root of all cases of Duchenne muscular dystrophy, was found to be preserved in a *miniDystrophin* gene that, when delivered to a mouse model of the disease was able to effect at least some improvement in the muscular phenotype (Koppanati et al., 2010). Recently one group has reported the rescue of the retinal degeneration phenotype in an induced zebrafish model of *CEP290* disease using just such a *miniCEP290* (Baye et al., 2011). To date, however, there have been no publications on the efficacy of this *miniCEP290* in any other models of disease.

Concluding thoughts

So, this was the state of the field when I began my work to elucidate CEP290 function. I was lucky to begin my dissertation in a field that had only recently emerged but, at the same time, was beginning to move forward at a rapid pace. I had a chance to experience the strange mix of excitement and anxiety whenever a new publication with the word “CEP290” was loaded onto PubMed but the good fortune to have made it to this stage of the game without being scooped.

I hope that this introduction has adequetly explained the background necessary to understand the work that follows while at the same time has impressed upon the reader the drastic need for a better understanding of ciliary biology and the immense need for novel ciliopathy therapeutics. It was also my intent to begin to establish certain ideas and paradigms in this introduction that will be more thoroughly fleshed out by the presentation of my work that follows. It is my hope that the reader, following these common threads through the next three chapters and into the discussion, finds the story that my dissertation tells novel, compelling, and exciting.

Originally published in the *Journal of Clinical Investigation*

CHAPTER 2: DISRUPTION OF NOVEL CEP290 MICROTUBULE/MEMBRANE BINDING DOMAINS CAUSES RETINAL DEGENERATION

Theodore G. Drivas, [1] Erika L. F. Holzbaur, [2] and Jean Bennett[1]

2. Kirby Center for Molecular Ophthalmology, Perelman School of Medicine, University of Pennsylvania, Philadelphia, PA 19104, USA

3. Department of Physiology and the Pennsylvania Muscle Institute, Perelman School of Medicine , University of Pennsylvania, Philadelphia, PA 19104, USA

Abstract

Mutations in the gene *CEP290* cause an array of debilitating and phenotypically distinct human diseases, ranging from the devastating blinding disease Leber congenital amaurosis (LCA) to Senior Løken Syndrome, Joubert syndrome, and the lethal Meckel-Grüber syndrome. Despite its critical role in biology and disease, we know only little about CEP290's function. Here we identify four novel functional domains of the protein, showing that CEP290 directly binds to cellular membranes through an N-terminal domain that includes a highly conserved amphipathic helix motif, and to microtubules through a domain located within its myosin-tail homology domain. Furthermore, CEP290 activity was found to be regulated by two novel autoinhibitory domains within its N- and C-termini, both of which were also found to play critical roles in regulating ciliogenesis. Disruption of the novel microtubule-binding domain in the rd16 mouse LCA model was found to be sufficient to induce significant deficits in cilium formation leading to retinal degeneration. These data implicate CEP290 as an integral structural and regulatory component of the cilium and provide insight into the pathological mechanisms of LCA and related ciliopathies, illustrating how disruption of particular CEP290 functional domains might lead to particular disease phenotypes, and suggesting novel strategies for therapeutic intervention.

Introduction

Upon exit from the cell cycle and entry into G_0 nearly every human cell sequesters its centrosome in a structure known as the primary cilium (Kobayashi and Dynlacht, 2011). Until recently the functional role of the primary cilium, a single antenna-like projection of the apical membrane, had not been well studied or appreciated. It is now clear that this organelle has important sensory roles affecting multiple cellular processes (Davenport et al., 2007; Han et al., 2009; Wong et al., 2009) and that defects in primary cilium formation and function are responsible for a variety of human diseases and developmental disorders, collectively termed ciliopathies (Waters and Beales, 2011).

While the ciliopathies are diverse in both phenotype and etiology, specific genes, including *CEP290,* have been implicated as having causative roles in multiple cilium-associated disorders (D'Angelo and Franco, 2009). *CEP290* mutations have been described in up to 20% of cases of the devastating inherited blinding disease Leber congenital amaurosis (den Hollander et al., 2008; Perrault et al., 2007) and in numerous cases of other more debilitating ciliopathies, such as Joubert syndrome (Brancati et al., 2007; Sayer et al., 2006; Valente et al., 2006), Senior Løken Syndrome (Helou et al., 2007), and Meckel-Grüber syndrome (Baala et al., 2007). How the many identified mutations in *CEP290* contribute to these diverse pathologies remains unknown, and the protein's normal biological role has not been well-characterized.

Throughout the cell cycle CEP290 localizes to both the mother and daughter centrioles (Chang et al., 2006; Sayer et al., 2006) where it is maintained in an inhibited state by the protein CP110 (Tsang et al., 2008). During G_0 the kinase Ttbk2 mediates the removal and degradation of CP110

from CEP290 at the mother centriole (Goetz et al., 2012; Spektor et al., 2007) leading to ciliogenesis, the formation of the primary cilium. Ciliogenesis is driven by the highly regulated and specific transport of ciliary proteins into the ciliary compartment through a process known as intraflagellar transport (IFT) (Pedersen and Rosenbaum, 2008). Numerous studies have demonstrated that CEP290's function is critical for this process – in *CEP290* knockdown experiments proteins that would normally localize to the cilium fail to do so (Chang et al., 2006; Craige et al., 2010) and cilium formation is disrupted (Kim et al., 2008; Stowe et al., 2012).

Once the cilium is formed, CEP290 is found at the ciliary transition zone, the region of the organelle just proximal to the microtubule axoneme. Elegant structural work in the *Chlamydomonas* model system has localized CEP290 to the ciliary Y-links (Craige et al., 2010), dense, proteinaceous structures within the transition zone that closely couple the ciliary membrane to its microtubule core (Williams et al., 2011). The Y-links are thought to form a barrier to passive diffusion between the cilium and the cytosol (Hu and Nelson, 2011) and possibly act as a scaffold for the cellular machinery responsible for IFT (Kee et al., 2012). CEP290 likely plays an important role in the organization of this diffusion barrier and "ciliary pore" through the recruitment of a number of interacting partners, such as CC2D2A (Gorden et al., 2008), NPHP5 (Schäfer et al., 2008), and Rab8 (Kim et al., 2008), all of which are also involved in cilium function and disease. However, despite our expanding knowledge of CEP290 interacting partners and localization, the precise role CEP290 plays in ciliogenesis, IFT, and as a component of the Y-links is still unclear. No functional domains for the protein have been identified, and how mutations in particular regions of the gene affect protein function and cause disease remains completely unknown.

In this paper we present evidence that CEP290 directly binds to cellular membranes through a highly conserved region in its N-terminus and to microtubules through a domain located near its C-terminus. CEP290 activity was found to be regulated by autoinhibitory domains located within its N- and C-termini, both of which were found to play a critical role in regulating ciliogenesis. Furthermore, we show that the microtubule-binding domain we identified is completely disrupted In the rd16 mouse LCA model (Chang et al., 2006), resulting in significant deficits in cilium formation leading to retinal degeneration. These findings implicate CEP290 both as a key structural component of the ciliary Y-links and as a terminal regulator in the pathway leading to ciliogenesis. Our study also provides the first evidence of a mechanistic and pathological basis for *CEP290*-related LCA and related ciliopathies and suggests novel strategies for therapeutic intervention.

Results

Mutations in the *CEP290* gene have been implicated in a variety of human diseases (Moradi et al., 2011), but their effects on protein function have not yet been characterized. Mutations clustering in particular regions of the gene might be indicative of important functional domains, but no mutational hotspots or functional domains have been identified to date (Figure 2.1A) (Coppieters et al., 2010). To better understand the role CEP290 plays in cilium function, ciliogenesis, and human disease, we performed a structure-function analysis using a panel of truncation constructs spanning the full length of *CEP290* to identify and define domains of novel functionality.

CEP290 associates with ARL13B-positive cellular membranes via its N-terminus

The first two CEP290 truncations we tested displayed distinct localization patterns. When overexpressed as GFP fusion proteins the N-terminal fragment of CEP290 (spanning aa 1-580) showed an exclusively punctate localization pattern while the C-terminal fragment of CEP290 (from aa 580 to the end of the protein, aa 2479) showed a striking fibrillar localization (Figure 2.1B). Both of these patterns were occasionally observed in cells overexpressing the full-length CEP290 construct, but not with the same frequency as in cells expressing the truncations (data not shown). We generated two additional truncations of the N-terminal region of the protein to better define the domain responsible for the punctate localization. The truncation spanning CEP290 aa 1-362 showed a punctate pattern similar to that observed for the complete N-terminal fragment, while the truncation spanning aa 380-580 was present only diffusely throughout the cytoplasm (Figure 2.1B). Further truncation of the protein was not effective in

resolving the domain responsible for punctate localization beyond aa 1-362, implying either that this is the minimum region needed for punctate staining or that further truncation significantly interferes with protein function.

The CEP290-positive puncta observed by microscopy were found to display robust co-staining with ARL13B (Figure 2.1B), a membrane protein important in the trafficking of vesicles to the primary cilium (Barral et al., 2012; Cevik et al., 2010; Li et al., 2010), suggesting that these puncta might be cilium-destined cellular vesicles. Detergent-free post-nuclear supernatants of cells expressing our CEP290 truncations were prepared and ARL13B-positive membranes were magnetically immunoprecipated and analyzed by western blotting. Both CEP290 aa 1-580 and CEP290 aa 1-362 were significantly enriched in the ARL13B membrane immunoprecipitate, while neither CEP290 aa 380-580 nor GFP alone were found in significant quantities (Figure 2.2B). Thus, CEP290 aa 1-362 were found to be necessary and sufficient to mediate CEP290 localization to ARL13B-positive membranes. In only very few cases did the CEP290-positive puncta exhibit any co-staining with LAMP2, a marker of the lysosomal compartment (Figure 2.2D), suggesting that CEP290 membrane localization was not an artifact of protein overexpression.

To confirm that the puncta observed by microscopy were truly membranous organelles we performed a series of membrane co-flotation assays on cells expressing CEP290 aa 1-580. Roughly 40% of total CEP290 aa 1-580 was found to co-float in the membrane-associated fractions (Figure 2.2A, fractions 1-3), indicating that a substantial portion of the protein was, in fact, associated with cellular membranes. ARL13B, the Na/K ATPase, and Annexin A2 were all

found to similarly co-float in the membrane-associated fractions, while Tubulin was found almost exclusively in the soluble fraction (Figure 2.2A).

The dual distribution of CEP290 aa 1-580 within both the membrane-associated and soluble fractions along with the absence of a signal peptide from CEP290's amino acid sequence was suggestive of peripheral, rather than integral, membrane association (Mu et al., 1995; Seaman et al., 1996). To confirm this, membrane fractions of cells transfected with our CEP290 truncations were prepared and peripheral membrane proteins were eluted from the membrane with a high pH buffer. The remaining integral membrane proteins were subsequently solubilized with detergent. For both CEP290 aa 1-580 and aa 1-362 the majority of each truncation was found in the peripheral membrane protein fraction (Figure 2.2C). This same pattern was observed for the peripheral membrane protein Annexin A2 (Klee, 1988), while the majority of the Na/K ATPase, an integral membrane protein, was found in the integral membrane protein fraction (Figure 2.2C). CEP290 aa 380-580, on the other hand, was not found in significant amounts in either fraction. Taken together, these data indicate that CEP290 aa 1-362 are necessary and sufficient for robust peripheral membrane association.

CEP290's capacity for membrane association is increased by truncation of its C-terminus

To further investigate CEP290's membrane association, we performed a series of subcellular fractionation experiments on cells expressing each of our CEP290 truncations. The CEP290 truncation spanning aa 580-2479 that produced a fibrillar localization pattern by microscopy

was found almost exclusively in the cytoskeletal fraction, while truncations lacking this region were completely absent from the cytoskeletal fraction (Figure 2.13A). On the other hand, truncations that included CEP290 aa 1-362 were again found to be significantly present in the membrane fraction when compared to either GFP-alone or our fractionation controls (Figure 2.13A). Roughly 30% each of both CEP290 truncations aa 1-580 and aa 1-362 were found to be associated with cellular membranes while roughly 10% of full-length CEP290 was also found in the membrane fraction (Figure 2.13B). This distribution agrees with what was observed by fluorescence microscopy – specifically, that full-length CEP290 occasionally displayed vesicular localization, but to a lesser extent than CEP290 truncations lacking the C-terminus of the protein but containing aa 1-362.

CEP290 directly binds membranes in vitro and contains a highly conserved membrane-binding amphipathic α-helix motif

To determine whether CEP290's membrane association was mediated by a direct or indirect interaction we performed a series of liposome co-flotation assays on purified recombinant CEP290 aa 1-580 (Figure 2.14A). CEP290 aa 1-580 associated with liposomes robustly, with a majority of the protein found in the liposome-associated fraction (Figure 2.3A). Flotation of the truncation occurred only in the presence of liposomes, and liposome co-flotation was not observed for a control protein, BSA (Figure 2.3A). The ability of this region of CEP290 to directly bind liposomes suggests that the observed association between the N-terminus of CEP290 and cellular membranes is mediated by a direct interaction

Projecting CEP290 aa 1-362 onto an α-helical wheel, a segment from aa 257 to 292 was predicted to form a canonical amphipathic α-helix (Figure 2.3B). Such helices have been shown to be critical in mediating robust interactions between peripheral membrane proteins and various cellular membranes (Cornell and Taneva, 2006). Comparing this stretch of the protein across a variety of species, we found the amphipathic helix motif to be very highly conserved. Where there was divergence in the amino acid sequence, there was usually conservation of polarity and charge between the divergent residues (Figure 2.3C). Taken together, these data suggest that the highly conserved amphipathic helix located within the membrane binding region of CEP290 may be mediating CEP290's novel membrane binding function.

CEP290 aa 1695-1966 mediate colocalization with microtubules

CEP290 aa 580-2479 appeared both by microscopy and subcellular fractionation to be associated with the cytoskeleton (Figures 2.1B, 2.2D, 2.13A). To further investigate this phenomenon, we constructed a library of additional *CEP290* truncations to thoroughly interrogate CEP290's cytoskeletal association (Figure 2.4). Overexpression of these truncations as GFP fusions revealed that those truncations containing CEP290 aa 1695-1966, referred to as region M, displayed a fibrillar localization pattern similar to that which was observed for CEP290 aa 580-2479 while truncations lacking CEP290 region M never display any fibrillar localization (Figure 2.5A-B). These fibrils were noted to co-localize with the microtubule network implicating CEP290 region M as necessary and sufficient for microtubule co-localization.

The degree to which different CEP290 truncations displayed a fibrillar localization pattern was found to be dependent upon which regions of the protein were included in the truncation. The full-length *CEP290* construct was noted to produce a fibrillar localization pattern in only about 10% of transfected cells (Figure 2.5B). Truncations lacking either the N- or C-terminus of CEP290, on the other hand, were found to display a fibrillar localization in roughly 20% and 60% of transfected cells, respectively. The truncation lacking both termini was found to display a fibrillar localization pattern in nearly 80% of transfected cells. These data indicated that the N- and C-termini of the protein have an inhibitory or regulatory effect on CEP290's microtubule binding ability.

It is interesting to note that all of our truncations displayed co-localization with pericentrin, a marker of the centriole (the normal site of CEP290 localization) (Figure 2.5A, insets). Homotypic interactions between endogenous CEP290, present at the centrioles, and our truncations (through CEP290's homo/heterodimerization domains (Schäfer et al., 2008)) might explain the observed centriolar localization of a number of our truncations. However, those truncations lacking both homo/heterodimerization domains are apparently still capable of localizing to the centriole, implying that multiple regions throughout CEP290 are capable of affecting centriolar localization.

CEP290 microtubule association results in microtubule acetylation and bundling

In cells transfected with *CEP290* constructs containing region M there was a dramatic increase in the intensity of acetylated α-tubulin staining, with bundles of acetylated microtubules looping throughout the cells (Figure 2.6A). These increases were not seen for truncations lacking region

M. The degree to which different CEP290 truncations increased the acetylation and bundling of microtubules was dependent upon which regions of the protein were included in the truncation. Full-length CEP290 and CEP290 truncations lacking either the N- or C-terminus increased microtubule acetylation and bundling in nearly 40% of transfected cells while CEP290 truncations lacking both the N- and C-terminus of the protein increased microtubule acetylation and bundling in nearly 75% of cells (Figure 2.6B). Less than 15% of cells transfected with truncations lacking region M were noted to have any change in microtubule acetylation or bundling.

CEP290 directly binds microtubules in vitro

A series of microtubule co-sedimentation assays performed on our CEP290 truncation constructs revealed that truncations containing region M were capable of significant microtubule association in vitro (Figure 2.7A-B). Again, the degree to which different CEP290 truncations associated with microtubules was found to be dependent on the inclusion of the N- and C-termini. Less than 50% of the full-length CEP290 construct and CEP290 constructs lacking either terminus were found to associate with microtubules, while nearly 100% of CEP290 constructs lacking both termini associated with microtubules (Figure 2.7B).

To test whether CEP290 region M's microtubules association was mediated by direct microtubule binding we recombinantly expressed and purified CEP290 region M (Figure 2.14B) and subjected this protein to a series of microtubule co-sedimentation assays using increasing concentrations of microtubules (Figure 2.7C-D). Region M was found to directly and robustly bind to microtubules in a concentration dependent manner (Figure 2.7D). The calculated K_D of

this interaction was found to be approximately 100nM, an affinity comparable to those of other microtubule binding proteins (Gustke et al., 1994; Kikkawa et al., 2000).

The N- and C-termini of CEP290 cooperate to inhibit protein function and regulate ciliogenesis

The observation that the N- and C-termini of CEP290 appeared to act in inhibiting the membrane and microtubule binding activity of the protein (Figures 2.4, 2.5B, 2.6B, 2.7B, 2.13B) suggested that these regions might be regulatory domains mediating the autoinhibition of the protein. To test this hypothesis, we transduced hTERT-RPE1 cells with lentiviral vectors encoding either the N- or C-terminus of the protein and observed the cells for deficits in primary cilium formation. To our surprise, we found that overexpression of either of these regulatory regions resulted not in deficiencies in primary cilium formation, but instead in significant increases in the percent of cells forming primary cilia, with more than twice as many cells forming primary cilia than those cells treated with a control vector (Figure 2.8A-B). The length of cilia formed by cells overexpressing either regulatory region was also significantly increased by more than 25% compared to cells treated with the control vector (Figure 2.8C-D). These increases were only observed in cells maintained in media supplemented with serum, a condition in which CEP290 is normally inhibited (Stowe et al., 2012), implying that these regulatory domains act through the same pathway that mediates normal CEP290 inhibition. It is also interesting to note that dysregulation of CEP290 by overexpression of either regulatory region was sufficient to initiate aberrant primary cilium formation, suggesting that there is no further downstream regulation of ciliogenesis beyond CEP290.

Interestingly, in both the serum starved and serum fed state it was noted that occasional cells transduced with the N-terminus of CEP290 appeared to produce multiple ciliary axonemes at the same centrosome (Figures 2.8A, 2.9A-C). These axonemes always emanated from a single focus of pericentrin (Figure 2.8B) and were often found at 90˚ to each other. In some, but not all cases, one or more of these axonemes co-stained with ARL13B (Figure 2.9A), a protein associated with the ciliary membrane (Cevik et al., 2010), indicating that at least some of these multi-axoneme structures were fully formed cilia.

The rd16 mouse Cep290 gene encodes a version of the protein deficient in microtubule binding

The rd16 mouse is a retinal disease model of *CEP290* deficiency characterized by a rapid and near-complete degeneration of photoreceptors. The rd16 *Cep290* gene encodes a protein containing an in-frame deletion of 298 amino acids (Chang et al., 2006) that significantly overlaps the region of human CEP290 we identified as being critical for microtubule binding (Figure 2.10A).

We generated two truncation mutants of human CEP290 containing either the region of the microtubule binding domain deleted in the rd16 mouse, or the region of the microtubule binding domain spared by the mouse deletion (Figure 2.10A). To our surprise, when overexpressed in hTERT-RPE1 cells both truncations displayed a diffuse localization pattern indicative of a primarily cytosolic localization (Figure 2.10B). In neither case was any significant co-localization with the microtubule network observed. We confirmed that neither of these constructs was capable of associating with microtubules by subjecting them to microtubule co-

sedimentation assays (Figure 2.10C). Neither construct was found to significantly co-sediment with microtubules (Figure 2.10D), indicating both that the rd16 deletion perturbs microtubule binding and that microtubule binding is conferred by a larger portion of the *CEP290* gene than was included in either of our truncations.

To confirm that rd16 Cep290 was in fact deficient in microtubule binding we subjected brain lysates from wild type (WT) and rd16 mice to microtubule co-sedimentation assays (Figure 2.10E). WT Cep290 showed very significant microtubule association, with roughly 60% of the protein associating with microtubules (comparable to full-length human CEP290 (Figure 2.7B)), while rd16 Cep290 was found to be completely deficient in microtubule binding (Figure 2.10F).

The rd16 mouse is deficient in cilium formation and structure

While the retinal phenotype of the rd16 mouse has been well documented (Cideciyan et al., 2011), no cellular phenotype regarding primary cilium formation or structure has yet been reported. To investigate the effect that ablation of Cep290 microtubule binding might have on primary cilium formation, we assayed primary dermal fibroblasts from rd16 and WT mice for deficiencies in cilium formation and structure. In both serum starved and serum fed conditions, rd16 fibroblasts were found to be significantly deficient in primary cilium formation, with roughly 50% fewer cells forming cilia than WT controls (Figure 2.11C-D). The cilia produced by rd16 fibroblasts were also found to be more than 25% shorter than those produced by WT fibroblasts (Figure 2.11A-B), further suggesting that the microtubule binding functionality of CEP290 is critically important in the maintenance and formation of the primary cilium and, when disrupted, capable of causing severe retinal disease.

Discussion

CEP290 plays a critical role in the formation and function of the primary cilium and, when mutated, is responsible for a variety of devastating human diseases (Coppieters et al., 2010). Our understanding of the protein's function has been, until now, inadequate to explain how disruption of CEP290 might lead to human pathology (Moradi et al., 2011). The findings presented here begin to implicate CEP290 as a vital structural and regulatory element of the ciliary transition zone, elucidate some of its molecular functionality, and place it at the center of the critically important and disease-relevant pathways of ciliogenesis and IFT.

CEP290 as a bridge between the ciliary membrane and the microtubule axoneme

To date, how CEP290 functions as a component of the ciliary Y-links has been unclear. Here we have shown that CEP290 is capable of directly binding to both cellular membranes and microtubules, possibly anchoring the two to each other and likely playing a key structural role in the maintenance of the cilium. Furthermore, we have described the particular domains of CEP290 responsible for mediating these specific functions. The N-terminus of the protein, containing a highly conserved amphipathic helix, mediates CEP290's membrane binding activity. Such helices have previously been shown to be critical in mediating robust, reversible interactions between various membrane binding proteins and cellular membranes (Cornell and Taneva, 2006). Multiple experiments determined that a region near the C-terminus of CEP290, encompassing much of the protein's myosin-tail homology domain, was necessary and sufficient to mediate microtubule binding. Myosin-tail homology domains have been reported to be

critical in mediating the microtubule binding activity of several other cytoskeleton-associated proteins (Moen et al., 2011; Weber et al., 2004).

The location of these two functional domains at opposite ends of CEP290 immediately suggests a potential structural role for the protein, anchoring the ciliary membrane to the axoneme at a fixed distance. Our data also indicate that, in addition to binding microtubules, CEP290 is capable of mediating their acetylation and bundling, two hallmarks of the microtubules that make up the ciliary axoneme (Alieva et al., 1999), suggesting that CEP290 might play an important role in the stabilization, bundling, and organization of microtubules during ciliogenesis.

A novel mechanism for the inhibition of CEP290

An overarching theme that emerged from our analysis of CEP290's membrane and microtubule binding activities was that the full-length protein exhibited attenuated activity when compared to truncation mutants lacking the N- or C-terminus. Confirming a role for these domains in the regulation of the protein's function and ciliogenesis, we found that overexpression of either domain interfered with the normal regulation of CEP290 and was sufficient to initiate aberrant primary cilium formation, suggesting that there is no further downstream regulation of ciliogenesis beyond CEP290. Overexpression of the regulatory regions in serum-starved cells, where CEP290 is known to be relieved of inhibition, did not result in any increase in CEP290 activity, implying that these regulatory domains act through the same pathway that mediates normal CEP290 inhibition.

These data present at least two possibilities for a mechanism of CEP290 regulation. Both regulatory loci might be acted upon by extraneous inhibitory factors to mediate CEP290 inhibition. In fact, it has been shown that the protein CP110 acts as just such an inhibitory factor, binding to the N-terminus of CEP290 and inhibiting protein activity (Spektor et al., 2007; Tsang et al., 2008). Accordingly, we found that, in some cells, overexpression of CEP290's N-terminus led to the growth of multiple ciliary axonemes. This is consistent with what would be expected upon competition between endogenous CEP290 and the overexpressed N-terminal fragment for CP110, normally removed from only one end of the mother centriole to initiate ciliogenesis (D'Angiolella et al., 2010). Nonspecific depletion of CP110 from both ends of both centrioles by the overexpressed N-terminus could have resulted in the growth of multiple ciliary axonemes in the cells we observed.

Our data cannot, however, be fully explained by this mechanism alone. If inhibition were solely dependent on the binding of a finite pool of endogenous inhibitory factor, then overexpression of the full-length protein should result in competition for the inhibitory factor and only minimal, if any, observed inhibition of the overexpressed protein. Additionally, we would not expect to see inhibition of the full-length construct in in vitro assays where inhibitory factors should not be present at meaningful concentrations. In all our experiments assessing protein activity, we found that full-length CEP290 was significantly inhibited compared to truncation mutants lacking the novel inhibitory regions, arguing against extraneous factors such as CP110 being solely responsible for CEP290 regulation.

We propose an alternative model for CEP290 regulation that is more consistent with our findings and with previous data showing that both the N- and C-termini of CEP290 are capable of binding both themselves and each other (Schäfer et al., 2008). Perhaps the two novel regulatory regions of the protein cooperate to inhibit CEP290 function, binding to each other and causing a conformational change in the protein, stabilized by the binding of CP110, that obscures important functional domains and decreases protein function (Figure 2.12). Thus, the overexpression of either regulatory domain would saturate endogenous CEP290 regulatory domains, resulting in a paradoxical increase in protein function, and the full-length protein, of its own accord, would be expected to display innate inhibition regardless of experimental conditions. These are exactly the results we observed in all of our experiments.

Interestingly, this mechanism of inhibition has been described for a variety of other proteins, such as Vinculin, Ezrin, and the ERM domain proteins, all of which act to link the cell membrane to the actin cytoskeleton (Smith et al., 2003; Song et al., 2012). These proteins depend on amphipathic helices for their membrane binding activity, and these helices have also been shown to act in the inhibition of these proteins, binding to and obscuring their actin-binding domains (Cornell and Taneva, 2006). It is plausible that this mechanism of autoinhibition, conserved among membrane-to-actin cytoskeleton bridging proteins, is operative and conserved for membrane to microtubule bridging proteins as well. CEP290 would be the first protein in this class shown to rely upon this mechanism of inhibition. This model is also supported by observations made in the rd16 mouse, such as the apparent increased affinity of rd16 Cep290, compared to WT, for RPGR (Chang et al., 2006). The rd16 deletion of the

microtubule binding/regulatory region may thus result in decreased autoinhibition and a higher affinity of Cep290 for its interacting partners, as was observed.

Implications for human disease

As we continue to learn more about the key functional domains of CEP290 we will begin to better understand how mutations in particular protein domains contribute to pathology. The microtubule binding function of CEP290 is clearly of critical importance to the function of the protein on a cellular level and, as we have shown, critical in disease. The rd16 mouse *Cep290* gene was found to encode a version of the protein completely deficient in microtubule binding, resulting in deficiencies in primary cilium formation and structure in cultured fibroblasts. While rd16 photoreceptors do seem capable of forming connecting cilia, the function and maintenance of the connecting cilium and photoreceptor outer segment is perturbed in these animals, resulting in dramatic and rapid retinal degeneration, implying that deficiencies in CEP290 microtubule binding can lead to significant pathology. Over 24 unique mutations identified in human CEP290 patients map to the microtubule binding domain we report here (Figure 2.1A). Almost all of these mutations are expected to have truncating effects on the protein (Coppieters et al., 2010), which, as in the rd16 mouse, would result in significant deficiencies in microtubule binding, potentially explaining the mechanism underlying the disease phenotype seen in these individuals.

Perhaps most interesting, however, are the implications that the discovery of novel regulatory domains of CEP290 has for the development of therapeutic interventions. The extension, to CEP290 patients, of recombinant adeno-associated virus (AAV)-based therapeutics, which have

proven safe and effective in the treatment of another genetic cause of LCA (Maguire et al., 2009), has been hindered by CEP290's large size, precluding it from packaging in AAV (Wu et al., 2010). Truncation mutants of CEP290 lacking the novel inhibitory domains we have described but maintaining the other functional regions of the protein may exhibit normal, or even enhanced, CEP290 function, while at the same time being small enough to fit in AAV. The delivery of such a therapeutic to terminally differentiated tissues, such as the retina, where permanent activation of CEP290 would not be expected to be problematic, might prove effective in the treatment of CEP290-related diseases such as LCA.

Methods

Plasmid construction

CEP290 truncations were generated by PCR amplification using Gateway® cloning (Invitrogen) compatible primers from a human codon-optimized *CEP290* plasmid synthesized by DNA 2.0. Amplified products were cloned into pDONR221 (Invitrogen) by Gateway® cloning to generate entry clones. For cell transfection and in vitro transcription and translation assays, entry clones were shuttled into the plasmid pcDNA-DEST53 (Invitrogen) by Gateway® LR clonase reactions to create N-terminally-tagged GFP fusions. For bacterial expression, entry clones were shuttled into pDest-527 (a gift of Dominic Esposito (Frederick National Laboratory for Cancer Research, Frederick, MD. Addgene plasmid #11518)) to create N-terminally-tagged 6xHis fusions. For lentivirus production, entry clones were shuttled into pLXnGFP, a modified version of pLX302 (a gift of David Root (The Broad Institute, Cambridge, MA. Addgene plasmid #25896)), to create N-terminally-tagged GFP fusion lentivirus production plasmids. Restriction digest and DNA sequencing were used to confirm the integrity of each expression construct.

Cell culture and treatments and lentivirus production

Wild type and rd16 mouse primary dermal fibroblasts and 293T cells were grown in DMEM supplemented with 10% FBS. hTERT RPE-1 cells were grown in DMEM:F12 supplemented with 10% FBS and 0.075% sodium bicarbonate. All cells were grown at 37˚ C in a humidified 5% CO_2 atmosphere. Transfections were performed with FuGENE 6 reagent (Promega) according to the manufacturer's protocol. Cells were induced to form primary cilia by serum starvation with Opti-MEM I (Invitrogen) for 48-72 hours.

Lentiviral vectors were produced by transfection of 80% confluent 293T cells in T25 culture flasks with 1 μg of lentivirus construct, 750 ng of PsPAX2 packaging plasmid, and 250 ng of pMD2.G envelope plasmid. Media was replaced after 24 hours, and lentiviral supernatants were harvested at 48 and 72 hours, combined, filtered through a 0.45 μm filter, and snap-frozen at -80° C. For lentivirus transduction, hTERT RPE-1 cells were plated in media containing 8 μg/mL polybrene. Filtered media containing the appropriate lentivirus particles was added and 24 hours after transduction cells were switched to selective media containing 10μg/mL puromycin.

Primary dermal fibroblast isolation

Primary dermal fibroblasts were isolated by washing neonatal mouse skin in 70% ethanol followed by 5 washes in PBS. The skin was minced in a culture vessel, covered with DMEM supplemented with 10% FBS, penicillin, and streptomycin, and incubated at 37˚ C in a humidified 5% CO_2 atmosphere. One week after harvesting the skin was removed and discarded and fibroblasts were passaged into a larger vessel.

Antibodies, immunofluorescence, and immunoblotting

Antibodies used in this study were rabbit anti-human CEP290 (Abcam, ab105383), rabbit anti-mouse Cep290 (Abcam, ab128231), mouse anti-α tubulin (Abcam, AB7291), rabbit anti-pericentrin (Abcam, AB4448), mouse anti-GFP (Roche 11 814 460 001), mouse anti-Bovine serum albumin (Thermo, MA5-15238), rabbit anti-6xHis (Abcam, AB1187), rabbit anti-GAPDH (Sigma, SAB2103104), mouse anti-Na/K ATPase α-1 (Novus, NB300-146), mouse anti-Lamin A/C (Sigma, SAB4200236), mouse anti-Acetylated α-tubulin (Sigma, T7451), rabbit anti-LAMP2 (Novus, NBP1-71692), rabbit anti-Annexin A2 (Cell Signaling, 8235), rabbit anti-ARL13B

(Proteintech, 17711-1-AP), HRP-conjugated goat anti-mouse (GE, NA931V), HRP-conjugated goat anti-rabbit (GE, NA934V), Cy5 conjugated goat anti-rabbit (KPL, 072-02-15-06), and AlexaFluor 594-conjugated goat anti-mouse (Invitrogen, A1100S).

For immunofluorescence, cells were grown in chamber slides and fixed with 3% PFA in PBS for 20 minutes at 37˚ C. Cells were permeabilised with 1% Triton X-100 in PBS for 5 minutes, and blocked in 2% BSA in PBS for 30 minutes prior to incubation with primary antibody. Secondary antibodies used were donkey anti-mouse or anti-rabbit, conjugated to Cy5 or AlexaFluor 594. Slides were mounted in mounting medium containing DAPI. Confocal imaging was performed with an LSM510 META NLO laser scanning confocal on a Zeiss Axiovert 200M inverted microscope using a Plan-Apo 63x/1.4 oil objective and the LSM510 4.2 software. Laser lines used were 488nm (for green labeling, from argon laser), 543nm (for red labeling, HeNe laser), 633nm (for cy5 channel, HeNe laser), and 740nm (for DAPI channel, from a Coherent Chameleon tunable two photon laser). For normal fluorescence microscopy, slides were imaged using an Axio Imager.M2 microscope using an either EC Plan-Neofluar 40x/0.75 M27 or an EC Plan-Neofluar 63x/1.25 Oil M27 objective and captured using an AxioCamMR3 camera and the AxioVs40 software, version 4.8.2.0. Primary cilium length was measured using the same AxioVs40 software.

For immunoblotting, samples were subjected to SDS-PAGE and transferred to nitrocellulose membrane using standard techniques. Membranes were blocked in 5% nonfat milk for 1 hour at room temperature and subsequently incubated in primary antibody overnight at 4° C. Membranes were washed three times with PBST (0.1% Tween-20 in PBS), incubated with HRP-

conjugated secondary antibody for 1 hour at room temperature, washed, and developed using ECL2 reagent (Pierce), and scanned on a Typhoon 9400 instrument (GE). Immunoblots were densitometrically quantified using ImageJ 1.44p.

Membrane flotation, membrane protein fractionation, and vesicle immunoprecipitation

Cultured cells were washed three times with ice cold PBS. Cells were resuspended in a 250mM Sucrose solution containing 4mM immidazole and a protease inhibitor cocktail and passaged through a 25G needle 20 times. The resulting lysate was centrifuged at 1,000x g for 10 minutes at 4˚C to pellet nuclei and unlysed cells and the resulting post-nuclear supernatant was centrifuged at 100,000x g for 60 minutes at 4˚C to pellet the membrane-enriched fraction.

Membrane flotation was performed by resuspending the membrane-enriched fraction in 250 µL of 80% sucrose in PBS. This solution was added to the bottom of a 2mL centrifuge tube, overlaid with 1.5 mL of 50% sucrose in PBS and with 250 µL of 5% sucrose in PBS. Sucrose gradients were then centrifuged at 100,000x g for 16 hours at 4˚C. Equal fractions were subsequently taken from the top to the bottom of the gradient and analyzed by western blotting as indicated.

Peripheral membrane proteins were extracted from membrane preparations by resuspending and incubating the membrane-enriched fraction of cultured cells in a high pH buffer (100nM Na_2CO_3, pH 11.3) for 30 minutes at 4˚C. The membranes were pelleted at 100,000x g for 60 minutes at 4˚C and the resulting supernatant was saved as the peripheral membrane fraction.

Integral membrane proteins were subsequently extracted by resuspending and incubating the resulting membrane pellet in 4% Triton-X100 in PBS for 30 minutes at 4˚C.

Vesicle immunoprecipitation was performed on post-nuclear supernatants of hTERT-RPE1 cells expressing various CEP290 truncations. A sample of the total post nuclear extract was saved as the input fraction. Protein G Dynabeads (Invitrogen) were washed and incubated with 2 µg of anti-ARL13B antibody for 20 minutes at room temperature, magnetically collected, and washed in PBS. 350 µL of post-nuclear supernatant was added to the antibody-dynabead complex and incubated with gentle agitation for 20 minutes at room temperature. The beads and immunoprecipitated complexes were magnetically collected and washed three times with PBS. A sample of the unbound fraction was saved and the immunoprecipitated material was eluted by resuspension in 4X SDS PAGE sample buffer.

Subcellular fractionation

Subcellular fractionation was performed using the QProteome Cell Compartment kit (Qiagen) according to the supplied protocol.

Recombinant protein expression and purification

6xHis tagged CEP290 truncation M and N were expressed from pDest-527 in E.coli BL21(DE3)pLysS (Invitrogen) and purified using the Ni-NTA Fast Start Kit (Qiagen) according to the manufacturer's protocol. Purified protein products were subjected to SDS-PAGE and stained with Coomassie Brilliant Blue to assess purity and determine protein concentration.

Liposome flotation assay

100 nm liposomes (total lipid concentration of 5mg/mL in PBS) with a lipid composition of a 60:40 molar ratio of phosphatidylserine to cholesterol were purchased from Encapsula NanoSciences and used within 2 weeks of formulation. 20 µL (1.5 µg) of recombinant CEP290 truncation N, or an equivalent amount of BSA, was incubated with 230 µL of liposomes, or an equal volume of PBS alone, at 37˚ C for 30 minutes. Each reaction was then mixed 1:1 with a solution of 80% sucrose in PBS and added to the bottom of a 2mL ultracentrifuge tube. Reactions were overlaid with 1.3 mL of 30% sucrose in PBS and with 200 µL of PBS and centrifuged at 100,000x g for 90 minutes at 30˚ C. Five 400 µL fractions were taken, starting at the top of sucrose gradient, and equal amounts of each were analyzed by SDS-PAGE and western blotting.

In vitro transcription and translation reactions

Plasmid DNA was transcribed and translated using the TNT T7 reticulocyte lysate system (Promega) according to the manufacturer's protocol.

Microtubule polymerization

Pure bovine tubulin (Cytoskeleton) was diluted 1:1 in BRB80 buffer (80mM Pipes, 1mM $MgCl_2$, 1mM EGTA, pH 6.8) and cleared of insoluble material by centrifugation at 20,000x g for 10 minutes. The soluble fraction was supplemented with 1 mM GTP and incubated at 37˚ C for 15 minutes to polymerize microtubules. The polymerized microtubules were treated with 10 µM taxol and incubated at room temperature for an additional 15 minutes to stabilize the microtubules. Microtubules were pelleted at 48,000x g for 30 minutes at 30˚ C and resuspended

in BRB80 supplemented with 1mM GTP and 10 µM taxol. Microtubules were used within one week of preparation.

Microtubule Binding Assays

Crude TNT T7 reaction products were diluted 1:1 in BRB80 supplemented with 1mM GTP and 10 µM taxol. The diluted products were then incubated at 30˚ C for 30 minutes in either the presence or absence of pure, pre-polymerized microtubules. Reactions were centrifuged through a 40% sucrose cushion at 48,000x g for 30 minutes, the supernatant was collected, and the pellet washed once with warm BRB80 and resuspended in 1x SDS PAGE sample buffer. Both fractions were subjected to SDS-PAGE and transferred to nitrocellulose. The presence of tubulin in the pellets was confirmed by Ponceau staining.

For microtubule binding assays performed on mouse brain homogenate, 0.5 g of mouse brain was mechanically homogenized in 0.5 mL of 1% NP40 in BRB80 buffer containing a protease inhibitor cocktail. The homogenate was cleared of insoluble material by centrifugation at 48,000x g for 30 minutes at 4˚ C, and the resulting supernatant was either used immediately or snap-frozen at -80˚ C for later use. Homogenates were incubated either at 37˚ C for 30 minutes with 1mM GTP and 10µM taxol to promote microtubule polymerization, or at 4˚ C for 30 minutes to inhibit microtubule polymerization. The resulting reactions were then layered over a 40% sucrose cushion, centrifuged at 48,000x g for 30 minutes to pellet the microtubules and microtubule-associated proteins, and processed as above.

For the direct microtubule binding assay, 1μM of recombinantly expressed and purified 6xHis tagged CEP290 truncation M was incubated at 30˚ C for 30 minutes with increasing amounts of pure, pre-polymerized microtubules. Reactions were centrifuged and subjected to SDS-PAGE as above, and tubulin and CEP290 truncation M were detected by Coomassie blue staining.

Bioinformatic Analysis

The helical wheel projection in Figure 2.3B was adapted from the Helical Wheel Projection applet available at http://rzlab.ucr.edu/scripts/wheel/wheel.cgi. The multiple sequence alignment presented in Figure 2.3C was adapted from GeneDoc 2.7.000.

Statistical analysis

The statistical significance of the difference between two means was determined using a two-tailed Student's t-test. The statistical significance of the difference between three or more means was determined using a two-way ANOVA and Tukey's HSD test. Statistical analysis was performed using GraphPad Prism Software 5.0b. p-values < 0.05 were considered significant.

Study approval

The genetics and cell studies were approved by the University of Pennsylvania IRB, Philadelphia, PA (protocol 808828, J. Bennett, PI). The animal studies were approved by the University of Pennsylvania IACUC, Philadelphia, PA (protocol 802901, J. Bennett, PI).

Acknowledgments

We are grateful to Dr. Jeannette Bennicelli, Dr. George T. Drivas, Dr. Michael P. Hart, and Adam Wojno for their many suggestions, conversations, and critical reading of this manuscript. We would also like to thank Jasmine Zhao for her technical support. Plasmids purchased from Addgene were kindly deposited by Dominic Esposito and David Root. Studies in this work were supported by the Wyk Grousbeck Family Foundation and were performed in collaboration with Project CEP290. Additional support was provided by Foundation Fighting Blindness, Research to Prevent Blindness, NIH R24Ey019861, 8DP1EY023177, TreatRush (European Union), the Mackall Foundation Trust, the Penn Genome Frontiers Institute, and the F.M. Kirby Foundation.

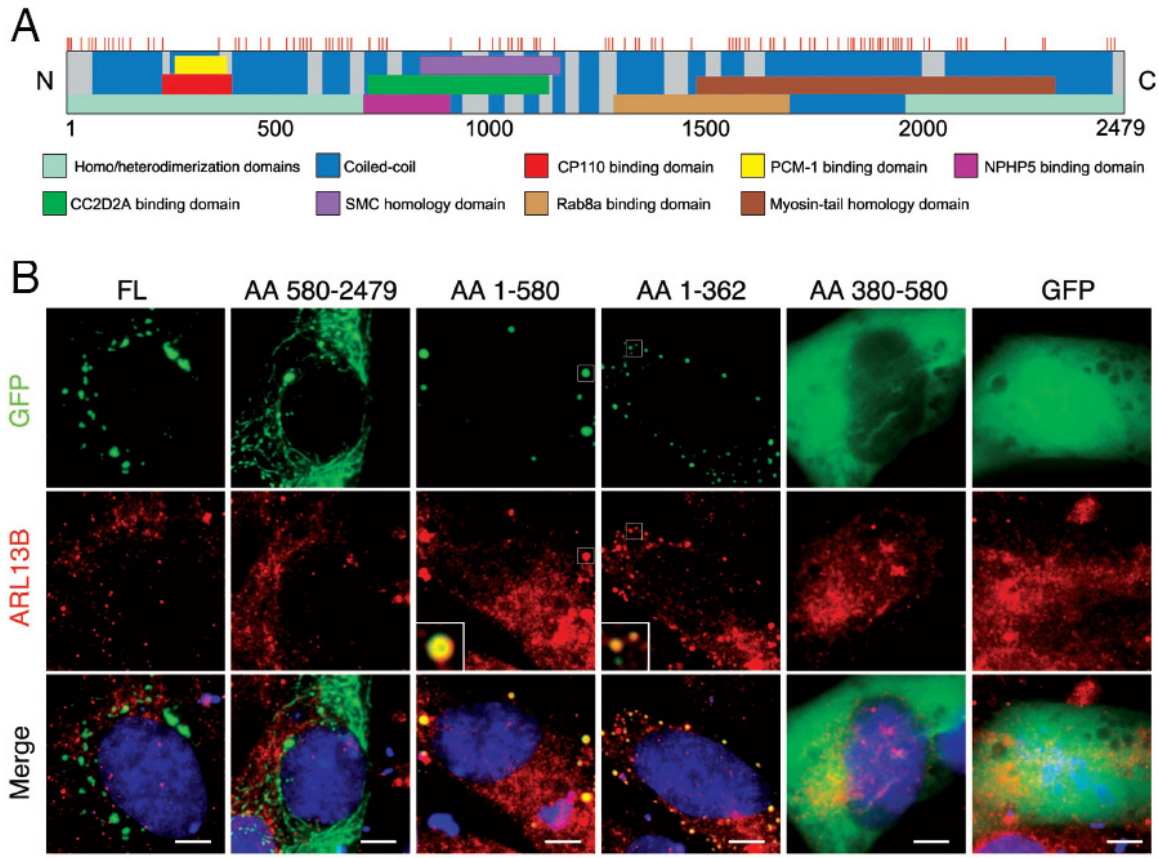

Figure 2.1. CEP290 aa1-362 mediate punctuate localization

(A) Scale representation of human CEP290. Known human CEP290 mutations are noted by red tick marks. The indicated domains and mutations are adapted from (Coppieters et al., 2010).

(B) Fluorescence microscopy images showing the localization pattern of GFP fusions of full-length (FL) and truncated CEP290 constructs in cycling hTERT-RPE1 cells. Cells were stained with an antibody against ARL13B and with DAPI. Scale bars are 5 µm. Insets show 3x magnified views of areas (in boxes) of colocalization between CEP290 truncations and ARL13B. Pearson correlation coefficient for colocalization between ARL13B and CEP290 aa 1-580 is 0.53 and for CEP290 aa 1-362 is 0.65.

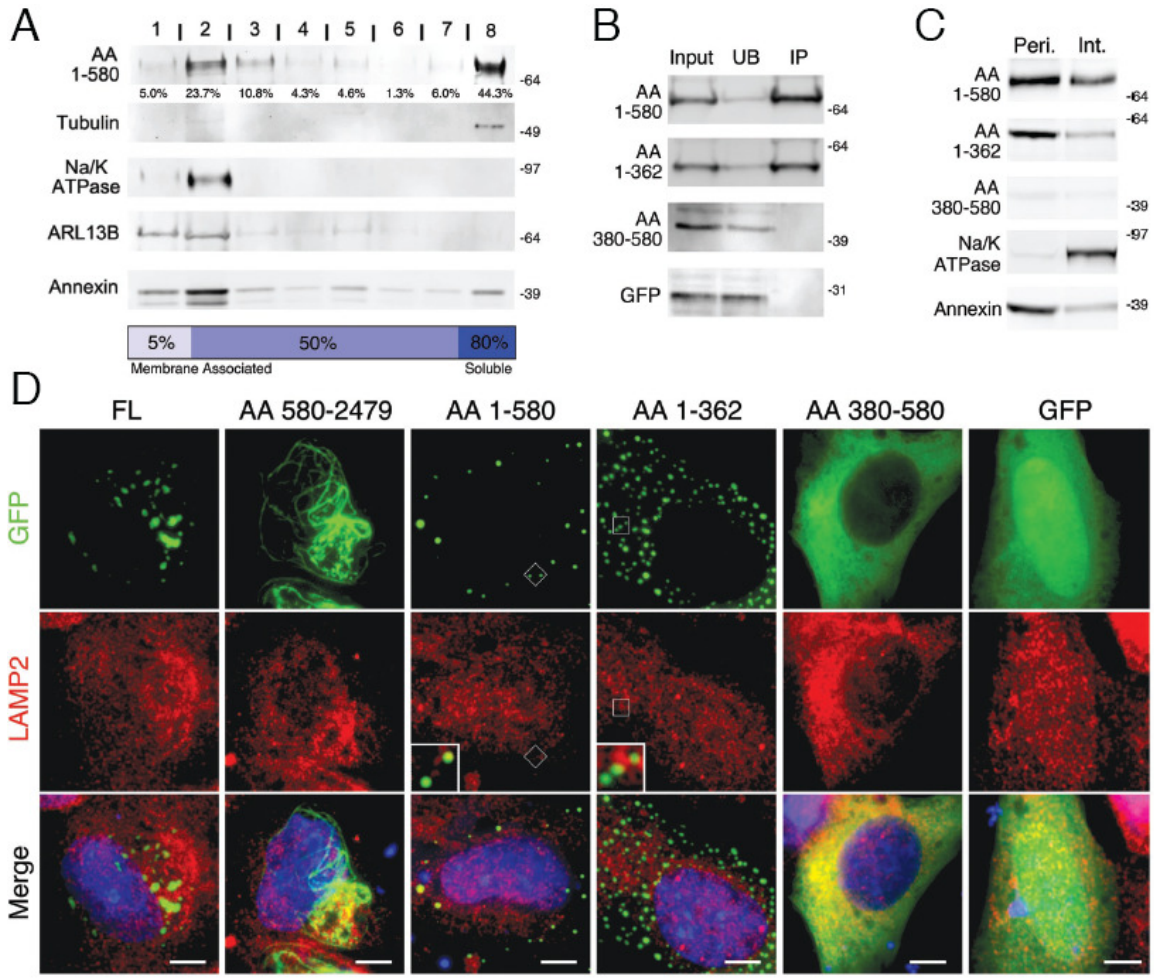

Figure 2.2. CEP290 aa1-362 mediate peripheral membrane association

(A) Equal amounts of each of five fractions, beginning from the top (1) and ending at the bottom (8) of the sucrose gradient of a membrane flotation assay performed on hTERT-RPE1 cells overexpressing CEP290 aa 1-580. Sucrose percentages and the percent of CEP290 aa 1-590 found in each fraction are indicated. Blots were probed for GFP to detect CEP290 aa 1-580 and for the indicated controls.

(B) ARL13B positive membranes immunoprecipitated from postnuclear supernatants of hTERT-RPE1 cells expressing the indicated GFP-fused CEP290 truncations or GFP alone were probed with an anti-GFP antibody. 15% of the input fraction, 15% of the unbound fraction (UB) and the entire immunoprecipitated fraction (IP) were loaded.

(C) The peripheral (Peri.) and integral (Int.) membrane protein fractions of hTERT-RPE1 cells expressing the indicated GFP-fused CEP290 truncations were isolated and probed for GFP and for the indicated controls.

(D) Fluorescence microscopy images showing the localization pattern of GFP-fused full-length (FL) and truncated CEP290 constructs in hTERT-RPE1 cells stained for LAMP2 and with DAPI (blue). Scale bars are 5 µm. Insets show 3x magnified views of areas (in boxes) illustrating lack of colocalization between CEP290 truncations and LAMP2.

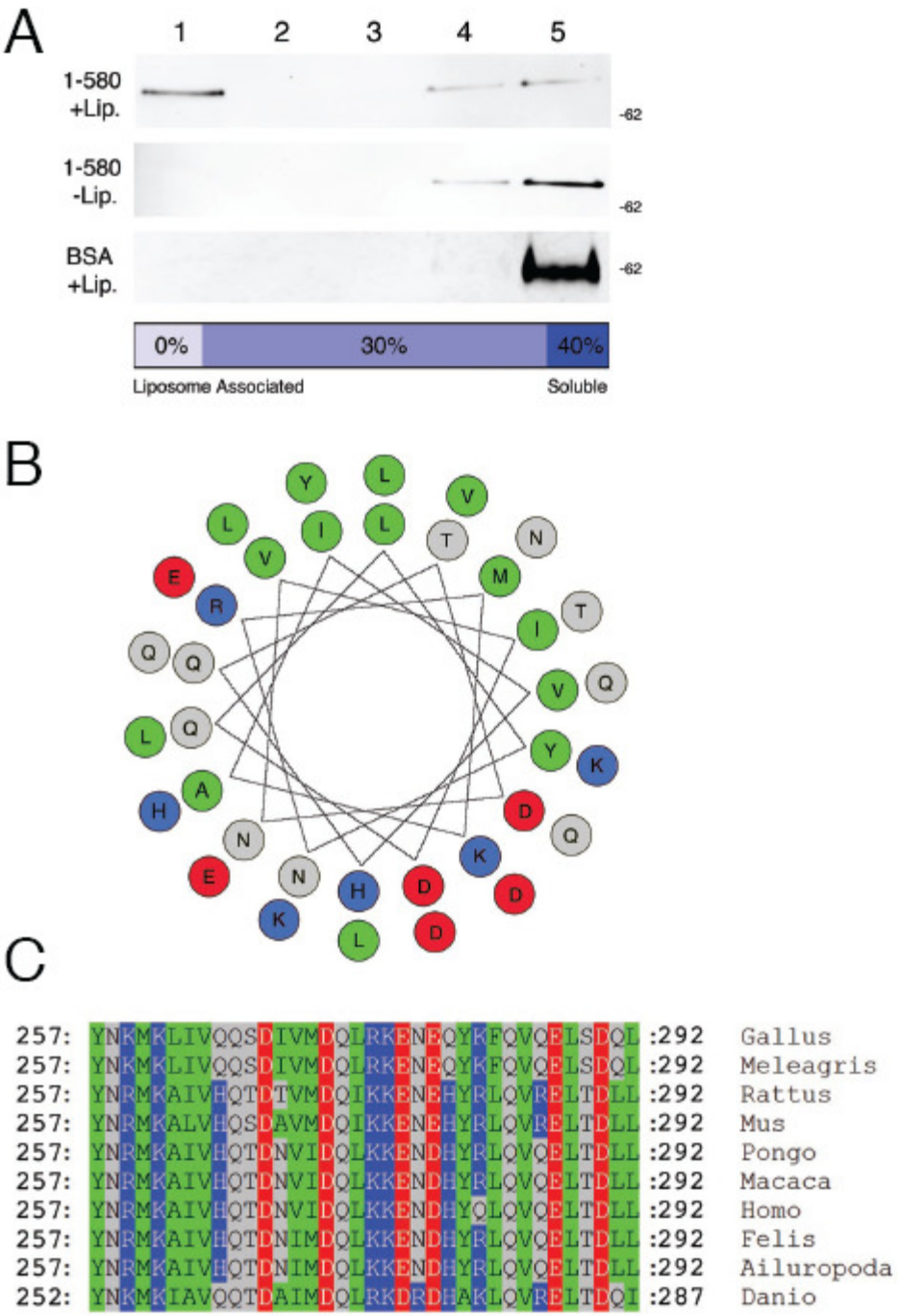

Figure 2.3. CEP290 aa1-362 mediates direct membrane binding

(A) Liposome co-flotation assays performed on purified CEP290 aa 1-580, both with and without liposomes, and with BSA as a control. Equal amounts of each of five fractions, beginning from the top (1) and ending at the bottom (5) of the sucrose gradient were analyzed. Sucrose percentages and the expected protein composition of each fraction are indicated.

(B) Helical wheel projection of CEP290 aa 257-292. Red circles represent negatively charged amino acids, blue circles represent positively charged amino acids, grey circles represent polar, uncharged amino acids, and green circles represent nonpolar amino acids.
(C) Multiple sequence alignment of CEP290's predicted amphipathic helix. Amino acids are color-coded using the same scheme as in panel F.

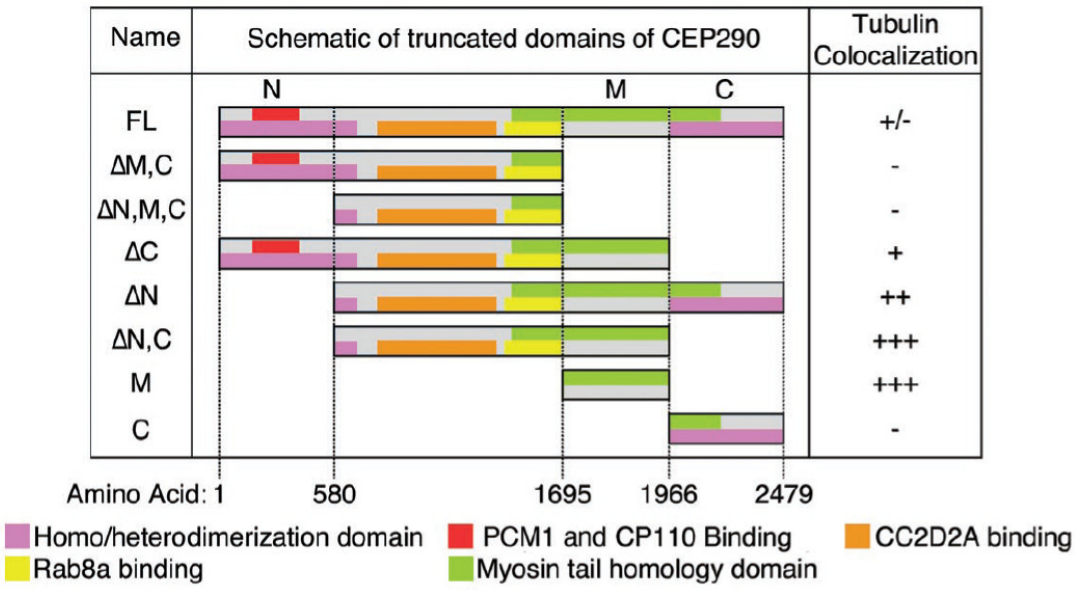

Figure 2.4. Schematic of CEP290 truncations

Scale representations of the CEP290 truncations tested in Figures 2.5, 2.6, and 2.7. Included is a summary of the extent of colocalization with tubulin, rated on a scale ranging from negative (-) to highly positive (+++).

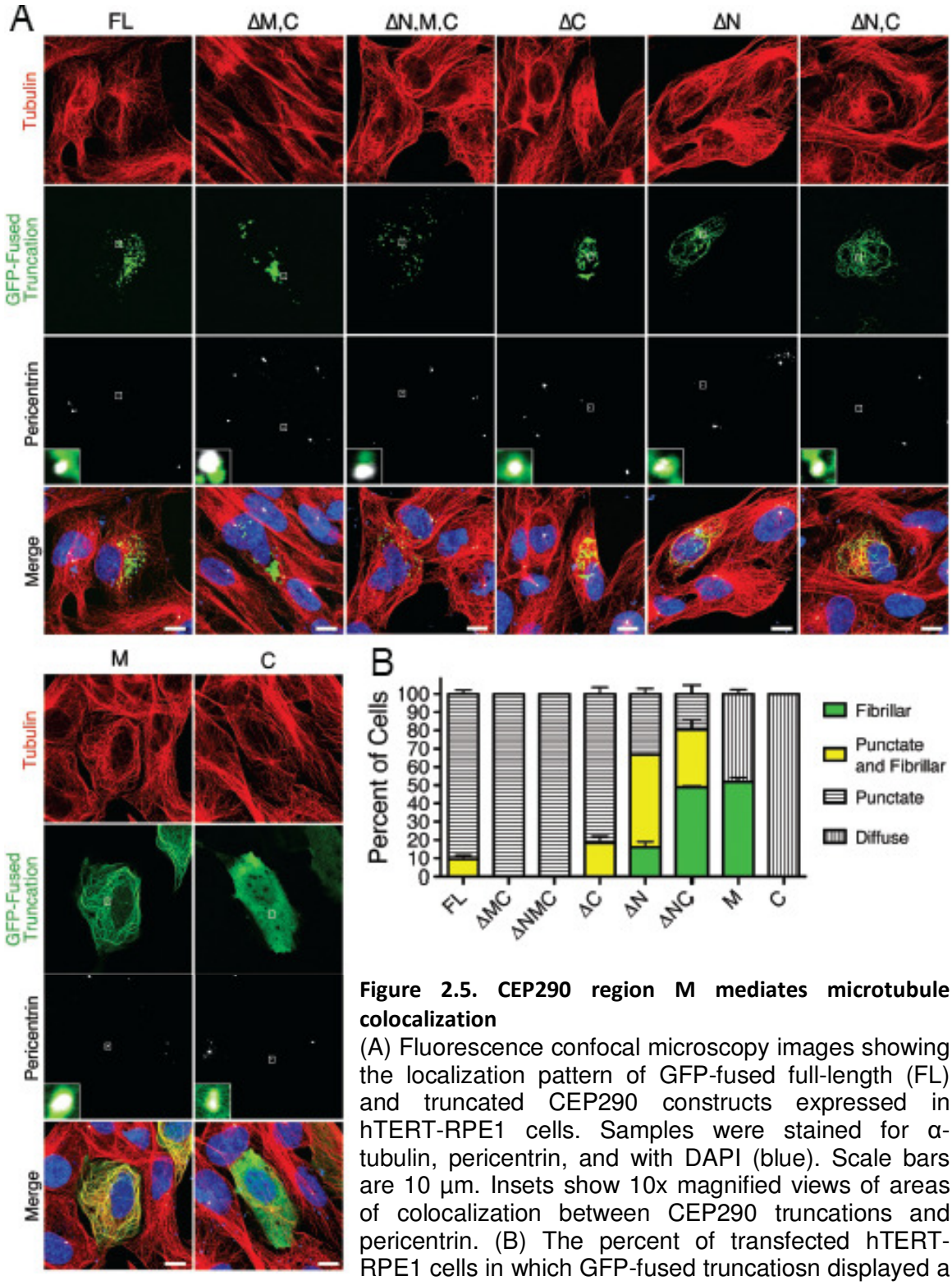

Figure 2.5. CEP290 region M mediates microtubule colocalization

(A) Fluorescence confocal microscopy images showing the localization pattern of GFP-fused full-length (FL) and truncated CEP290 constructs expressed in hTERT-RPE1 cells. Samples were stained for α-tubulin, pericentrin, and with DAPI (blue). Scale bars are 10 µm. Insets show 10x magnified views of areas of colocalization between CEP290 truncations and pericentrin. (B) The percent of transfected hTERT-RPE1 cells in which GFP-fused truncatiosn displayed a fibrillar localization pattern. At least 100 cells were counted per experiment. Data are presented as mean ± SD, n=3.

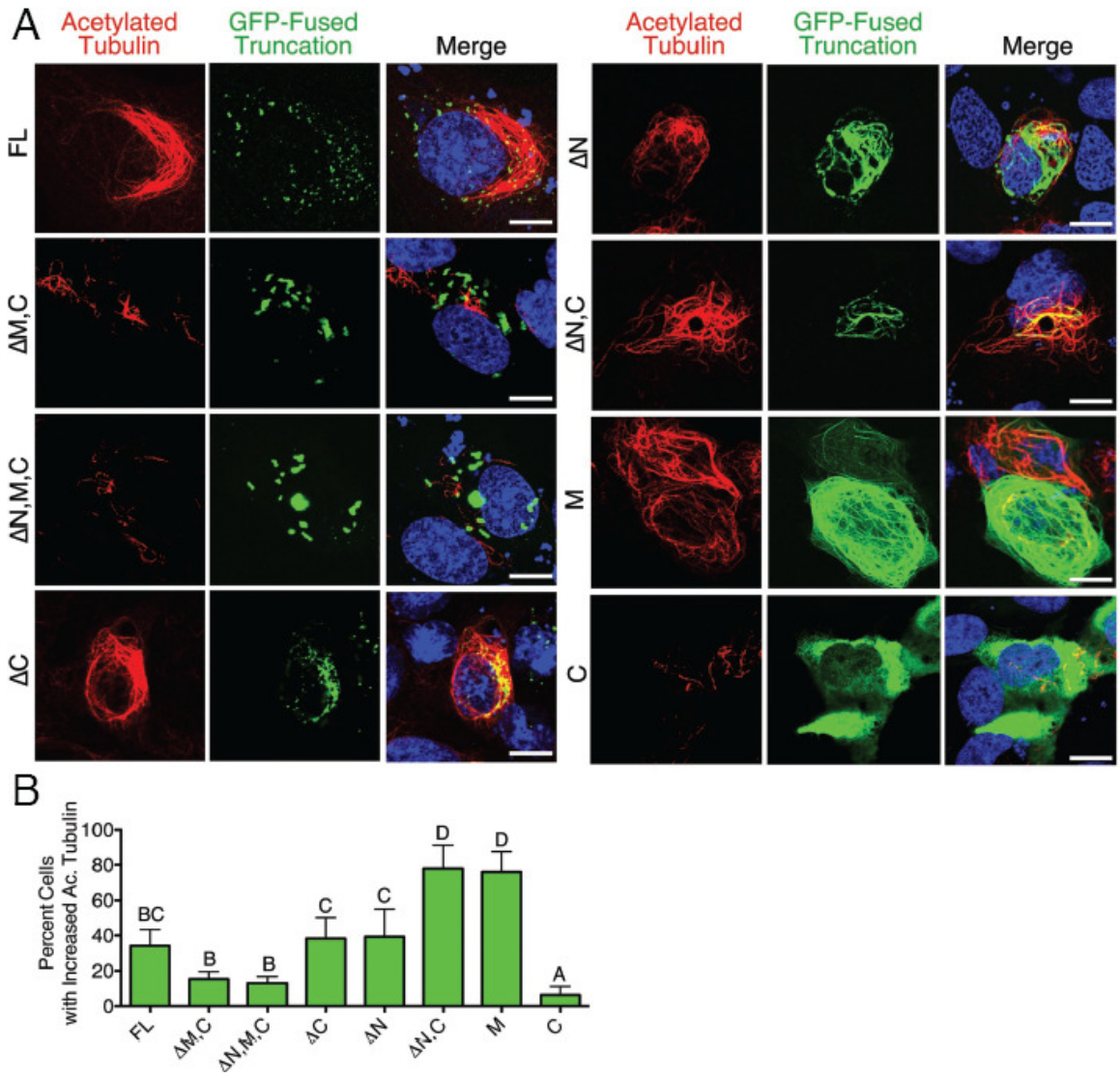

Figure 2.6. CEP290 region M mediates tubulin acetylation

(A) Representative confocal fluorescence microscopy images of GFP-fused full-length (FL) and truncated CEP290 constructs expressed in hTERT-RPE1 cells stained for acetylated α-tubulin and with DAPI (blue). Scale bars are 10 μm.

(B) Percent of 293T cells showing an increase in the intensity of acetylated α-tubulin staining following transfection with CEP290 constructs. 100 transfected cells were counted per experiment. Data are presented as mean ± SD, n=5. Means with different letters are significantly different.

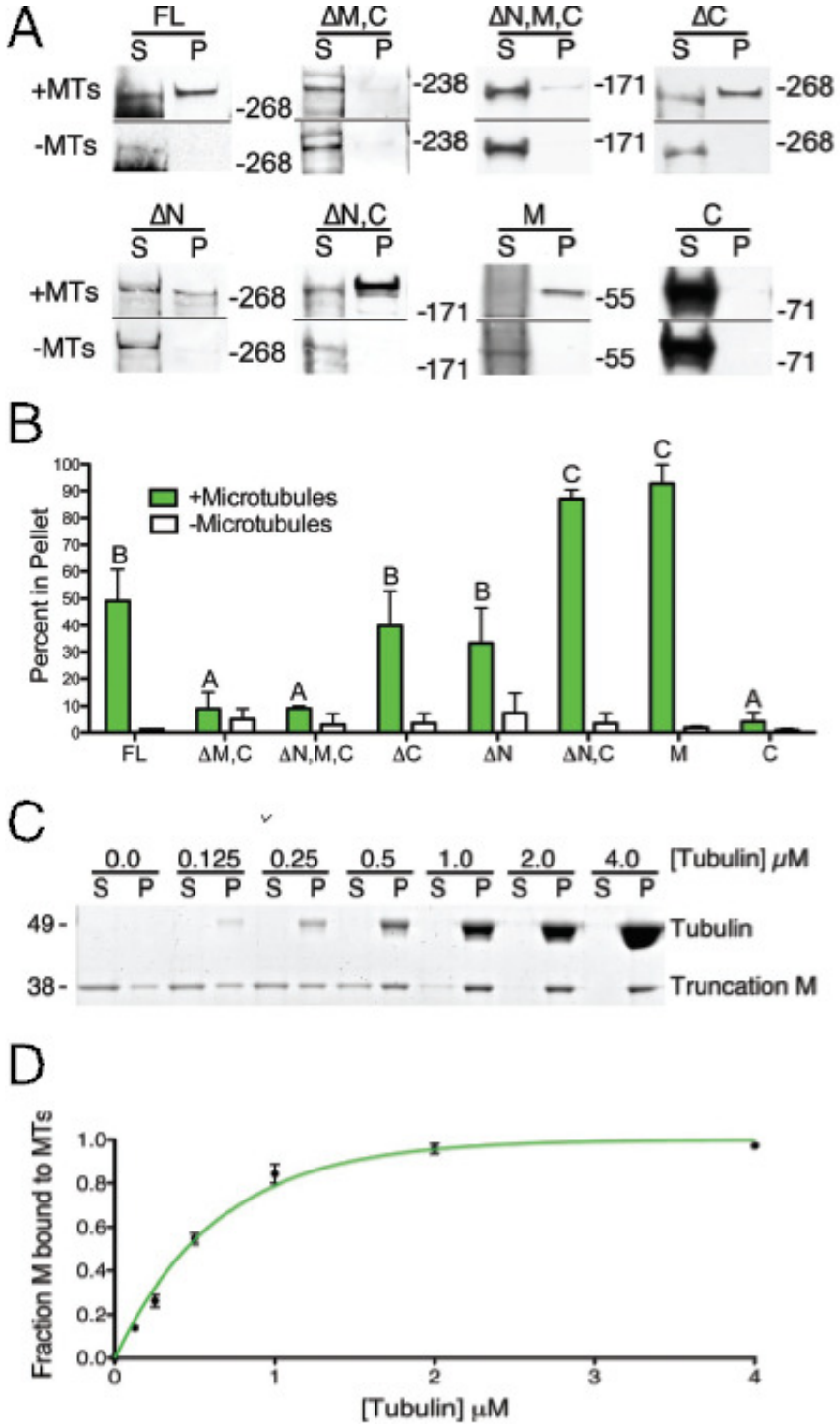

Figure 2.7. CEP290 region M mediates direct microtubule binding

(A) Microtubule co-sedimentation assays for in vitro transcribed and translated CEP290 truncations. The supernatants (S) and microtubule pellets (P) are shown for assays performed both with (+MT) and without (-MT) microtubules.

(B) Percent of each truncation co-sedimenting with microtubules. Data are presented as mean ± SD, n=3. Means with different letters are significantly different.
(C) Coomassie-stained gel of microtubule co-sedimentation assays performed with purified CEP290 truncation M and increasing concentrations of microtubules. The supernatants (S) and microtubule pellets (P) are shown.
(D) Binding curve of microtubules cosedimentation assays as in panel E. The fraction of truncation M present in the pellet in the absence of microtubules was subtracted from all data points. Data are presented as means ± SD, n=3.

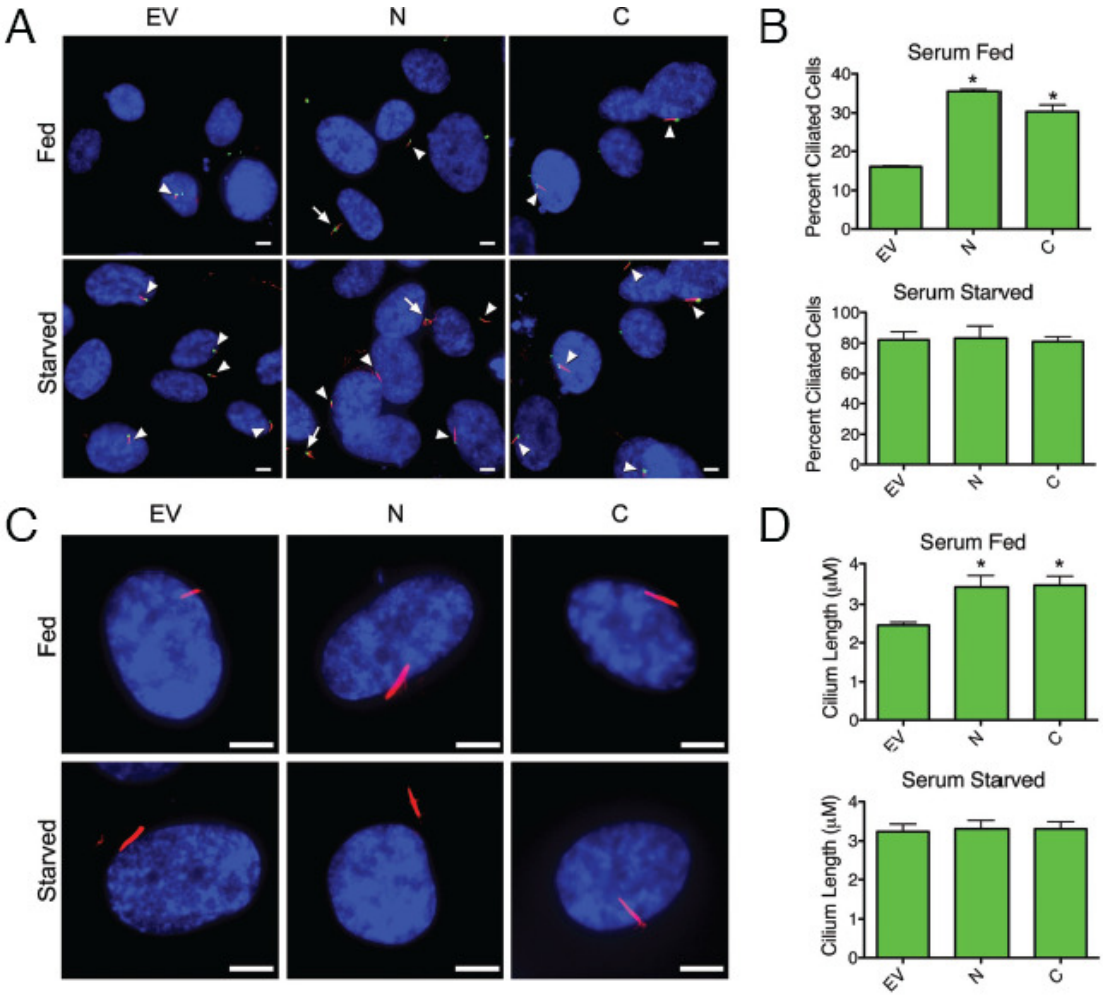

Figure 2.8. Overexpression of either N- or C-terminal regulatory region of CEP290 ablates normal CEP290 inhibition

(A) Fluorescence microscopy fields of hTERT-RPE1 cells transduced with lentiviral empty vector (EV), or vectors encoding either the N- (aa 1-580) or C-terminus (aa 1966-2479) of CEP290. Cells were stained for acetylated α-tubulin (red) and pericentrin (green) to detect primary cilia and with DAPI. Arrowheads indicate primary cilia. Arrows indicate cells with multiple axonemes originating from the same focus of pericentrin. Scale bars are 10 μm.

(B) Percent of lentivirus-treated cells forming primary cilia. Data are presented as mean ± SD, n=3. 100 cells were counted per experiment.

(C) Fluorescence microscopy images of hTERT-RPE1 cells transduced with lentiviral vectors as in panel A. Cells were stained for acetylated α-tubulin to detect primary cilia and with DAPI. Scale bars are 5 μm.

(D) Average primary cilium length for hTERT-RPE1 cells as in panel C. Data are presented as mean ± SD, n=3. A total of at least 150 cilia were measured per condition.

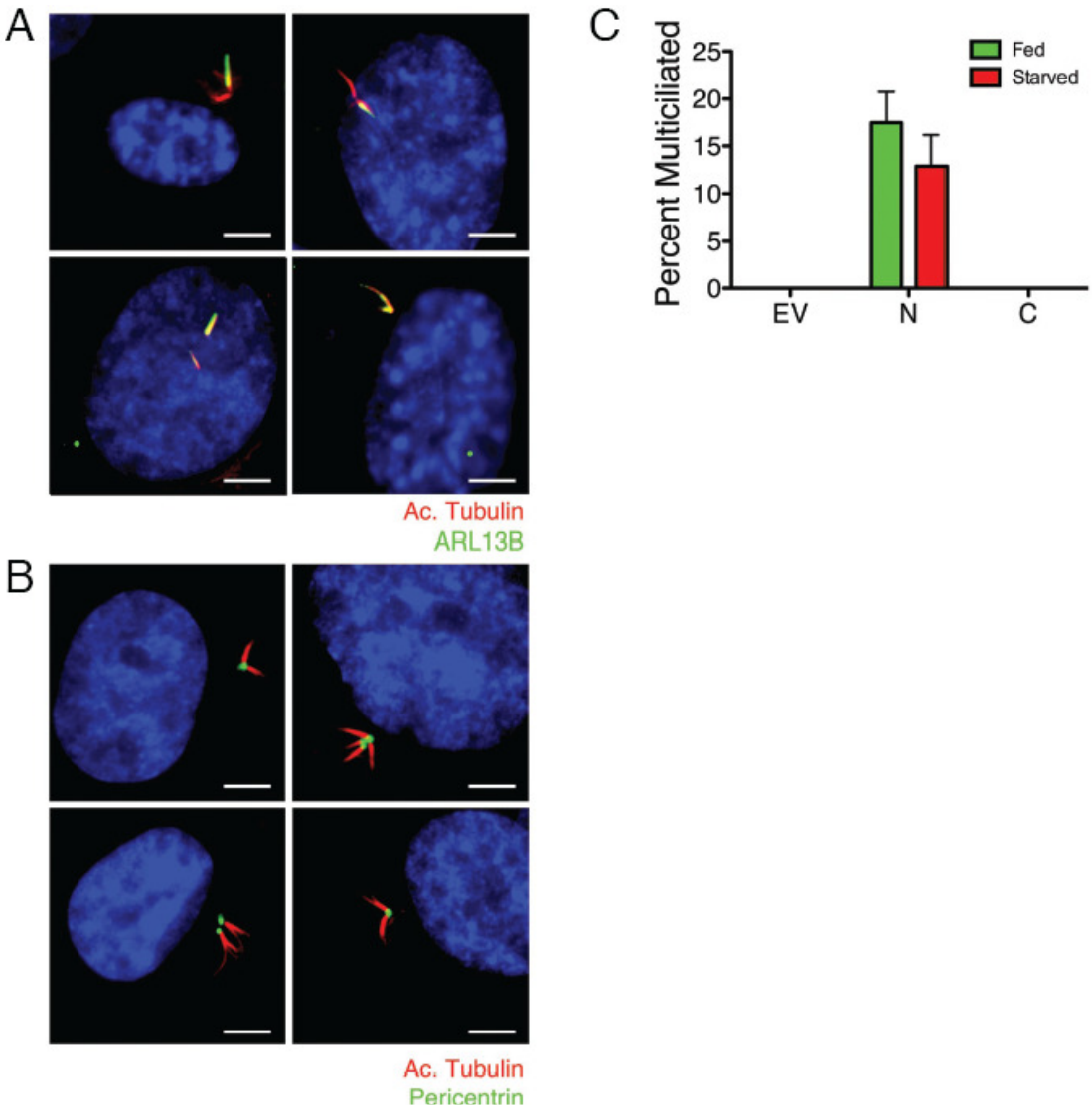

Figure 2.9. Overexpression of the N-terminal regulatory region of CEP290 results in multiple ciliary axonemes

(A-B) Fluorescence microscopy images of hTERT-RPE1 cells that formed multiple cilia after transduction with lentiviral vector encoding the N-terminus of CEP290. Cells were stained for either ARL13B or pericentrin, and for acetylated α-tubulin and with DAPI (blue). Scale bars are 5μm.

(C) Percent of lentivirus transduced hTERT-RPE1 cells forming multiple cilia. At least 100 cells were counted per experiment. Data are presented as mean ± SD, n=3.

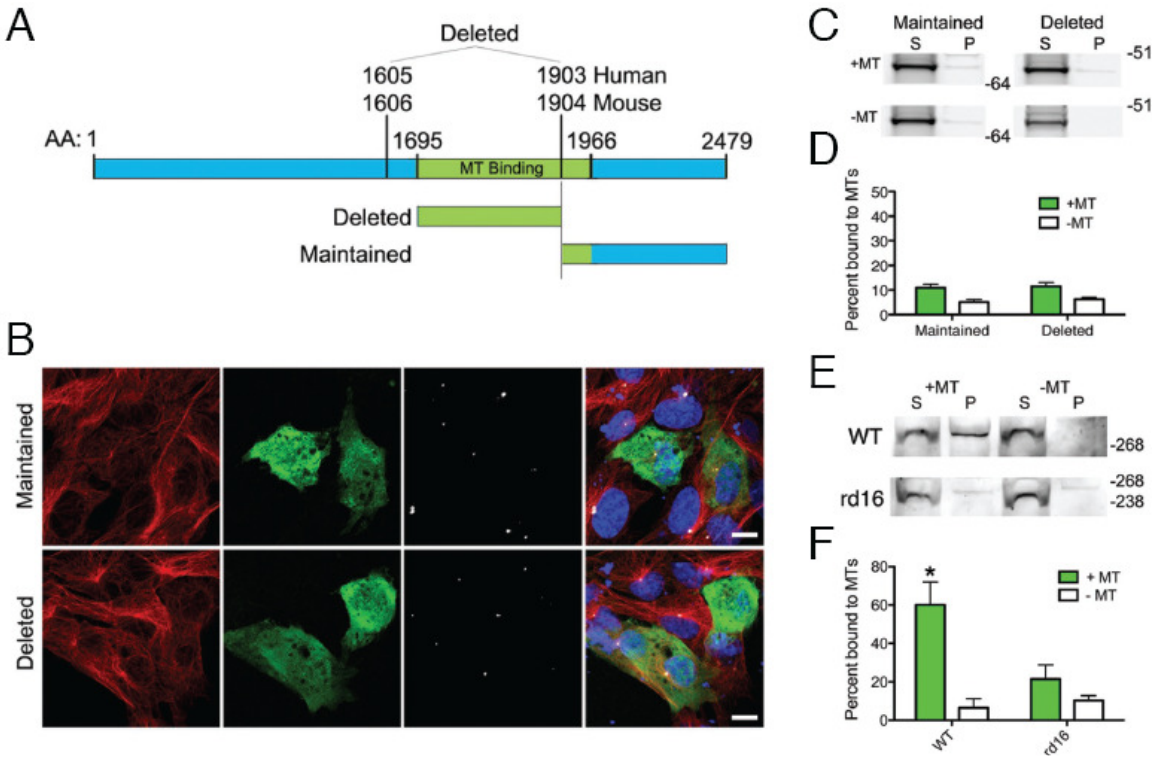

Figure 2.10. An in-frame deletion in *Cep290* in the rd16 mouse ablates Cep290's microtubule binding activity

(A) Schematic representation of the microtubule binding region of human CEP290 in relation to the rd16 mouse deletion (Chang et al., 2006). Truncations of CEP290 representing the part of the microtubule binding region deleted in the rd16 mouse and the part of the microtubule binding region maintained in the rd16 mouse were created as shown.

(B) Confocal fluorescence microscopy images showing the localization pattern of GFP-tagged "Maintained" and "Deleted" CEP290 truncations. Cells were stained for α-tubulin (red), pericentrin (white) and with DAPI (blue). Scale bars are 10 µm.

(C) Microtubule co-sedimentation assays for in vitro transcribed and translated "Maintained" and "Deleted" CEP290 truncations. The supernatant (S) and microtubule pellet (P) fractions are shown in assays performed both with (+MT) and without (-MT) microtubules.

(D) Percent of each truncation co-sedimenting with microtubules. Data are presented as mean ± SD, n=2.

(E) Microtubule co-sedimentation assays performed on full-length WT and rd16 Cep290 from mouse brain homogenate. The supernatant (S) and microtubule pellet (P) fractions are shown in assays performed on samples induced to polymerize microtubules (+MT) and samples treated to prevent microtubule polymerization (-MT).

(F) Percent of WT and rd16 Cep290 co-sedimenting with microtubules. Data are presented as mean ± SD, n=3. Asterisks indicate statistical significance over –MT samples.

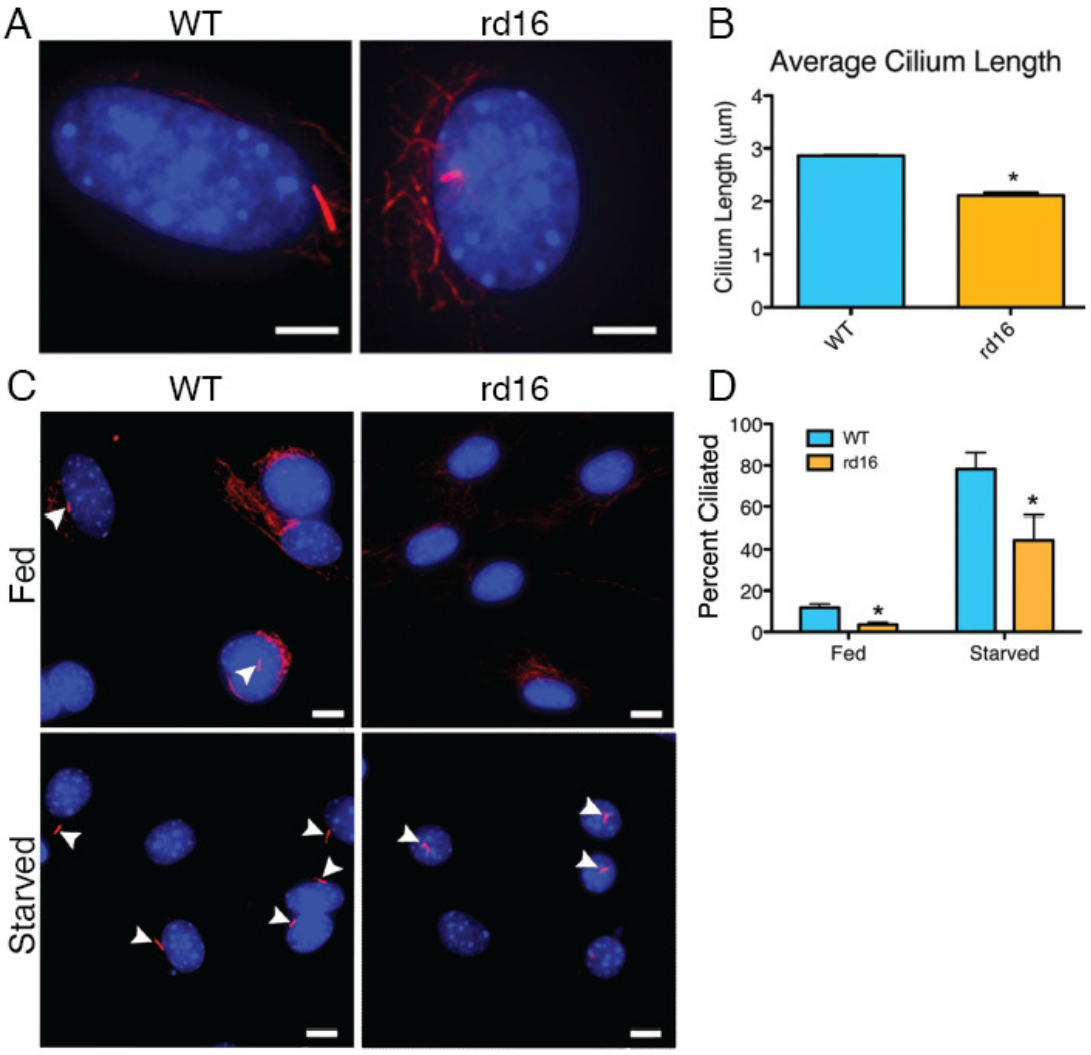

Figure 2.11. rd16 mouse fibroblasts are deficient in primary cilium formation

(A) Fluorescent microscopy images of serum-starved WT and rd16 primary dermal fibroblasts stained for acetylated α-tubulin (red) to identify primary cilia, and stained with DAPI (blue). Scale bars are 5 µm.

(B) Average cilium length of serum starved WT and rd16 primary dermal fibroblasts. Quantification was based on separate experiments on fibroblasts coming from 3 different animals per genotype. At least 50 cilia were measured per experiment, and a total of 400 cilia were measured for both the WT and rd16 fibroblasts. Data are presented as mean ± SD, n=5.

(C) Fluorescence microscopy fields of WT and rd16 primary dermal fibroblasts stained for acetylated α-tubulin (red) to identify primary cilia, and stained with DAPI (blue). Fibroblasts were grown in media with (Fed) or without (Starved) serum. Arrowheads indicate primary cilia. Scale bars are 10 µm.

(D) Percent of WT and rd16 primary dermal fibroblasts that form primary cilia in serum fed and serum starved conditions. Quantification was based on separate experiments on fibroblasts coming from 3 different animals per genotype. At least 100 cells were counted per experiment. Data are presented as mean ± SD, n=5.

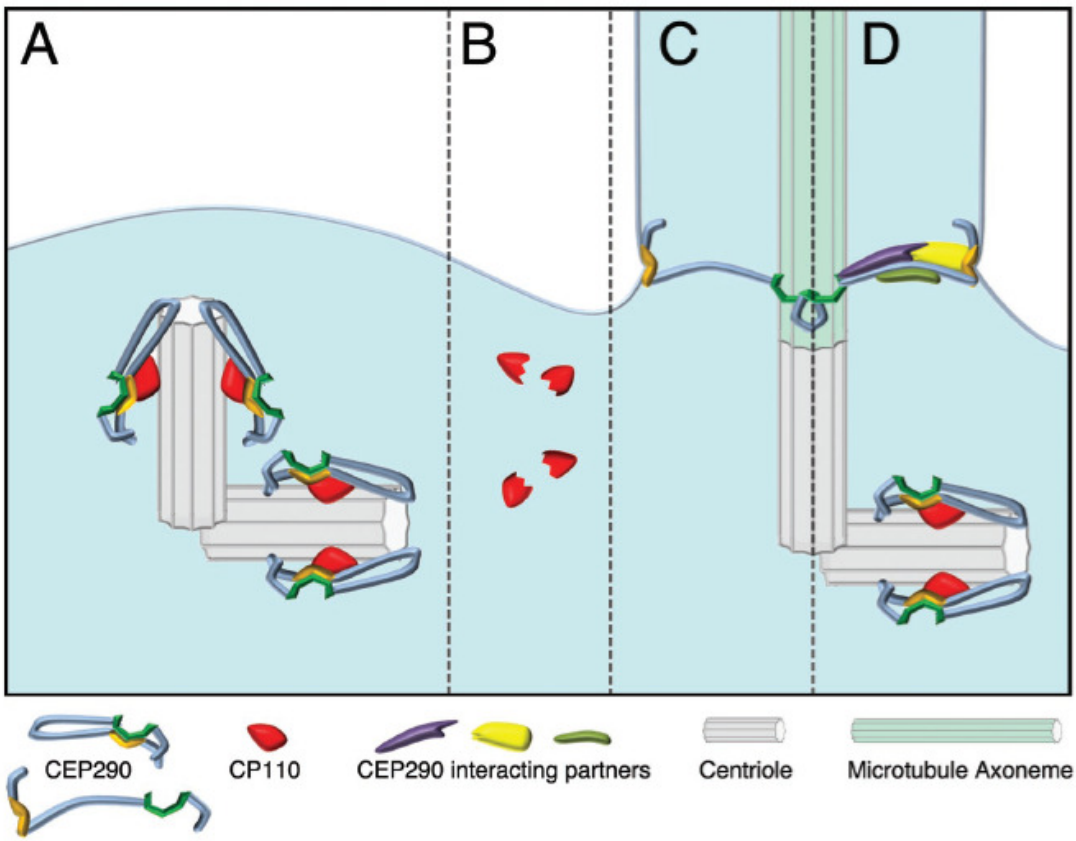

Figure 2.12. A speculative model for CEP290 activity at the primary cilium
CEP290 is maintained in a closed, inhibited state by its N- and C-termini and CP110 during the cell cycle (A). Upon degradation of CP110 at the mother centriole (B), a conformational change in the protein frees and activates CEP290's membrane binding (orange) and microtubule binding (green) domains (C) and CEP290 is able to recruit additional interacting partners to initiate IFT and ciliogenesis (D).

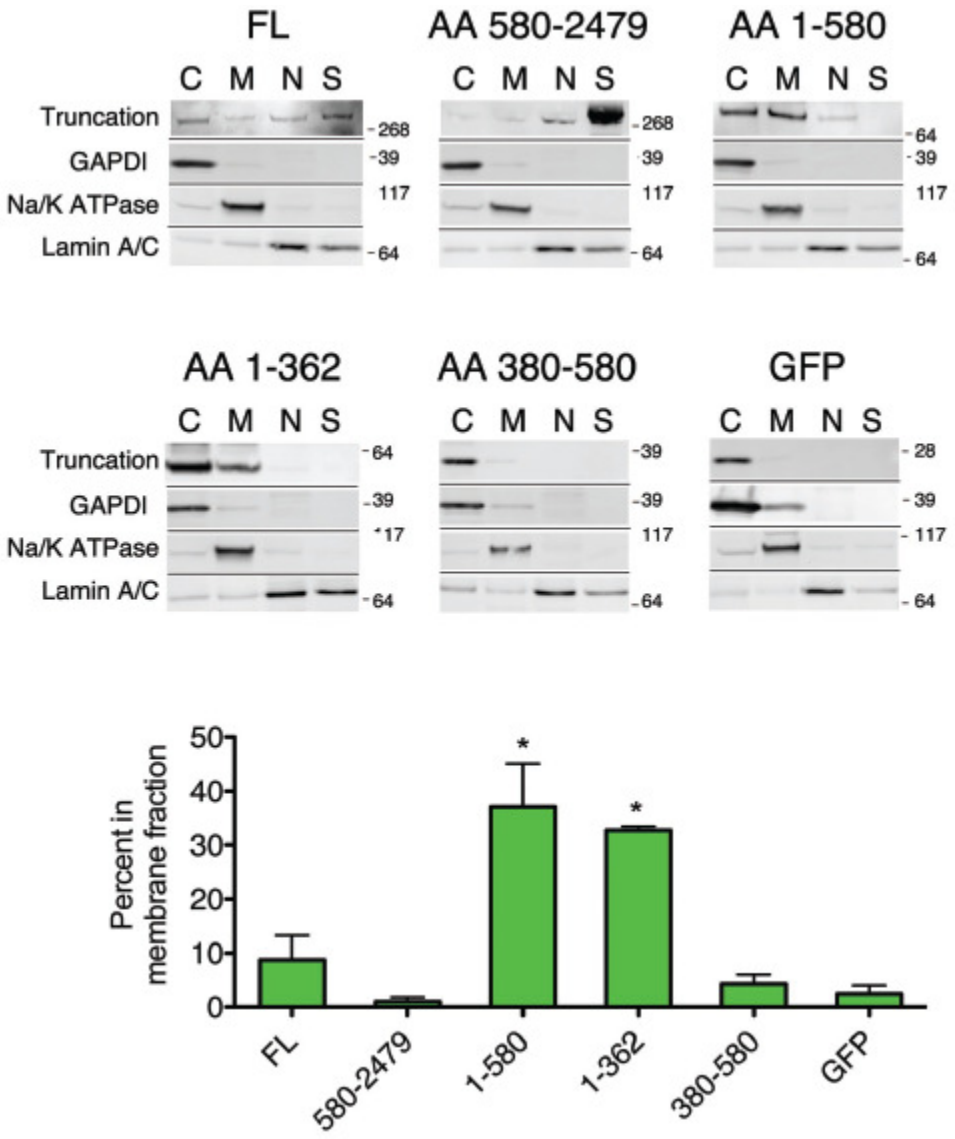

Figure 2.13. Truncation of CEP290's C-terminus increases CEP290 membrane association
(A) Subcellular fractionation experiments performed on 293T cells expressing CEP290 constructs. Cells were fractionated into cytoplasmic (C), membrane (M), nuclear (N), and cytoskeletal (S) fractions and analyzed by western blotting. Relevant molecular weight markers are shown in kDa.
(B) Percent of each truncation present in the membrane fraction. Data are presented as mean ± SD, n=3. Asterisks indicate statistical significance over GFP-alone.

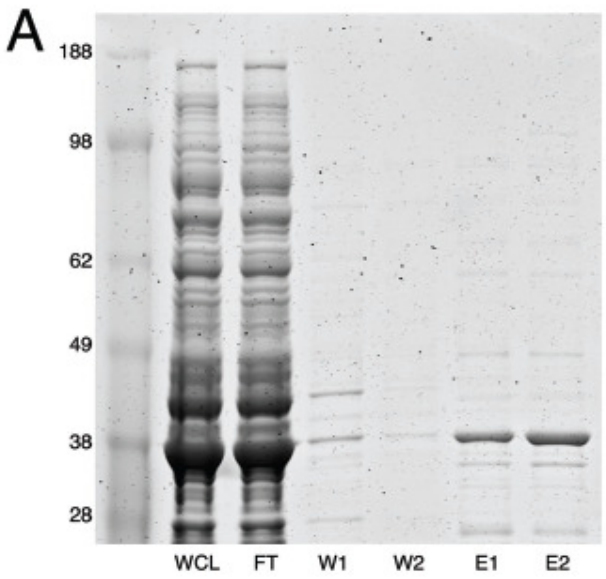

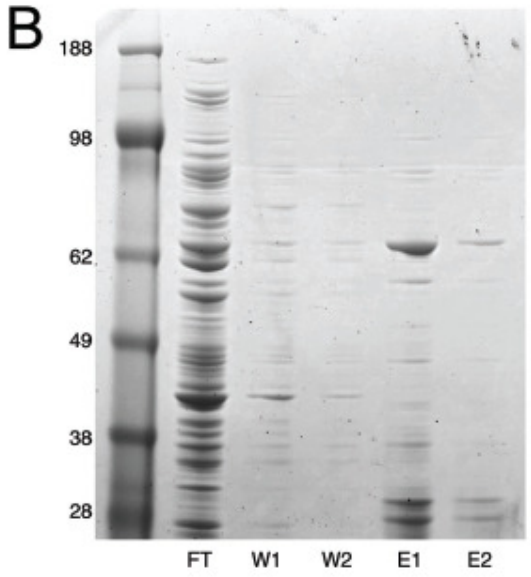

Figure 2.14. Expression and purification of CEP290 truncation mutants in bacterial cells
CEP290 regions M (A) and aa 1-580 (B) were expressed from pDest-527 in E.coli BL21(DE3)pLysS by IPTG induction and purified by nickel affinity chromatography. WCL is the whole bacterial cell lysate. FT is the fraction of lysate that did not bind to the Ni-NTA resin. W1 and W2 are the material that washed off the resin during the first and second washes, respectively. E1 is the first elution fraction. E2 is the second elution fraction. Relevant molecular weights are indicated in kDa

CHAPTER 3: A NEW MODEL FOR CEP290 DISEASE PATHOGENESIS

Theodore G. Drivas,[1,*] Adam Wojno, [1,*] Jean Bennett, [1] Bud Tucker, [2] and Edwin Stone[2]

1. Kirby Center for Molecular Ophthalmology, Perelman School of Medicine, University of Pennsylvania, Philadelphia, PA 19104, USA
2. Department of Ophthalmology and Visual Sciences , University of Iowa Carver College of Medicine , Iowa City , IA 50309, USA

* These authors contributed equally to the work

Introduction

Mutations in the ciliopathy disease gene *CEP290* are associated with a spectrum of devastating and phenotypically distinct human disease syndromes ranging in severity from isolated retinal degeneration to embryonic lethality.(Perrault et al., 2007) The pathology observed in these diseases is due to CEP290's essential role in the development and maintenance of the primary cilium (D'Angelo and Franco, 2009), but how different mutations in the same gene can lead to such dramatically different phenotypes remains unknown. Here we have developed a novel model that, taking into account the phenomenon of basal exon skipping, accurately predicts patient CEP290 protein levels in a mutation-specific fashion. Predicted CEP290 protein levels were found to robustly correlate with disease severity for all reported CEP290 patients. Applying our model to CC2D2A, another similar ciliopathy disease gene, we found the same correlation to hold true. Our model establishes a new paradigm for the pathogenesis of the ciliopathies and, for the first time, helps to explain the diversity of ciliopathy disease in general.

Results

Rationale

Mutations in the gene *CEP290* are associated with a spectrum of devastating and phenotypically distinct human syndromes ranging in severity from the isolated retinal degeneration of Leber congenital amaurosis (LCA) (den Hollander et al., 2008; Perrault et al., 2007) to the cerebellar, renal, and retinal disease of the Joubert syndrome related disorders (JSRD)(Brancati et al., 2007; Sayer et al., 2006; Valente et al., 2006) and the multi-organ system pathology and embryonic lethality of Meckel syndrome (MKS) (Baala et al., 2007). The varied pathology seen in these disease states is thought to be due to CEP290's essential role in the development and maintenance of the primary cilium,(D'Angelo and Franco, 2009; Waters and Beales, 2011) a cellular organelle critical for signaling and growth,(Davenport et al., 2007; Han et al., 2009; Wong et al., 2009) but how different mutations in the same gene can cause such drastically different phenotypes remains unknown.

CEP290 pathology is almost always associated with truncating, rather than missense mutations.(Coppieters et al., 2010) This has lead to a number of theories as to how different truncating mutations might lead to different diseases, none of which, unfortunately, have proven true. It has also been reported that the truncating p.R151X mutation in exon 7 of the *CEP290* gene induces skipping of the mutated exon, resulting in the production of small amounts of a near-full-length *CEP290* message containing an intact open reading frame (Littink et al., 2010). We speculated that such nonsense-induced alternative splicing, or NAS (Chang et al., 2007; Puisac et al., 2013; Vuoristo et al., 2004; Wang et al., 2002; Figure 1a), might lead to selective exon skipping and the partial correction of truncating mutations in *CEP290* patients in

general, with levels of full-length and near-full-length CEP290 protein correlating with disease severity.

Formulating a model

To formulate and assess our model we first classified all 142 known human *CEP290* mutations(Coppieters et al., 2010; Halbritter et al., 2012; Otto et al., 2011; Papon et al., 2010; Wiszniewski et al., 2011; Yzer et al., 2012) based on their predicted coding effects (Figure 1b). Mutations were divided into three categories – mild, moderate, and severe. Mild mutations (green) were those that were predicted to have only small or moderate effects on the levels of CEP290 protein. These included all known *CEP290* missense mutations and the common intronic c.1655A>G mutation, which results in only a roughly 50% reduction in normal *CEP290* transcript (den Hollander et al., 2006).

All truncating mutations were classified as either moderate or severe. Moderate mutations (orange) were those that resulted in the introduction of a premature stop codon (due either to a missense, frame-shift, or splicing mutation) within an exon beginning and ending in the same reading frame. Transcripts including the mutated exon and premature stop codon should be subject to nonsense mediated decay (NMD) (Baker and Parker, 2004; Maquat, 2004), resulting in little or no protein production, whereas those few transcripts skipping the mutated exon, through the process of NAS, should result in the production of low levels of near-full-length CEP290 (Figure 1a.I-II).

Severe mutations (red), on the other hand, were those that resulted in the introduction of a premature stop codon within an exon beginning and ending in different reading frames. Thus transcripts either including the mutated exon or those skipping the mutated exon (resulting in a frame-shift) should both contain premature stop codons and be subject to NMD, resulting in no full length or near-full-length CEP290 protein (Figure 1a.III-IV).

Accurate correlation of CEP290 patient phenotype with genotype

Using this classification system we established a model for the prediction of total full-length and near-full-length CEP290 protein levels for any patient, given both *CEP290* disease alleles (Figure 1c). Hypothesizing that the predicted protein levels might correlate with different *CEP290* disease phenotypes, we categorized different phenotypes by predicted protein level as part of our model. Applying our model to all 231 published *CEP290* patients(Coppieters et al., 2010; Halbritter et al., 2012; Otto et al., 2011; Papon et al., 2010; Wiszniewski et al., 2011; Yzer et al., 2012) a striking correlation was immediately apparent -- predicted protein levels were significantly associated with disease severity with $p < 0.0001$ (Fisher's exact test). More than 90% of patients with LCA, the least severe *CEP290* phenotype, were predicted to have high to medium levels of CEP290. CEP290 levels in Senior Løken syndrome and Joubert syndrome patients were predicted to be more evenly distributed, from high to low, whereas 100% of Meckel-like and Meckel syndrome patients, with the most severe phenotypes, were predicted to have low to absent CEP290 levels (Figure 2a).

Identification of domains critical to CEP290 function

While predicted protein levels clearly and significantly correlated with the severity of *CEP290* disease, 48 patients presented with phenotypes and genotypes not completely consistent with our model. Examining the mutations harbored by these patients, a pattern quickly became clear. Greater than 70% (n=23) of patients whose phenotypes were worse than what was predicted by our model were found to harbor truncating mutations within exons 6, 9, 40, or 41 (Figure 2b). Although each of these mutations was considered only moderate by our model, each of these patients presented with very severe disease. An explanation for the deleterious nature of these particular mutations immediately became apparent when we mapped them to CEP290's known functional domains – exons 6 through 9 lie at the center of CEP290's recently discovered membrane association domain, while exons 40 and 41 make up the core of CEP290's critical microtubule binding domain (Figure 2c) (Chapter 2; Drivas et al., 2013). Splice variants lacking any of these four exons might escape nonsense mediated decay and result in low levels of near-full length protein, all of which, however, would lack regions critical to CEP290's function. It is interesting to note that a majority of Meckel syndrome and Meckel-like syndrome patients were found to harbor mutations in these particular exons, suggesting that patients expressing low-levels of CEP290 lacking critical functional regions are worse off than those expressing no CEP290 at all. Taking the critical nature of exons 6,9,40, and 41 into account, we modified our model to predict functional, rather than absolute, levels of CEP290. Applying this model to all published *CEP290* patients predicted functional protein levels were again significantly associated with disease severity with $p < 0.0001$ (Fisher's exact test).

Validating the model

To more rigorously interrogate our model we assembled a cohort of *CEP290* patients with diverse genotypes and symptoms. These patients and their records were carefully examined by a single clinician masked to the patients' genotypes (Figure 2a). We applied our modified model to each of the patients and saw that, again, predicted functional CEP290 levels accurately correlated with patient phenotype. All patients predicted to have high to medium levels of CEP290 were diagnosed only with LCA, while patient 582, predicted to have very low levels of CEP290 protein, carried a diagnosis of Joubert syndrome with retinal degeneration. Interestingly, this small but well characterized cohort of patients revealed an even finer correlation between predicted protein levels and patient phenotypes. Patient 54, predicted to have high levels of CEP290, was found to have a visual acuity of 20/80, the best of the patients we looked at. Similarly, patients 62, 619, and 620, all predicted to have medium levels of CEP290 (with a mild/moderate genotype), were found to have at least some residual light perception despite having advanced retinal degeneration. On the other hand, patients 294 and 182, both predicted to have medium levels of CEP290 protein, but with mild/severe genotypes, were found to have no residual light perception.

Accurate prediction of CEP290 protein levels

To confirm that the protein levels predicted by our model correlated with actual CEP290 protein levels, we analyzed CEP290 levels in primary dermal fibroblasts from each of these patients and from three normal controls by western blotting (Figure 3b, c). Strikingly, CEP290 protein levels perfectly correlated with the levels predicted by our model – patient 54, predicted to have high

protein levels, was found to have roughly 50% of normal levels of CEP290. Patients predicted to have medium protein levels were found to have roughly 33% of normal levels of CEP290. Patient 582, predicted to have very low protein levels, was found to have only 8.5% of normal CEP290 levels (Figure 3d).

CEP290 basal exon skipping is a common occurrence

To test whether the mechanism of NAS could be the cause of the low levels of CEP290 protein detected in our experiments we designed nested PCR primers to selectively amplify across the exon junctions between *CEP290* exons 5, 6, and 7. Suspecting that patient 182 (known to harbor a truncating mutation in *CEP290* exon 6) might produce small amounts of *CEP290* transcript skipping exon 6, as per our model, we used these primers to amplify through the exon 6 splicing junctions for each of our patients and controls. To our surprise, we discovered that for each patient and control a small amount of *CEP290* transcript lacking exon 6 was detectable (Figure 3.4), indicating that basal-level exon skipping (BES) is a common occurrence, even outside of the context of nonsense mutations. Such basal exon skipping is a plausible mechanistic explanation for the levels of full-length and near-full-length CEP290 protein we detected in our patients, suggesting that the basal skipping of exons occurs with some frequency in all the CEP290 patients that we investigated.

Applying the model to other ciliary disease proteins

To determine if the implications of BES and our findings extended beyond *CEP290* and to other disease genes we applied our model to Coiled-Coil and C2 Domain containing 2A (*CC2D2A*), a ciliopathy gene that, similar to *CEP290*, is associated with a spectrum of clinical presentations (Bachmann-Gagescu et al., 2012; Doherty et al., 2010; Gorden et al., 2008; Mougou-Zerelli et al., 2009; Noor et al., 2008; Tallila et al., 2008). Even without accounting for any CC2D2A functional domains, we found that predicted CC2D2A protein levels were significantly correlated with disease severity with $p < 0.0001$ (Fisher's exact test). 100% of patients with uncomplicated Joubert syndrome were predicted to have high to medium levels of CC2D2A. Patients with Joubert syndrome with retinal or renal disease were found to have a more even distribution across different predicted protein levels. 80% of patients with Meckel syndrome, on the other hand, were predicted to have very low or absent levels of CC2D2A protein (Figure 2e).

Discussion

To date, the pleiotropic nature of ciliary dysfunction has defied explanation despite significant scientific investigation and analysis. In particular, how mutations in single ciliary disease genes such as *CEP290* can result in such drastically different phenotypes in different patients remained completely unknown. Here we have presented data that, for the first time, accurately and robustly correlates CEP290 mutations with clinical presentation and have described the mechanism by which these mutations, through alternative splicing and exon skipping, result in predictable levels of CEP290 protein and predictable disease phenotypes.

Our model relies on the concepts of alternative splicing and exon skipping, phenomena that have recently been shown to occur with high frequency within the retina (Farkas et al., 2013) and which have been overlooked as a potential source of pleiotropy. The canonical splicing of a gene transcript to yield an annotated mRNA is often treated as a rule, leaving little room for the exceptions of haphazard exon skipping and stochastic splicing, and imposing an artificial uniformity on the cell transcriptome. Here we have shown this idea to be false –basal levels of non-canonical exon skipping were found to occur in every one of the 10 human samples we investigated, yielding abundant transcript variety and posing a potential solution to the problem of pleiotropy.

Our data indicate that, in the face of premature stop mutations, basal exon skipping (BES) may provide nature a potential workaround, supplying the cell with low levels of alternatively spliced transcript lacking the mutated exon producing low levels of near-full length, functional protein. This workaround is, of course, dependent on the affected exon – exons beginning and ending in

different reading frames provide no benefit when skipped, as such transcripts would contain frame shifts and almost certainly premature termination codons. We found BES to faithfully and robustly explain the pleiotropy associated both with CEP290 mutations and with mutations in the CC2D2A gene. With continued investigation, it will be interesting to see if this mechanism extends beyond the ciliopathies and ciliary disease genes. In fact, the mechanism of BES may provide a new genetic paradigm, changing our understanding of the cellular transcriptome and helping to explain the genetics of pleiotropy and human disease.

Acknowledgements

We must thank the CEP290 patients and their families who so graciously made this work possible through the donations of their samples and time. Studies in this work were performed in collaboration with Project CEP290. Primary dermal fibroblasts were provided by Drs. Budd Tucker and Edwin Stone, University of Iowa. Support was provided by the Wyk Grousbeck Family Foundation. Additional support was provided by the Foundation Fighting Blindness, Research to Prevent Blindness, NIH R24Ey019861 and 8DP1EY023177, TreatRush (European Union), the Mackall Foundation Trust, the Penn Genome Frontiers Institute, and the F.M. Kirby Foundation.

Methods

Mutation Analysis

Human mutations in CEP290 were compiled from published articles and from the CEP290 mutation database (http://medgen.ugent.be/cep290base/) (Coppieters et al., 2010). The coding effect of each mutation was noted, particularly with respect to whether an exon was predicted to be disrupted by a premature stop codon (due to either nonsense or frame shift mutations) or skipped due to a mutation affecting splicing. Mutations were then sorted into three color-coded groups. Mild (green) mutations were those that were predicted to have little effect on total CEP290 protein levels (in frame deletions, missense mutations, truncating mutations occurring within the last exon, and splicing mutations in which there is evidence for high levels of normal transcript production). Moderate (orange) mutations were those that were predicted to significantly reduce CEP290 protein levels (those that resulted in a premature stop codon within (or splicing mutation likely to result in the skipping of) an in-frame exon). Severe (red) mutations were those that were predicted to act as null alleles (those that resulted in a premature stop codon within (or splicing mutation likely to result in the skipping of) an out-of-frame exon). The sorted mutations are listed in figure 1B. Mutations in the gene CC2D2A were sorted in an identical fashion. For our modified CEP290 model, mutations affecting exons 6, 9, 40, or 41 were considered severe. These exons encode domains of the CEP290 protein critical in membrane and microtubule binding (Chapter 2, Drivas et al., 2013).

CEP290 patient protein level and disease phenotype prediction

A model, as in figure 1C, for predicting the amount of full-length and near-full-length CEP290 protein levels in patients for whom both CEP290 disease alleles were known was devised as follows. Any patient with two CEP290 alleles encoding mild mutations was predicted to have high levels of full-length or near-full-length CEP290. Patients with alleles encoding one mild mutation were predicted to have medium levels of CEP290. Patients with alleles encoding two moderate CEP290 mutations were predicted to have low levels of CEP290. Patients with alleles encoding one moderate and one severe mutation were predicted to have very low levels of CEP290. Patients with two severe alleles were predicted to produce no CEP290. The same model was applied to CC2D2A patients.

Cells and cell culture

Primary dermal fibroblasts were isolated from patient skin punches and grown in DMEM supplemented with 10% FBS and 1% pen-strep at 37˚ C in a humidified 5% CO_2 atmosphere. Fibroblasts were passaged fewer than 10 times before analysis.

Patient Assessment

Patients were see in either the University of Iowa or the Children's Hospital of Philadelphia retinal degenerations clinic where a family history was ascertained and the individuals received standard clinical examinations including assessments of visual acuity, visual fields, and retinal structure. The diagnosis of LCA was made by electroretinogram. Molecular genetic testing was

carried out after appropriate IRB-approved consent/assent (plus parental permission) was obtained.

CEP290 protein levels

Patient fibroblasts were washed with PBS and $5x10^6$ cells were lysed by incubation in 50 µL of RIPA buffer () supplemented with a protease inhibitor cocktail for 30 minutes at 4˚ C. Cell lysates were centrifuged at 20,000x g for 15 minutes to remove insoluble material and the resulting supernatant was analyzed by SDS PAGE and immunoblotting using standard techniques. Blots were probed with antibodies against CEP290 (Abcam, AB105383) and α-tubulin (Abcam, AB7291) and imaged with a Typhoon 9400 instrument (GE).

Exon junction detection

cDNA was isolated from patient fibroblasts using Qiagen's RNeasy kit and Invitrogen's SuperScript III First-Strand Synthesis kit, following the manufacturers' protocols. A set of primers was designed to amplify across the exon junctions from CEP290 exons 4 to 8. A nested primer set was designed to amplify across the exon junctions from CEP290 exons 5 to 7. 10 cycles of amplification were run using the initial primer set with patient/control cDNA as template. Subsequently, 30 cycles of amplification were run using the nested primer set and 2 µL of the initial reaction as template. The resulting PCR products were resolved by agarose gel electrophoresis, imaged, gel excised, and submitted for Sanger sequencing.

Statistical Analysis

The statistical significance of the difference between three or more means was determined using a two-way ANOVA and Tukey's HSD test. Statistical analysis was performed using GraphPad Prism Software 5.0b. p-values < 0.05 were considered significant.

a

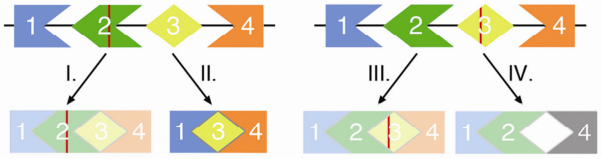

b

Mild	Missense	c.2T>G*, c.1A>G*, c.21G>T, c.95T>C, c.829G>C, c.1985A>T, c.1991A>G, c.2915T>C, c.4661_4663del, c.5777G>C
	Cryptic exon	c.2991+1655A>G
Moderate	Frame Shift	c.136G>T, c.265dup, c.270_274delAGTAA, c.287del, c.381_382delinsT, c.384_387del, c.384_385del, c.437del, c.679_680del, c.2118_2122dup, c.4452_4455delAGAA, c.4656del, c.5256_5257del, c.5434_5435del, c.5445-8delAACT, c.5493del, c.5515_5518del, c.5519_5537del, c.5611_5614del, c.5649dup c.6277del, c.6604del, c.7318_7321dup, c.7341dup, c.7366_7369del
	Splicing Event	c.2218-15_2220del, c.2218-4_2222del, c.2218-2A>C, c.5226+1G>A, c.5226+5_8delGTAA, c.5587-1G>C, c.6271-8T>G
	Early Stop	c.322C>T, c.451C>T, c.566C>G, c.613C>T, c.2213delT, c.2249T>G, c.2251C>T, c.2695C>T, c.2906dup, c.4393C>T, c.5311G>T, c.5344C>T, c.5668G>T, c.6331C>T
Severe	Early Stop	c.1078C>T, c.1236delG, c.1429C>T, c.1550del, c.1593C>A, c.1645C>T, c.1709C>G, c.1936C>T, c.1984C>T, c.1987A>T, c.3043G>T, c.3175del, c.3292G>T, c.3793C>T, c.3802C>T, c.3811C>T, c.3814C>T, c.3922C>T, c.4723A>T, c.4732G>T, c.4771C>T, c.4882C>T, c.4966G>T, c.5046del, c.5162G>T, c.5218C>T, c.5722G>T, c.5824C>T, c.5866G>T, c.5932C>T, c.5941G>T, c.6031C>T, c.6072C>A
	Frame Shift	c.164_167del, c.1219_1220del, c.1260_1264del, c.1361del, c.1419_1423del, c.1666del, c.1682_1683del, c.1830delA, c.1859_1862del, c.1860_1861del, c.1992del, c.2505_2506delAG, c.3175dup, c.3176del, c.3178delA, c.3185delT, c.3422dup, c.4001del, c.4028del, c.4791_4794del, c.4962_4963del, c.4965_4966del, c.5163del, c.5734del, c.5776C>T, c.5813_5817del, c.5850del, c.5865_5867delinsGG, c.6869del, c.6870delc.4115_4116del, c.4114_4115del
	Splicing Event	c.103-13_103-18del, c.180+1G>T, c.180+2T>A, c.1066-1G>A, c.1189+1G>A, c.1711+5A>G, c.1824G>A c.1910-2A>C, c.3104-1G>A, c.3104-2A>G, c.3310-1G>C, c.3310-1_3310delinsAA, c.4195-1G>A

** These point mutations disrupt the start codon, likely resulting in translation initiation at an in frame AUG codon at c.31-33 creating near normal levels of a protein product lacking only the first 10 amino acids*

c

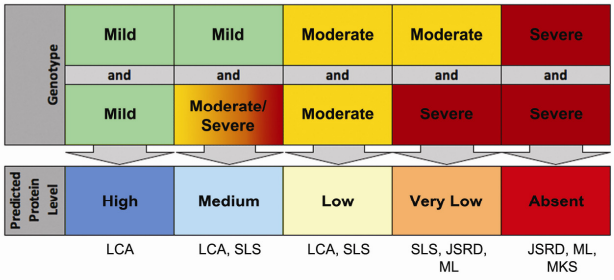

Figure 3.1. A model to predict CEP290 protein levels

(a) A schematic of nonsense-induced alternative splicing (NAS), illustrating the combined effects of nonsense mutations, alternative splicing and nonsense-mediated decay (NMD) on protein levels. (I and III) The coding sequence of a gene containing a nonsense mutation (red line) is spliced together to yield the full-length transcript. In both cases, the inclusion of the exon harboring the nonsense mutation targets the transcript for NMD. (II) Alternative splicing yields a transcript lacking exon 2 and the premature stop codon. The message persists and results in a slightly truncated protein product. (IV) Alternative splicing yields a transcript lacking exon 3 and the premature stop codon but containing a frame-shift from the splicing together of incompatible exon ends. The frame shift results in premature stop codons and nonsense-mediated decay.
(b) Human CEP290 mutations were classified based on their predicted coding effects. In green are mutations predicted to result in medium to high levels of CEP290 protein. In orange are mutations that, through the mechanism described in panel A.II, are predicted to result in low levels of CEP290 protein. In red are mutations that, through the mechanisms described in panel A.III-IV, are predicted to act as null mutations.
(c) A model for predicting CEP290 protein levels in individual patients for whom both CEP290 disease alleles are known. Listed below are the CEP290 disease phenotypes predicted to be associated with each protein level. LCA, Leber congenital amaurosis; SLS, Senior Loken syndrome; JSRD, Joubert syndrome and related disorders; ML, Meckel-like syndrome; MKS, Meckel syndrome.

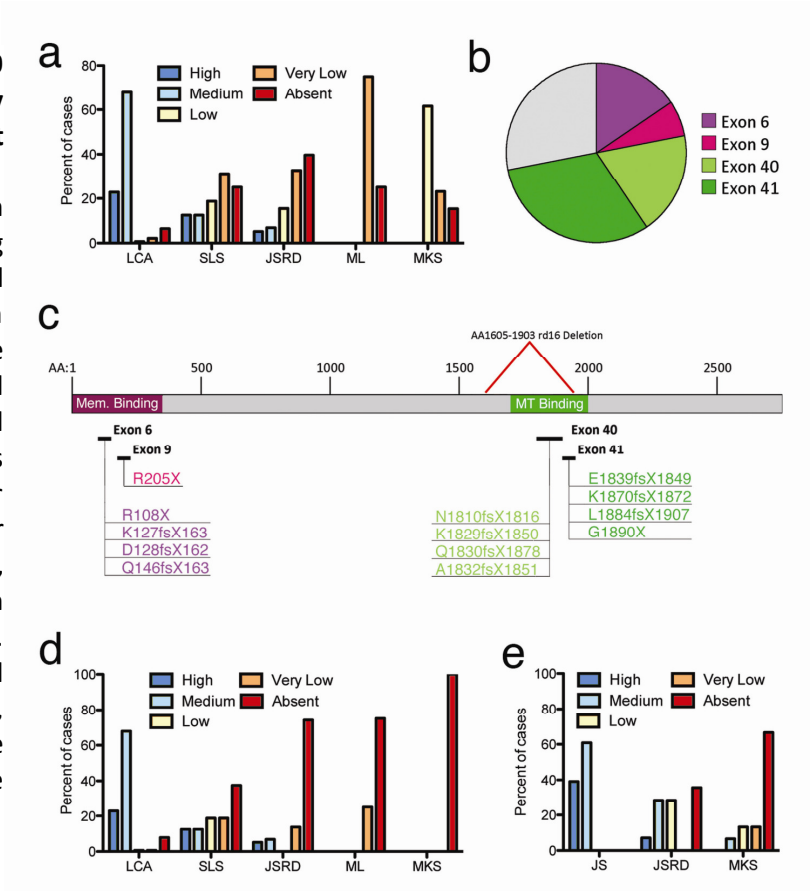

Figure 3.2. Predicted CEP290 protein levels strongly correlate with patient phenotype

(a) Predicted CEP290 protein levels were determined, using our model, for all published patients for whom both CEP290 disease alleles were known. Patients were sorted by phenotype and predicted protein levels were plotted as a percent of total cases for each phenotype. Leber congenital amaurosis (LCA), n=140. Senior Løken syndrome (SLS), n=16. Joubert syndrome and related disorders (JSRD), n=58. Meckel-like syndrome (ML), n=4. Meckel syndrome (MKS), n=13.

(b) Of those patients whose phenotypes were more severe than predicted by our model, 70% harbored mutations in exons 6, 9, 40, or 41.

(c) A scale representation of the CEP290 protein indicating the location of the mutations identified in panel B. The mutations within exons 6 and 9 fall within CEP290's membrane binding region. The mutations within exons 40 and 41 fall within CEP290's critical microtubule binding region (Chapter 2; Drivas et al., 2013).

(d) Predicted functional CEP290 protein levels were determined using a modified model taking into account the critical nature of exons 6, 9, 40 and 41 for all published patients for whom both CEP290 disease alleles were known. Patients were sorted by phenotype and predicted functional protein levels were plotted as a percent of total cases for each phenotype as in panel a.

(e) Our model for predicting protein levels applied to a different ciliopathy disease gene, CC2D2A. Patients were sorted by phenotype and predicted protein levels were plotted as a percent t of total cases for each phenotype. Joubert syndrome (JS), n=23. Joubert syndrome with extra-CNS involvement (JSRD), n=14. Meckel syndrome (MKS), n=15.

a

Patient	Age	Gender	Nucleotide Alteration	Coding Effect	Predicted Protein Level	Ocular Symptoms*	CNS Symptoms	Renal Symptoms	Diagnosis
54	9 yrs	F	IVS26 + 1655 A>G IVS26 + 1655 A>G	Cryptic Exon Cryptic Exon	High	20/80, VF	*N/A*	*NRD*	LCA
62	23 yrs	M	IVS26 + 1655 A>G Val247 739delG	Cryptic Exon Exon 10 FS	Medium	LP s P, VFNA	*N/A*	*NRD*	LCA
182	7 yrs	F	IVS26 + 1655 A>G Lys127 379delA 380delA	Cryptic Exon Exon 6 FS	Medium	NLP	MR	*NRD*	LCA
294	14 yrs	M	IVS26 + 1655 A>G Thr835 2503delA 2504delC	Cryptic Exon Exon 24 FS	Medium	NLP	*N/A*	*NRD*	LCA
582	19 yrs	M	Arg549Stop 1645 C>T Lys1882 5643_5644 insA	Exon 17 S Exon 41 FS	Very Low	20/100, VFNA	JS	*NRD*	JS+LCA
619	5 yrs	M	IVS26 + 1655 A>G Val2093 6277delG	Cryptic Exon Exon 46 FS	Medium	20/1400, VFNA	*N/A*	*NRD*	LCA
620	4 yrs	M	IVS26 + 1655 A>G Val2093 6277delG	Cryptic Exon Exon 46 FS	Medium	LP c P, VFNA	*N/A*	*NRD*	LCA

FS, frame shift; S, premature stop codon; LCA, Leber congenital amaurosis; SLS, Senior Loken syndrome; JSRD, Joubert syndrome and related disorders; ML, Meckel-Like syndrome; VF, measurable visual fields; VFNA, visual fields not assesable; LP s P, light perception without projection; LP c P, light perception with projection; NLP, no light perception; MR, mental retardation; JS, MRI-confirmed Joubert Syndrome; N/A, not assessed; NRD, no overt renal disease

* Visual acuity, if measurable, is indicated

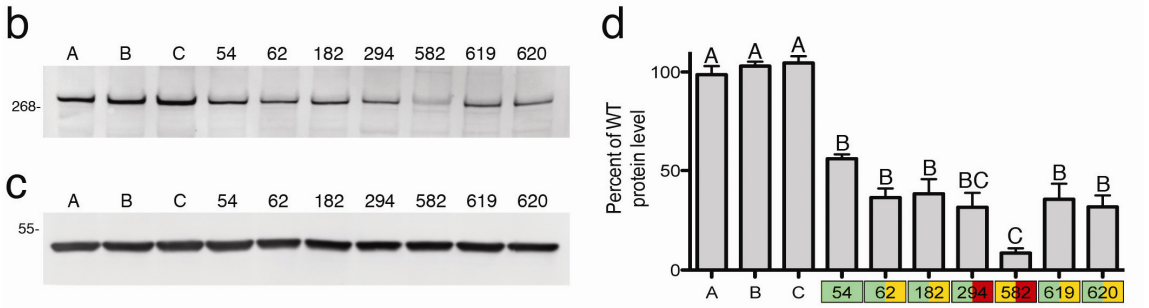

Figure 3.3. Actual CEP290 protein levels robustly correlate with predicted protein levels and are predictive of clinical phenotype.

(a) Table listing the clinical features, mutations, and predicted protein levels of seven CEP290 patients. Color coding is as in Figure 1. Boxes with orange and red stripes indicate mutations expected to produce low levels of dysfunctional CEP290 lacking critical exons 6 or 41.

(b) Immunoblot showing relative levels of CEP290 protein in fibroblasts isolated from seven CEP290 patients and three normal controls (A, B and C). Relevant molecular weights are indicated in kiloDaltons.

(c) Loading control for panel B, probing for levels of αTubulin. Relevant molecular weights are indicated in kiloDaltons.

(d) Densitometric analysis of CEP290 protein levels from seven CEP290 patients and three normal controls as in panel B. Data are presented as mean ± SD, n=4. Means with different letters are significantly different.

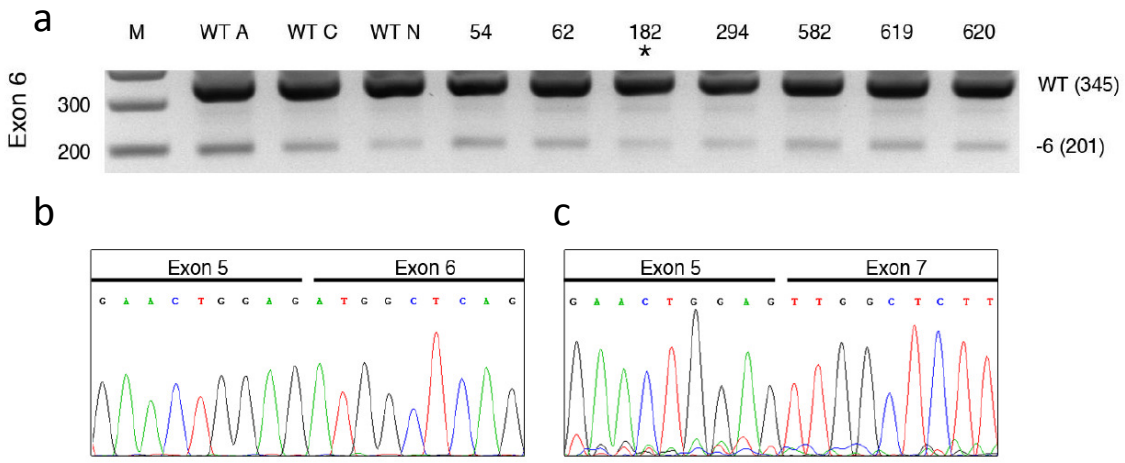

Figure 3.4. Basal exon skipping (BES) of CEP290 exon 6 occurs in all samples

(a) Nested PCR primers were designed to amplify across the exon junctions between exons 5-7. PCR products amplified, using these primers, from cDNA prepared from patient fibroblasts were resolved by gel electrophoresis. Patient 182 (asterisk) is known to harbor a truncating mutation in CEP290 exon 6. In every sample a major band of roughly 350 bp was detected (the size expected for PCR products containing exons 5, 6, and 7) along with a minor band of roughly 200 bp (the size expected for PCR products containing only exons 5 and 7).

(b) Gel extraction and sequencing of the major band revealed that it corresponded to a PCR product containing exons 5, 6, and 7.

(c) Gel extraction and sequencing of the minor band revealed that it corresponded to a PCR product lacking exon 6, with exon 5 being spliced directly onto exon 7.

Dx	Allele 1	Allele 2
JSRD	Exon 2 P	Exon 2 P
JSRD	Exon 20 S	Exon 46 FS
JSRD	Exon 22 S	Exon 50 FS
JSRD	Exon 28 FS	Exon 28 FS
JSRD	Exon 28 FS	Exon 41 S
JSRD	Exon 31 S	Exon 42 FS
JSRD	Exon 31 S	Exon 42 FS
JSRD	Exon 32 S	Exon 43 FS
JSRD	Exon 32 S	Exon 43 FS
JSRD	Exon 34 S	Exon 36 S
JSRD	Exon 36 FS	Exon 36 FS
JSRD	Exon 36 FS	Exon 41 S
JSRD	Exon 36 FS	Exon 41 S
JSRD	Exon 37 FS	Intron 2
JSRD	Exon 37 S	Exon 41 FS
JSRD	Exon 37 S	Exon 43 S
JSRD	Exon 38 FS	Exon 38 FS
JSRD	Exon 38 S	Exon 44 S
JSRD	Exon 40 FS	Exon 41 S
JSRD	Exon 41 FS	Exon 42 FS
JSRD	Exon 41 FS	Exon 42 FS
JSRD	Exon 41 FS	Exon 42 FS
JSRD	Exon 41 S	Exon 41 S
JSRD	Exon 41 S	Exon 41 S
JSRD	Exon 41 S	Exon 41 S
JSRD	Exon 42 S	Exon 42 S
JSRD	Exon 42 S	Exon 42 S
JSRD	Exon 44 S	Exon 54 FS
JSRD	Exon 44 S	Exon 54 FS
JSRD	Intron 12	Exon 39 FS
JSRD	Intron 28	Intron 45
JSRD	Exon 40	Exon 39
JSRD	Exon 41	Exon 41
JSRD	Exon 41	Exon 41
JSRD	Exon 41	G397 P
JSRD	Exon 41	Exon 3
JSRD	Exon 46	Exon 38
JSRD	Exon 41 S	Exon 41 S
JSRD	Exon 42 S	Exon 42 S
JSRD	Exon 42 S	Exon 42 S
JSRD	Exon 37 S	Exon 41 FS
JSRD	Exon 41 S	Exon 41 S
JSRD	Exon 42 S	Exon 42 S
JSRD	Exon 42 S	Exon 42 S
JSRD	Exon 17 FS	Exon 31 S
JSRD	Exon 17 FS	Exon 44 S
JSRD	Exon 36 S	Exon 36 S
JSRD	Exon 36 S	Exon 36 S
JSRD	Exon 36 S	Exon 36 S
JSRD	Exon 37 S	Exon 41 FS
JSRD	Exon 42 S	Exon 42 S
JSRD	Exon 54 FS	Exon 29 FS
JSRD	Exon 54 FS	Exon 54 FS
JSRD	Exon 54 FS	Exon 54 FS
JSRD	Exon 6 FS	Exon 17 S
JSRD	Intron 40	Exon 31 S
JSRD	Exon 36 S	Exon 36 S
JSRD	Intron 17,	Intron 40
LCA	Exon 16 S	Exon 2 P
LCA	Exon 18, loss	Exon 2 P
LCA	Exon 20 S	Exon 48 FS
LCA	Exon 21	Intron 35
LCA	Exon 36 S	Exon 17 S
LCA	Exon 36 S	Exon 35 P
LCA	Exon 36 S	Exon 36 S
LCA	Exon 36 S	Exon 36 S
LCA	Exon 36 S	Exon 36 S
LCA	Exon 36 S	Exon 36 S
LCA	Exon 36 S	Exon 36 S
LCA	Exon 36 S	Exon 36 S
LCA	Exon 36 S	Exon 36 S
LCA	Exon 36 S	Exon 36 S
LCA	Exon 42 FS	Exon 35 D
LCA	Exon 42 FS	Intron 40
LCA	Exon 7 S	Intron 26
LCA	G1544 D	Exon 17
LCA	Intron 26	Exon 5 FS
LCA	Intron 26	Exon 10 FS
LCA	Intron 26	Exon 10 FS
LCA	Intron 26	Exon 10 P
LCA	Intron 26	Exon 14 FS
LCA	Intron 26	Exon 14 FS
LCA	Intron 26	Exon 14 FS
LCA	Intron 26	Exon 14 S
LCA	Intron 26	Exon 14 S
LCA	Intron 26	Exon 16 S
LCA	Intron 26	Exon 16 S
LCA	Intron 26	Exon 19 FS
LCA	Intron 26	Exon 19 FS
LCA	Intron 26	Exon 19 FS
LCA	Intron 26	Exon 20 FS
LCA	Intron 26	Exon 21 FS
LCA	Intron 26	Exon 22 S
LCA	Intron 26	Exon 24 FS
LCA	Intron 26	Exon 25 S
LCA	Intron 26	Exon 28 FS
LCA	Intron 26	Exon 28 FS
LCA	Intron 26	Exon 28 FS
LCA	Intron 26	Exon 28 S
LCA	Intron 26	Exon 28 S
LCA	Intron 26	Exon 29 FS
LCA	Intron 26	Exon 29 FS
LCA	Intron 26	Exon 31 FS
LCA	Intron 26	Exon 31 FS
LCA	Intron 26	Exon 31 FS
LCA	Intron 26	Exon 31 S
LCA	Intron 26	Exon 31 S
LCA	Intron 26	Exon 31 S
LCA	Intron 26	Exon 31 S
LCA	Intron 26	Exon 32 FS
LCA	Intron 26	Exon 32 FS
LCA	Intron 26	Exon 34 S
LCA	Intron 26	Exon 35 FS
LCA	Intron 26	Exon 35 FS
LCA	Intron 26	Exon 36 S
LCA	Intron 26	Exon 36 S
LCA	Intron 26	Exon 36 S
LCA	Intron 26	Exon 37 FS
LCA	Intron 26	Exon 37 FS
LCA	Intron 26	Exon 37 S
LCA	Intron 26	Exon 37 S
LCA	Intron 26	Exon 37 S
LCA	Intron 26	Exon 37 S
LCA	Intron 26	Exon 38 FS
LCA	Intron 26	Exon 38 Fs
LCA	Intron 26	Exon 38 FS
LCA	Intron 26	Exon 38 S
LCA	Intron 26	Exon 39 S
LCA	Intron 26	Exon 40 FS
LCA	Intron 26	Exon 40 FS
LCA	Intron 26	Exon 40 FS
LCA	Intron 26	Exon 41 S
LCA	Intron 26	Exon 41 S
LCA	Intron 26	Exon 41 S
LCA	Intron 26	Exon 42 FS
LCA	Intron 26	Exon 42 FS
LCA	Intron 26	Exon 42 FS
LCA	Intron 26	Exon 42 FS
LCA	Intron 26	Exon 42 P
LCA	Intron 26	Exon 43 FS
LCA	Intron 26	Exon 43 S
LCA	Intron 26	Exon 48 FS
LCA	Intron 26	Exon 48 FS
LCA	Intron 26	Exon 48 FS
LCA	Intron 26	Exon 48 FS
LCA	Intron 26	Exon 48 FS
LCA	Intron 26	Exon 5 FS
LCA	Intron 26	Exon 54 FS
LCA	Intron 26	Exon 6 FS

LCA	Intron 26	Exon 6 FS
LCA	Intron 26	Exon 6 FS
LCA	Intron 26	Exon 6 S
LCA	Intron 26	Exon 9 S
LCA	Intron 26	Intron 13
LCA	Intron 26	Intron 13
LCA	Intron 26	Intron 19
LCA	Intron 26	Intron 21
LCA	Intron 26	Intron 26
LCA	Intron 26	Intron 26
LCA	Intron 26	Intron 26
LCA	Intron 26	Intron 26
LCA	Intron 26	Intron 26
LCA	Intron 26	Intron 26
LCA	Intron 26	Intron 26
LCA	Intron 26	Intron 26
LCA	Intron 26	Intron 26
LCA	Intron 26	Intron 26
LCA	Intron 26	Intron 26
LCA	Intron 26	Intron 26
LCA	Intron 26	Intron 26
LCA	Intron 26	Intron 26
LCA	Intron 26	Intron 26
LCA	Intron 26	Intron 26
LCA	Intron 26	Intron 26
LCA	Intron 26	Intron 26
LCA	Intron 26	Intron 26
LCA	Intron 26	Intron 26
LCA	Intron 26	Intron 26
LCA	Intron 26	Intron 26
LCA	Intron 26	Intron 26
LCA	Intron 26	Intron 26
LCA	Intron 26	Intron 26
LCA	Intron 26	Intron 26
LCA	Intron 26	Intron 26
LCA	Intron 26	Intron 26
LCA	Intron 26	Intron 26
LCA	Intron 26	Intron 28
LCA	Intron 26	Intron 28
LCA	Intron 26	Intron 28
LCA	Intron 26	Intron 3
LCA	Intron 26	Intron 38
LCA	Intron 26	Intron 4
LCA	Intron 26	Intron 40
LCA	Intron 26	Intron 40
LCA	Intron 26	Intron 40
LCA	Intron 26	Intron 40
LCA	Intron 26	Intron 40
LCA	Intron 40	Exon 13 S
MKS	Exon 14 FS	Exon 32 FS
MKS	Exon 28 FS	Exon 28 FS
MKS	Exon 40 FS	Exon 40 FS
MKS	Exon 40 FS	Exon 40 FS
MKS	Exon 40 FS	Exon 40 FS
MKS	Exon 40 FS	Exon 40 FS
MKS	Exon 6 FS	Exon 19 FS
MKS	Exon 6 FS	Exon 6 FS
MKS	Exon 6 FS	Exon 6 FS
MKS	Exon 9 S	Exon 9 S
MKS	Exon 9 S	Exon 9 S
MKS	Intron 3	Exon 6 FS
MKS	Intron 3	Exon 6 FS
ML	Exon 26 S	Exon 31 S
ML	Exon 41 FS	Exon 42 FS
ML	Exon 41 FS	Exon 42 FS
ML	Exon27 S	Intron 27
SLS	Exon 2 P	Exon 2 P
SLS	Exon 2 P	Exon 15 S
SLS	Exon 26 P	Exon 26 P
SLS	Exon 36 S	Exon 34 S
SLS	Exon 36 S	Exon 34 S
SLS	Exon 41 FS	Intron 32
SLS	Exon 41 FS	Exon 42
SLS	Intron 21	Intron 21
SLS	Intron 21	Intron 21
SLS	Exon 2 P	Intron 38
SLS	Exon 20 S	Exon 36 S
SLS	Exon 20 S	Exon 36 S
SLS	Exon 31 S	Exon 36 S
SLS	Exon 35 FS	Exon 36 S
SLS	Intron 13	Exon 36 S
SLS	Exon 5 FS	Exon 46 FS

Table 1. Genotype and diagnosis for all reported CEP290 patients.

Disease diagnoses in green agree with our model. Disease diagnoses in red do not agree with our model. Color coding of alleles and abbreviations are identical to those in Figure 1, taking into account the effect of mutations affecting exons 6, 9, 40, or 41.

CHAPTER 4: WORK TOWARDS A NOVEL CEP290 THERAPEUTIC

Theodore G. Drivas[1]

1. Cell and Molecular Biology Graduate Group and the F.M. Kirby Center for Molecular Ophthalmology, Perelman School of Medicine, University of Pennsylvania, Philadelphia, PA 19104, USA

Introduction

Dysfunction of the centrosomal and ciliary protein CEP290 is the chief cause of the devastating blinding disease Leber congenital amaurosis (LCA), with more than 20% of LCA cases being linked directly to mutations in the *CEP290* gene (Perrault et al., 2007). LCA as a disease stands out as being one of the first genetic disorders to be successfully and safely treated by gene therapeutic approaches utilizing adeno-associated virus (AAV) vectors (Maguire et al., 2009), but the extension of recombinant AAV-based therapeutics to CEP290 patients has been hindered by CEP290's large size.

The natural DNA capacity of the AAV virus is 4.7 kb, with therapeutic cassettes of up to 5.0 kb having been successfully packaged within the viral capsid (Wu et al., 2010). CEP290, however, with an open reading frame of 7.8kb, is much too long for AAV packaging (Chang et al., 2006). A considerable amount of effort in the gene therapy community has been spent trying to package larger-than-normal genomes within AAV – in 2008 it was reported that full length *CEP290* cDNA had been successfully packaged within AAV serotype 5 (Allocca et al., 2008), but to date no group has been able to successfully replicate these results and *CEP290* patients remain without any effective treatments.

The recent discovery of novel autoinhibitory regions within the CEP290 gene, however, may present an alternative approach to the development of CEP290 therapeutics (Chapter 2; Drivas et al., 2013). Perhaps CEP290 truncation mutants lacking these inhibitory domains but maintaining the other important functional regions of the protein would exhibit normal, or even enhanced, CEP290 function while at the same time being small enough to fit within AAV. The

delivery of such a therapeutic to terminally differentiated tissues, such as the retina, where permanent activation of CEP290 is not expected to be problematic, might prove effective in the treatment of CEP290-related diseases such as LCA.

This is not a completely novel idea – a mini-gene approach has met some success in the treatment of muscular dystrophy where the functionality of dystrophin, a large structural protein that is at the root of all cases of Duchenne muscular dystrophy, was found to be preserved in a *miniDystrophin* gene (Koppanati et al., 2010). The AAV-vectored delivery of *miniDystrophin* to a mouse model of muscular dystrophy was able to affect at least some improvement in the disease phenotype (Koppanati et al., 2010). With this proof-of principle study in Duchenne muscular dystrophy and with our new-found knowledge of CEP290's autoregulatory and functional domains, we set out to design a *miniCEP290* gene for therapeutic intervention.

Results

Creation of a CEP290 knockdown cell line

To test the efficacy of our miniCEP290 therapeutic we first set out to create a CEP290-knockdown reporter cell line. Knockdown of *CEP290* in cultured cells has been reported to result in dramatic decreases in ciliation upon serum starvation (Gorden et al., 2008; Tsang et al., 2008), and rescue of this phenotype could serve as a good reporter for miniCEP290 protein function. Three *CEP290* shRNA constructs were generated and transfected into hTERT-RPE1 cells to assess their ability to knockdown levels of CEP290 protein. One week post transfection cell lysates were collected and assayed for CEP290 by western blotting. All three constructs were found to affect a greater than 50% reduction in CEP290 protein levels, even in only transient transfection (Figure 4.1 A, B).

To assay the effects of each of these constructs on cell ciliation, retrovirus vectors encoding each construct were generated and used to transduce hTERT-RPE1 cells. Control and transduced cells were stained for acetylated tubulin and observed by fluorescence microscopy for deficits in ciliation. Construct sh2 in particular was found to affect a profound decrease in cell ciliation, with only 50% of cells forming primary cilia, compared to 75% of control cells, upon serum starvation (Figure 4.1 C, D).

We decided to move forward with CEP290 shRNA construct 2 due to its efficiency in knocking down CEP290 protein levels and ability to affect a significant ciliary phenotype. CEP290 sh2 retrovirus-transduced hERT-RPE1 cells were selected for with puromycin and individual clones were isolated and assayed for CEP290 levels. All of the clones tested were found to exhibit

significant knockdown of CEP290 (Figure 4.2, A), but clones 2.5, 2.7, and 2.8 were each found to affect the greatest knockdown, with less than 30% of endogenous CEP290 remaining (Figure 4.2, B).

To test the ciliary phenotype of such significant knockdown of CEP290 protein, clonal lines 2.5, 2.7, and 2.8 were stained for acetylated tubulin, a marker of the primary cilium, and assayed by fluorescence microscopy for ciliation. Clone 2.8 in particular was characterized by a remarkably severe deficit in ciliation upon serum starvation (Figure 4.2, C), with only 5% of sh2.8 cells producing primary cilia, compared to greater than 75% of control cells (Figure 4.2, D). In the serum fed state, sh2.8 cells formed cilia only extremely rarely, making accurate quantification difficult (data not shown). We decided to move forward with the CEP290 shRNA 2.8 cell line as a reporter for miniCEP290 gene rescue.

Design of a miniCEP290 gene

We next set out to design a miniCEP290 gene small enough to fit within AAV's limited packaging capacity. To maintain as much of the protein as possible, we decided to include CEP290 amino acids 130-380, 700-1040, 1260-1605, and 1695-1990, making for a total open reading frame of only 3.7 kb, small enough for AAV packaging (Figure 4.3, A, B). miniCEP290 was thus strategically designed to include CEP290's membrane and microtubule binding domains (Chapter 2; Drivas et al., 2013) and almost all of CEP290's PCM-1, NPHP5, CC2D2A, and Rab8A binding domains (Chang et al., 2006; Gorden et al., 2008; Kim et al., 2008; Schäfer et al., 2008), while leaving out as much of CEP290's known autoregulatory domains as possible (Chapter 2; Drivas et al., 2013). The mini gene was codon optimized, both to increase expression levels and to harder the

transcript against the affects of the shRNA used to generate the CEP290 knockdown reporter cell line, and synthesized by DNA 2.0.

miniCEP290 localizes correctly in hTERT-RPE1 cells

As a preliminary test of miniCEP290's ability to recapitulate CEP290 functionality, we generated a GFP-fused miniCEP290 expression construct. Upon transfection into hTERT-RPE1 cells, miniCEP290 was found to localize to discrete puncta throughout the cytoplasm (Figure 4.3, C), a pattern similar to that observed for overexpressed full-length CEP290 (Chapter 2; Drivas et al., 2013). In cells where primary cilia were present, a punctus of miniCEP290 was always found exactly at the ciliary transition zone, immediately between the ciliary axoneme and centrosome (as indicated by acetylated tubulin and pericentrin staining, respectively; Figure 4.3, C), indicating that, at least in cells with endogenous CEP290 expression, miniCEP290 was capable of correctly localizing to the same compartment as its full-length counterpart.

Discussion

The work presented in this chapter represents the very beginning of an exciting attempt to apply what we have learned about the basic biology of CEP290 to the creation of a novel and inventive therapeutic. In the past few years it has become clear that CEP290 can be divided into a number of discrete functional domains, some of which promote the protein's function at the primary cilium and others which actively work to inhibit the protein (Drivas et al., 2013; Tsang et al., 2008). The generation of an intelligently engineered truncated version of the protein small enough to deliver using AAV-based viral vectors but large enough to retain some of the original protein's function is now a real possibility. Whether or not the *miniCEP290* gene we propose in this study will ultimately prove useful to this end remains to be seen, but the general strategy seems to be the most promising one currently available.

A number of additional studies on the *miniCEP290* gene described are needed to determine whether or not it will prove to be of any utility in rescuing CEP290 deficiency. Many of these studies are currently underway –we have already shown that miniCEP290 localizes appropriately in hTERT-RPE1 cells (although it is a possibility that miniCEP290 localizes to the ciliary transition zone through homotypic interactions with endogenous CEP290, and not though an innate ability of the mini gene to correctly localize), and, perhaps more importantly we have shown that miniCEP290 doesn't seem to interfere with ciliogenesis (an important concern when overexpressing truncation mutants). We are now actively working to determine whether miniCEP290 is also capable of binding to microtubules and cellular membranes, two functions recently discovered to be critical to full-length CEP290's role in cilium formation. A panel of immunoprecipitation experiments will be performed to confirm that the mini gene is capable of

interacting with known CEP290 binding partners, an aspect of CEP290 biology likely critical to the protein's function at the cilium.

The next most logical step will be to assay miniCEP290's ability to rescue the ciliogenesis phenotype of the sh2.8 cell line described here. We are currently subcloning the miniCEP290 gene into a lentiviral vector for this exact purpose. Any promising results in cell culture will, of course, have to be validated in animal models to demonstrate a potential for therapeutic use. We could test the lentiviral vectors in early postnatal rd16 mice as this will lead to transduction of at least some photoreceptor precursor cells (Auricchio et al., 2001; Kong et al., 2008). Alternatively, AAV vectors encoding the *miniCEP290* gene can be generated and subretinally administered to rd16 mice. If miniCEP290 does, in fact, recapitulate even some of full-length CEP290's function, we would expect to see at least partial correction of the rd16 retinal degeneration phenotype in the treated eyes.

It is too early to tell when miniCEP290 will make it out of the culture dish and into preclinical testing, but what is certainly clear is that novel therapeutic approaches are sorely needed for people suffering from *CEP290*-based disease. Regardless of whether or not miniCEP290 pans out as a therapeutic tool, it is undeniable that whatever we may learn in our examination of miniCEP290 activity will be invaluable to the development of therapeutic interventions in the future.

Methods

Cell culture and treatments

hTERT RPE-1 cells were grown in DMEM:F12 supplemented with 10% FBS and 0.075% sodium bicarbonate. All cells were grown at 37˚ C in a humidified 5% CO_2 atmosphere. Transfections were performed with FuGENE 6 reagent (Promega) according to the manufacturer's protocol. Cells were induced to form primary cilia by serum starvation with Opti-MEM I (Invitrogen) for 48-72 hours.

miniCEP290 synthesis

The miniCEP290 construct was codon optimized, synthesized, and sequenced by DNA2.0.

Plasmid construction

shRNA constructs were created as follows. Three regions of the human *CEP290* coding sequence without homology to other transcripts were selected as shRNA targets. Oligonucleotides encoding the target sequence in the context of a DNA hairpin were synthesized, annealed, and ligated into the pSIREN-RetroQ retrovirus vector (Clontech). Efficiency of knockdown was assayed as described in the results section.

The mammalian expression vector encoding GFP-fused miniCEP290 was created by the amplification of the miniCEP290 gene by PCR using primers compatible with Gateway® cloning (Invitrogen). Amplified products were cloned into pDONR221 (Invitrogen) by Gateway® cloning

to generate entry clones and subsequently shuttled into the plasmid pcDNA-DEST53 (Invitrogen) by Gateway® LR clonase reactions to create N-terminally-tagged GFP fusions.

Retrovirus production and transduction

Retroviral vectors were produced by transfection of 80% confluent 293T cells in 100mm culture dishes with 10 μg of retrovirus construct and 10 μg of pCL10A1 packaging plasmid. Media was replaced after 24 hours, and retroviral supernatants were harvested at 48 and 72 hours, combined, filtered through a 0.45 μm filter, and snap-frozen at -80° C. For retrovirus transduction, hTERT RPE-1 cells were plated in media containing 8 μg/mL polybrene. Filtered media containing the appropriate retroviral particles was added and 24 hours after transduction cells were switched to selective media containing 10μg/mL puromycin.

Antibodies, immunoblotting, and immunofluorescence

Antibodies used in this study were rabbit anti-human CEP290 (Abcam, ab105383), rabbit anti-pericentrin (Abcam, AB4448), rabbit anti-GAPDH (Sigma, SAB2103104), mouse anti-Acetylated α-tubulin (Sigma, T7451), HRP-conjugated goat anti-mouse (GE, NA931V), HRP-conjugated goat anti-rabbit (GE, NA934V), Cy5 conjugated goat anti-rabbit (KPL, 072-02-15-06), and AlexaFluor 594-conjugated goat anti-mouse (Invitrogen, A1100S).

For immunofluorescence, cells were grown in chamber slides and fixed with 3% PFA in PBS for 20 minutes at 37˚ C. Cells were permeabilized with 1% Triton X-100 in PBS for 5 minutes, and blocked in 2% BSA in PBS for 30 minutes prior to incubation with primary antibody. Secondary

antibodies used were donkey anti-mouse or anti-rabbit, conjugated to Cy5 or AlexaFluor 594. Slides were mounted in mounting medium containing DAPI. Images were acquired with an Axio Imager.M2 microscope using either an EC Plan-Neofluar 40x/0.75 M27 or an EC Plan-Neofluar 63x/1.25 Oil M27 objective and captured using an AxioCamMR3 camera and the AxioVs40 software, version 4.8.2.0.

For immunoblotting, samples were subjected to SDS-PAGE and transferred to nitrocellulose membrane using standard techniques. Membranes were blocked in 5% nonfat milk for 1 hour at room temperature and subsequently incubated in primary antibody overnight at 4° C. Membranes were washed three times with PBST (0.1% Tween-20 in PBS), incubated with HRP-conjugated secondary antibody for 1 hour at room temperature, washed, and developed using ECL2 reagent (Pierce), and scanned on a Typhoon 9400 instrument (GE). Immunoblots were densitometrically quantified using ImageJ 1.44p.

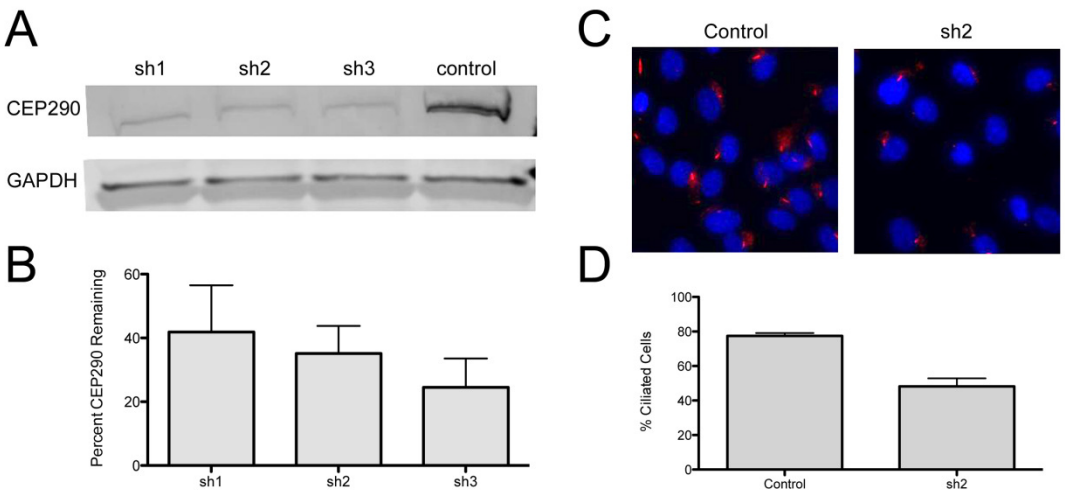

Figure 4.1. Generation and testing of CEP290 shRNA constructs

(A) hTERT-RPE1 cells transiently transfected with three different CEP290 shRNA constructs were lysed and analyzed by western blotting for CEP290 levels. Blots were reprobed for GAPDH as a loading control.

(B) Densitometric quantification of CEP290 protein levels in hTERT-RPE1 cells as in panel A. CEP290 levels were normalized using GAPDH as a loading control and the percent of CEP290 remaining, compared to untransfected hTERT-RPE1 cells, was determined.

(C) Immunofluorescence microscopy images of fields of hTERT-RPE1 cells, either untransfected or transfected with CEP290 shRNA construct 2, stained for acetylated tubulin (red) as a marker of the primary cilium.

(D) The percent of control and sh2 transfected hTERT-RPE1 cells, as in panel C, that formed cilia upon serum starvation.

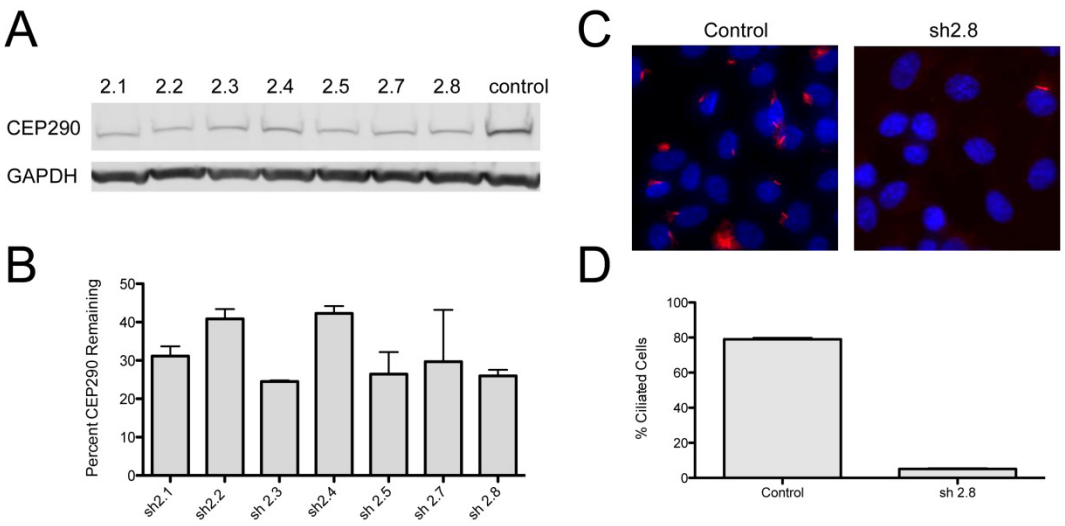

Figure 4.2. Isolation and testing of clonal CEP290 knockdown cell lines

(A) Clonal retrovirus-transduced hTERT-RPE1 cell lines expressing CEP290 shRNA 2 were lysed and analyzed by western blotting for CEP290 levels. Blots were reprobed for GAPDH as a loading control.
(B) Densitometric quantification of CEP290 protein levels in hTERT-RPE1 cells as in panel A. CEP290 levels were normalized using GAPDH as a loading control and the percent of CEP290 remaining, compared to untransfected hTERT-RPE1 cells, was determined.
(C) Immunofluorescence microscopy images of fields of control and sh2.8 hTERT-RPE1 cells stained for acetylated tubulin (red) as a marker of the primary cilium.
(D) The percent of control and sh2.8 hTERT-RPE1 cells, as in panel C, that formed cilia upon serum starvation.

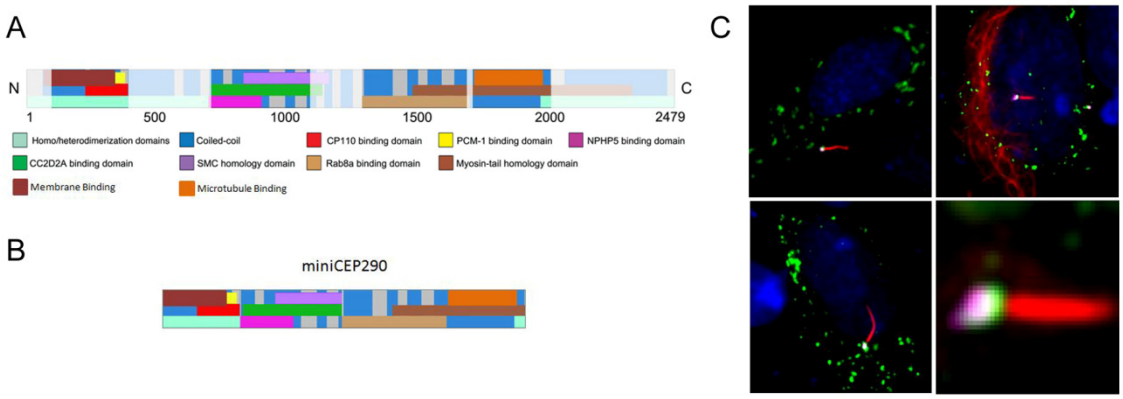

Figure 4.3 Construction and testing of a miniCEP290 construct

(A) Schematic representation of the CEP290 protein with identified functional domains, interacting domains, and protein motifs labeled. Grayed areas represent regions of the protein not included in the miniCEP290 construct.

(B) A schematic representation of miniCEP290. Color coding of functional domains is identical to panel A.

(C) Immunofluorescence images of hTERT-RPE1 cells transiently transfected with GFP-fused miniCEP290 and stained for acetylated tubulin (red) and pericentrin (magenta), and with DAPI (blue). The lower right panel represents a magnified view of a primary cilium, showing the localization of miniCEP290 to the ciliary transition zone.

CHAPTER 5: GENERAL CONCLUSIONS AND FUTURE DIRECTIONS

Theodore G. Drivas[1]

1. Cell and Molecular Biology Graduate Group and the F.M. Kirby Center for Molecular Ophthalmology, Perelman School of Medicine, University of Pennsylvania, Philadelphia, PA 19104, USA

Putting the pieces together

The work presented in the previous chapters represents an in-depth look at the function of CEP290 in ciliogenesis and in human disease. I presented data showing CEP290 to be both a membrane and microtubule binding protein, identified novel autoregulatory domains within CEP290 that appear to regulate the protein's activity and the initiation of ciliogenesis (Chapter 2), and described a novel model for *CEP290* disease pathogenesis that, for the first time, accurately and robustly links specific *CEP290* mutations with specific clinical diagnoses, while at the same time independently corroborating the critical nature of CEP290's membrane and microtubule binding domains (Chapter 3). Using the knowledge I gained in the first two chapters, I describe, in studies which are still ongoing, my attempt to create a *miniCEP290* gene with the ultimate goal of using such a gene as a novel therapeutic for the numerous patients living with *CEP290*-based disease (Chapter 4).

As it turns out, however, picking the problem apart has proved much easier than putting everything back together. Whether reconstructing a mini gene from scraps and fragments, assembling a model from hypothesis and databases, or synthesizing years of work into a single chapter, it's not always obvious how all the pieces fit together, even when one begins to recognize the broader picture that the pieces will ultimately paint. Often times the portrait of CEP290 that I thought I saw in the jumble turned out to be illusions – tightly-wound rings of microtubules masquerading as the nuclear envelope; unambiguous nuclear localization signals producing anything but unambiguous results – while at other times the most obvious pieces – bright, beckoning puncta of vesicular staining, for instance – lay on the top of the pile, in plain

view, completely overlooked or brushed aside in the pursuit of other seemingly more interesting stories.

Regardless of how the pieces were won or how they were fit together, they ultimately paint a picture and tell a story that is their own. The full, unabridged, and definitive version of CEP290's story is certainly still years in the making. While we wait, however, we have the exciting opportunity to tell our own versions of the CEP290 story. Hopefully we will all agree on the most important facts and, collectively, come close to approximating the true plotline. There is certainly room for multiple viewpoints, but what follows is the story of CEP290 that, based on my data and the data of other fantastic groups, I believe to be an accurate reflection of the protein's true identity.

CEP290: a primary player in the primary cilium

The story of CEP290 is undoubtedly a story of the protein's function (and dysfunction) at the primary cilium. Other groups have investigated the protein's putative role in the nucleus (Guo et al., 2004), at the centriolar satellites (Kim et al., 2008), and as a transcriptional activator (Sayer et al., 2006), but it seems to me (and to the field in general) that these excursions into poorly-charted CEP290 territory have been mostly diversions. At the very least, any role that CEP290 might be playing elsewhere in the cell has certainly taken a backseat to the protein's role in ciliogenesis and cilium function (Coppieters et al., 2010). This is not to say that the other functions ascribed to the protein are inconsequential to CEP290's role in the cell, but only that the protein's most important function, based on the data we currently have, appears to lie in promoting and maintaining cilium formation and function. We are now finally beginning to gain a firm grasp on the role that the protein plays in these processes, and as we have learned more about what CEP290 is doing we have begun to appreciate how important and central the protein is to the integrity of the cilium.

Bridging the gap

With the publication of the work presented in this thesis, and with consideration of the work published by other groups, we have finally defined the critical role that CEP290 plays at the primary cilium. We can now say with confidence that CEP290 directly bridges the gap between the ciliary membrane and microtubule axoneme at the transition zone of the organelle.

Since Craige et al.'s publication in 2010, CEP290 had been known to be a critical component of the ciliary Y-links, the dense, proteinaceous structures that appear to span the distance between

the transition zone membrane and axoneme. A *Chlamydomonas* mutant lacking CEP290 was found to exhibit significant deficits in ciliary Y-link formation, resulting in severe dysregulation of the protein components of the ciliary compartment. But in what capacity does CEP290 serve to stabilize or promote Y-link formation? It had been postulated, since CEP290's discovery, that the predominantly coiled-coiled nature of the protein might lend itself well to the structural bolstering of the cilium (Chang et al., 2006). But whether CEP290 serves merely as a structural connector, acting as a scaffold for the assembly of other Y-link components, or whether it plays a direct role in riveting the axoneme to the membrane has been up for debate. In fact, as recently as June of this year it had been proposed that CEP290 acts as nothing more than an adapter, serving to connect microtubule binding proteins at the axoneme to membrane binding proteins at the ciliary membrane (Wang et al., 2013).

The work on CEP290 presented in this dissertation lays that notion to rest. It is now clear that CEP290 itself directly anchors the microtubule core of the cilium to the overlying membrane. CEP290 contains a membrane binding domain within its N-terminus and a microtubule binding domain near its C-terminal end. The proper function of both of these domains is absolutely critical to the function of the protein – deletion of the microtubule binding domain in the rd16 mouse leads to profound and rapid retinal degeneration; human patients producing low levels of CEP290 lacking either domain were found to fare far worse than even those patients lacking CEP290 altogether. The fact that dysfunction of CEP290 and its membrane/microtubule binding domains leads to such significant disease and such dramatic disintegration of the ciliary Y-links speaks to the fact that CEP290's function at the cilium is completely indispensible. There appears to be no redundancy where CEP290 is concerned – no protein has yet been discovered

capable of masking CEP290 deficiency. This may be due to the unique, bispecific nature of the CEP290 protein – CEP290 is so far the only protein component of the transition zone shown capable of directly linking the ciliary membrane to the ciliary axoneme, and the protein's uniqueness in this regard may be at the root of its indispensability.

But why are the membrane-to-microtubule bridges of the ciliary Y-links so important for ciliary function? There are certainly a number of hypotheses, each of them valid. It has been suggested that the ciliary Y-links act as a pore, selectively allowing for the transport of ciliary cargo (Kee et al., 2012). Or perhaps the Y-links act, more simply, as a diffusion barrier, passively separating the ciliary compartment from the cytosol (Hu and Nelson, 2011). Some have even proposed that the ciliary Y-links are the site of IFT initiation, serving as specialized structures for the loading of IFT particles onto the intraflagellar highway (Craige et al., 2010).

But there are certainly other protein components of the ciliary Y-links, many of which bind either the ciliary membrane or axonemal microtubules, and many of which are known CEP290-interactors, yet none of these proteins is capable of rescuing CEP290 dysfunction (Gorden et al., 2008; Kim et al., 2008; Schäfer et al., 2008). Additionally, it is only CEP290 dysfunction that has been shown to result in the complete dissolution of the ciliary Y-links (Craige et al., 2010). Why is it that CEP290, in particular, is so essential to Y-link formation? I would propose that CEP290, always present and primed for ciliogenesis at the mother centriole (Tsang et al., 2008), forms the initial link between the axoneme and ciliary membrane – the grappling hook of the transition zone, if you will. Once CEP290 securely attaches itself to both components of the organelle it might then act as a scaffold for the elaboration of the structures we know as the

ciliary Y-links (Figure 5.1). Thus, disruption of CEP290 function leads to complete collapse of the Y-links and severe disease, while dysfunction of other Y-link components produces a less dramatic phenotype. This hypothesis will of course require significant experimental validation, but all the data that the field has gathered so far is at least in support of the notion.

Bending over backwards to stop ciliogenesis

It became clear from our studies of CEP290 function that the full-length CEP290 protein was significantly inhibited in both its membrane and microtubule binding activities when compared to truncation mutants lacking either CEP290's N- or C-terminus. Investigating this phenomenon further, we went on to discover that the N- and C-termini of the protein do indeed contain autoregulatory domains that act to inhibit CEP290 function and ciliogenesis. The natural inhibition of the protein may, in fact, be the reason why so many groups overlooked CEP290 as a membrane or microtubule binding protein in the first place – overexpressed full-length CEP290 does not obviously associate with either microtubules or membrane.

It had been known for some time that the N- and C- termini of the protein, each containing one of the autoregulatory domains we had identified, are both capable of homo- and heterodimerization (Schäfer et al., 2008). Additionally, in all cases examined, full-length CEP290 seemed to be intrinsically inhibited, suggesting that, whatever the mechanism, CEP290 inhibition is an inherent quality of the protein itself. Finally, we went on to show that overexpression of either terminal autoregulatory domain paradoxically increases, rather than decreases, CEP290 function and ciliogenesis. All of these data led me to the hypothesis that the N- and C-termini of the protein were interacting, cooperating to inhibit CEP290 function.

Perhaps the termini tightly bind to each other, folding the protein over on itself, obscuring important functional domains and inhibiting ciliogenesis (Figure 5.1).

As noted in the discussion of Chapter 2, this particular mechanism of protein inhibition is not novel – it is, in fact, employed by a multitude of human proteins. The ERM domain-containing proteins, for instance, which function to link the cell membrane to the actin cytoskeleton, depend upon this same mechanism to regulate their actin and membrane binding activities (Smith et al., 2003). In fact, the actin- and membrane-binding domains of these proteins aid in their autoinhibition, with the two domains binding to each other in the inhibited state, inhibiting their respective functions, and shutting the protein off (Cornell and Taneva, 2006). It is not surprising, then, that CEP290's membrane binding domain lies in the middle of the N-terminal

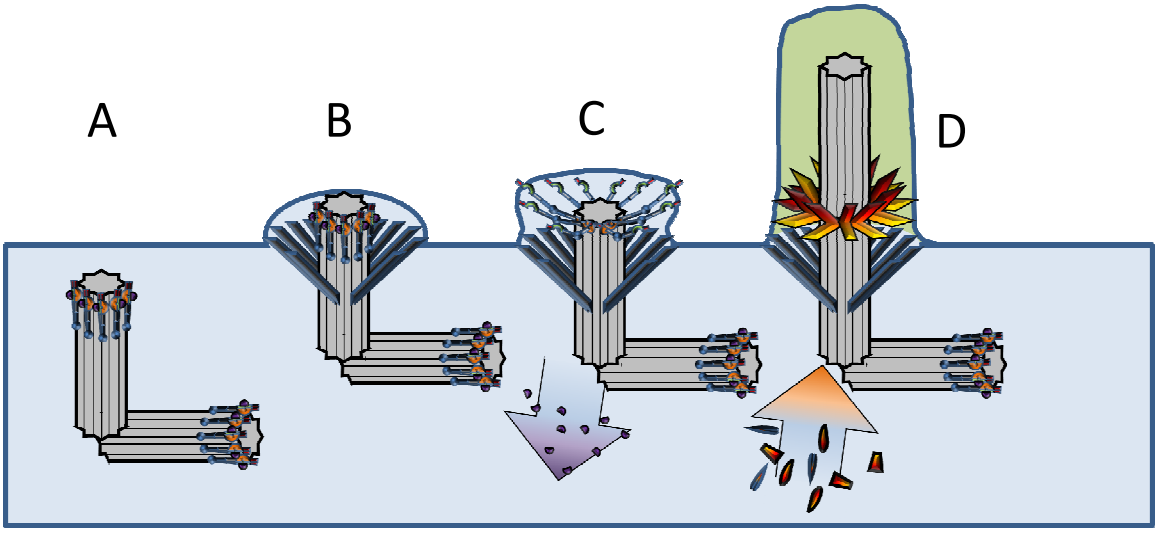

Figure 5.1 A model for CEP290 regulation
(A) The centrioles, each capped by a ring of CEP290, migrate towards the cell surface
(B) The distal appendages make contact with the membrane and form the thick transition fibers
(C) CP110 (purple) is removed from CEP290 at the mother centriole, allowing the protein to spring open and bridge the gap between the membrane and axoneme
(D) CEP290 recruits other transition zone proteins (red/orange), creating the ciliary Y-links, initiating axoneme extension, and establishing the distinct ciliary compartment

autoregulatory domain I identified, and that its microtubule binding domain lies immediately adjacent to the identified C-terminal inhibitory domain. It is likely that CEP290's membrane and microtubule binding domains play similar roles in inhibiting the protein's function.

Reviewing the literature, it became clear that there had been hints of this mechanism of regulation all along. It has been demonstrated that the protein CP110 is capable of binding to and inhibiting CEP290. In fact, CP110 binds CEP290 squarely in the middle of its membrane binding/N-terminal autoregulatory domain (Tsang et al., 2008). It is tantalizing to think that the binding of CP110 causes a conformational change within CEP290's membrane binding domain, rendering it incapable of binding membranes and promoting and stabilizing its binding to the C-terminal microtubule binding/autoregulatory domain. CP110 would thus keep the protein inhibited, folded head-to-tail, at the mother centriole throughout the cell cycle. The removal of CP110 at the initiation of ciliogenesis (Goetz et al., 2012) might allow CEP290 to spring open, freeing its membrane and microtubule binding domain to bridge the transition zone gap and promote Y-link formation (Figure 5.1).

A second hint to the existence of this mechanism of CEP290 inhibition came from the initial study of the rd16 mouse. When the rd16 Cep290 mutation was first described, the authors noted that rd16 Cep290 had a significantly higher affinity for its binding partners than full-length Cep290 did itself (Chang et al., 2006). The rd16 Cep290 deletion encompasses much of the protein's microtubule binding domain, which, as I have noted, may be playing a critical role in mediating Cep290 autoinhibition. The rd16 Cep290 deletion might thus be interfering with CEP290's innate regulation, preventing the protein from shutting off, and paradoxically

increasing its apparent affinity for its binding partners. The difficult-to-explain increase in affinity of rd16 Cep290 for its binding partners now makes perfect sense in the context of CEP290 autoregulation.

However, one last piece of the model is missing. One would hypothesize that CEP290 must contain some kind of a hinge, allowing the two autoregulatory domains at either end of the protein to come in contact with each other to affect CEP290 inhibition. As it turns out, we may have, unknowingly, already identified CEP290's hinge. CEP290 has long been known to contain, at its center, a Structural Maintenance of Chromosomes (SMC) homology domain (Coppieters et al., 2010). The SMC proteins themselves are composed of two coiled coil arms on either side of a molecular hinge that can be selectively swung open or closed to bind to and gather the cell's chromosomes (Melby et al., 1998). It had been assumed that CEP290's SMC homology domain was playing some kind of role in DNA binding (presumed, it seems, only because of the "chromosomes" part of the SMC name and not because of any evidence that CEP290 can actually bind DNA). The SMC homology domain now suddenly makes much more sense, potentially providing a hinge for the opening and closing – activation and inactivation – of CEP290.

To me, at least, this model for CEP290 inhibition makes perfect sense. It helps to explain so many pieces of previously difficult-to-explain data and synthesizes many aspects of CEP290 biology, both on a real and abstract level, into a compelling story, leaving very few loose ends. Significant experimentation is clearly needed to validate this hypothesis, but I eagerly anticipate any advances that may be made on this front.

CEP29opathy

Throughout this thesis I have belabored the point that CEP290 dysfunction results in significant and devastating disease, but this point cannot be stressed enough – accounting for up to 20% of all cases of Leber congenital amaurosis (LCA), *CEP290* is the single biggest cause of LCA yet discovered (den Hollander et al., 2008; Perrault et al., 2007). *CEP290* is also the only gene known to be involved in the pathogenesis of such a broad spectrum of ciliopathy disease, with mutations in the gene resulting in at least 7 distinct ciliopathy phenotypes, ranging in severity from isolated retinal degeneration to embryonic lethality (Coppieters et al., 2010). Up until now, however, we were at a loss when it came to describing the molecular mechanisms of *CEP290* disease pathogenesis. The work presented in this thesis has begun to elucidate some of these mechanisms, and we are now finally beginning to get a handle on the molecular mechanisms of *CEP290* disease.

Molecular mechanisms of CEP290 disease pathogenesis

Over the past 10 years, the number of reported disease-causing mutations in the human *CEP290* gene has exploded, with over 140 deleterious mutations identified throughout the gene's open reading frame (Coppieters et al., 2010). But even as the number of reported mutations increased, the effects that these mutations were having on CEP290 function remained unknown; in fact, CEP290's function in general continued to remain somewhat of a mystery. It is now clear that mutations in *CEP290*, in one way or another, interfere with the protein's critical role in bridging the gap between the ciliary membrane and axoneme: we found that the retinal pathology of the rd16 mouse, a model of *CEP290* disease characterized by a large in-frame deletion of the *Cep290* gene, was ultimately due to the complete disruption of Cep290

microtubule binding (Chapter 2); numerous human mutations in the *CEP290* gene map to this same critical microtubule binding domain, suggesting a potential molecular mechanism for human CEP290 disease.

But on closer inspection it becomes clear that the story isn't quite so simple. Of all the 142 identified human *CEP290* mutations, fewer than 10 are of the missense variety (Coppieters et al., 2010). All of the others are predicted to result in premature termination codons, either directly, through nonsense mutations, or indirectly, through deletions/insertions resulting in frame-shifts. The effects of these truncating mutations on CEP290 protein levels has not been thoroughly investigated, but it is reasonable to assume that, through the mechanism of nonsense-mediated decay (NMD), many of these mutations should act as null alleles (Baker and Parker, 2004), producing little if any CEP290 protein. Suddenly the mechanistic relevance of mutations in the microtubule and membrane binding domains of CEP290 seems greatly diminished – certainly these mutations should significantly interfere with CEP290 function, but so should truncating mutations affecting any other region of the protein, each of them acting, through NMD, to decimate CEP290 protein levels and eliminate CEP290 function.

These important observations and implications have received minimal discussion in the literature, but seem integral to CEP290 disease pathogenesis. If nearly every known CEP290 mutation should result in absent CEP290 protein, how can different CEP290 mutations result in such drastically different phenotypes?

While a number of hypotheses and models to explain the mechanisms and spectrum of *CEP290* disease have been proposed, none have held up to scientific scrutiny. In Chapter 3 of this dissertation, however, we propose a model for *CEP290* disease pathogenesis that, for the first time, robustly and accurately illustrates how different *CEP290* mutations result in different diseases. The model is based on a simple concept: through the mechanisms of NMD and basal exon skipping (BES), different *CEP290* mutations result in different CEP290 protein levels, with decreasing protein levels correlating with increased disease severity (Chapter 3).

Our model explains many of the inconsistencies the field has encountered in describing *CEP290* disease pathogenesis but, perhaps more importantly, it surprised us by highlighting the importance of CEP290's microtubule and membrane binding domains in disease pathogenesis. A number of patients with severe *CEP290* disease did not, at first glance, neatly fit our model. On closer inspection, it was discovered that the pathology seen in these patients stemmed from their production of low levels of CEP290 (levels high enough to potentially ameliorate disease), but of CEP290 lacking either the microtubule or membrane binding domain. In fact, these patients were found to fare worse than those patients producing no CEP290 at all. Disruption of CEP290's membrane or microtubule domains again proved to be the critical mechanism in the progression of *CEP290* disease.

And so our inquiry into CEP290 disease pathogenesis has come full circle. The membrane and microtubule binding functionality of the protein does, in fact, lie at the heart of CEP290 disease; it is this dual functionality that is critical to the protein's role in ciliary biology and human health. However, it is not mutations in these critical regions that are responsible for CEP290 pathology,

but rather mutations, in general, that diminish the levels of functional CEP290 protein. As CEP290 protein levels drop, the structural integrity of the ciliary Y-links is jeopardized. Eventually, the integrity of the ciliary compartment itself is compromised – trafficking into the organelle is hindered and normally excluded proteins begin to leak in. Thus, without enough CEP290 to bridge the gap between the transition zone membrane and axoneme, disease begins to manifest – first, with moderately reduced levels of CEP290, in the retina; with lower CEP290 levels, in the kidneys; finally, with lower CEP290 levels still, throughout the body. With this new understanding of the mechanisms underlying CEP290 pathology we can finally begin to consider novel therapeutic strategies to help those suffering from CEP290 disease.

Implications for therapeutic intervention

As illustrated in the work presented in this thesis, it is inevitable that any new understanding we gain of CEP290's basic biology will be critical in the development of innovative *CEP290* therapeutics. In our studies, the identification of novel CEP290 functional domains immediately suggested new avenues towards therapeutic approaches. For instance, it is now clear that any gene transfer strategy delivering *CEP290* or a *miniCEP290* gene must take into consideration the critical role the protein plays in bridging the transition zone gap, taking special care to preserve CEP290's membrane and microtubule binding functionality (Chapter 2). On the other hand, the identification of novel inhibitory domains within the protein presents numerous possibilities for therapeutic approach of a different sort. If these inhibitory domains are truly dispensable for CEP290 function in the retina, we may be one step closer to the design and delivery of a *miniCEP290* gene capable of replacing the full-length protein's function while being small enough to fit within the AAV class of viral vectors (Chapters 3, 4). Regardless of whether such a

mini gene strategy ultimately pays off, learning more about the regulation of CEP290 through the continued study of its inhibitory domains may present completely new paradigms for the treatment of CEP290 disease. With a finer understanding of how CEP290 is activated, the possibility exists that we might be able to potentiate what little CEP290 may still be present in the tissues of CEP290 patients by manipulating endogenous CEP290 regulation for therapeutic gain.

The activity of residual CEP290 protein levels is not only relevant to the design of therapeutics – it is now clear that CEP290 protein levels are critically important to human health. The sliding scale of *CEP290* disease (CEP29opathy, to coin a new term) indicates that there is no CE29opathy tipping point – incremental decreases in CEP290 protein levels result in incremental decreases in ciliary function. These findings have major, and not necessarily favorable, implications for therapeutic intervention. In Chapter 3 we discovered that even high levels of CEP290 protein (up to 50% of normal) were still associated with significant retinal degeneration. Low to absent levels of CEP290, on the other hand, were uniformly associated with severe disease. In terms of therapeutic approach, these data seem to indicate that relatively high levels of CEP290 expression will have to be achieved in the retina if there is any hope of halting the progression of *CEP290*-associated LCA. The renal disease common to so many CEP29opathies, on the other hand, may be rescuable with lower levels of CEP290 protein, as it is only at medium to low levels of CEP290 that renal symptoms are manifest. Unfortunately, the CNS and systemic deficits of Joubert syndrome and Bardet-Biedl syndrome will likely be refractory to any gene therapeutic approach since much of the pathology in these diseases occurs during the very earliest stages of embryonic development (Chen, 2007).

Regardless of how effective a gene transfer approach to *CEP290* disease might or might not be in ameliorating the pathology seen in different organ systems, the fact remains that we are still without any *CEP290* therapeutic. Some of the findings presented in this dissertation may someday aid in the development of such an intervention, perhaps through the use of a *miniCEP290* gene, as discussed, or perhaps through some as-of-yet undreamt of approach. Either way, I am glad to have contributed to the work towards this end. I can only hope that some small part of this thesis will go on to make difference in the lives of those CEP290 patients and supporters who have already made a difference in mine.

REFERENCES

Adams, N.A., Awadein, A., and Toma, H.S. (2007). The retinal ciliopathies. Ophthalmic Genet. *28*, 113–125.

Afzelius, B.A. (1976). A human syndrome caused by immotile cilia. Science *193*, 317–319.

Aguilar, A., Meunier, A., Strehl, L., Martinovic, J., Bonniere, M., Attie-Bitach, T., Encha-Razavi, F., and Spassky, N. (2012). Analysis of human samples reveals impaired SHH-dependent cerebellar development in Joubert syndrome/Meckel syndrome. Proc. Natl. Acad. Sci. *109*, 16951–16956.

Alieva, I.B., Gorgidze, L.A., Komarova, Y.A., Chernobelskaya, O.A., and Vorobjev, I.A. (1999). Experimental model for studying the primary cilia in tissue culture cells. Membr. Cell Biol. *12*, 895–905.

Allocca, M., Doria, M., Petrillo, M., Colella, P., Garcia-Hoyos, M., Gibbs, D., Kim, S.R., Maguire, A., Rex, T.S., Di Vicino, U., et al. (2008). Serotype-dependent packaging of large genes in adeno-associated viral vectors results in effective gene delivery in mice. J. Clin. Invest. *118*, 1955–1964.

Andersen, J.S., Wilkinson, C.J., Mayor, T., Mortensen, P., Nigg, E.A., and Mann, M. (2003). Proteomic characterization of the human centrosome by protein correlation profiling. Nature *426*, 570–574.

Anderson, R.G.W. (1972). The Three-Dimensional Structure of the Basal Body from the Rhesus Monkey Oviduct. J. Cell Biol. *54*, 246–265.

Van Asselt, S.J., de Vries, E.G., van Dullemen, H.M., Brouwers, A.H., Walenkamp, A.M., Giles, R.H., and Links, T.P. (2013). Pancreatic cyst development: insights from von Hippel-Lindau disease. Cilia *2*, 3.

Auricchio, A., Kobinger, G., Anand, V., Hildinger, M., O'Connor, E., Maguire, A.M., Wilson, J.M., and Bennett, J. (2001). Exchange of surface proteins impacts on viral vector cellular specificity and transduction characteristics: the retina as a model. Hum. Mol. Genet. *10*, 3075–3081.

Avidor-Reiss, T., and Gopalakrishnan, J. (2012). Building a centriole. Curr. Opin. Cell Biol.

Azimzadeh, J., and Marshall, W.F. (2010). Building the Centriole. Curr. Biol. CB *20*, R816–R825.

Baala, L., Audollent, S., Martinovic, J., Ozilou, C., Babron, M.-C., Sivanandamoorthy, S., Saunier, S., Salomon, R., Gonzales, M., Rattenberry, E., et al. (2007). Pleiotropic effects of CEP290 (NPHP6) mutations extend to Meckel syndrome. Am. J. Hum. Genet. *81*, 170–179.

Bachmann-Gagescu, R., Ishak, G.E., Dempsey, J.C., Adkins, J., O'Day, D., Phelps, I.G., Gunay-Aygun, M., Kline, A.D., Szczaluba, K., Martorell, L., et al. (2012). Genotype-phenotype correlation in CC2D2A-related Joubert syndrome reveals an association with ventriculomegaly and seizures. J. Med. Genet. *49*, 126–137.

Baker, K.E., and Parker, R. (2004). Nonsense-mediated mRNA decay: terminating erroneous gene expression. Curr. Opin. Cell Biol. *16*, 293–299.

BARNES, B.G. (1961). Ciliated secretory cells in the pars distalis of the mouse hypophysis. J. Ultrastruct. Res. *5*, 453–467.

Barral, D.C., Garg, S., Casalou, C., Watts, G.F.M., Sandoval, J.L., Ramalho, J.S., Hsu, V.W., and Brenner, M.B. (2012). Arl13b regulates endocytic recycling traffic. Proc. Natl. Acad. Sci. U. S. A. *109*, 21354–21359.

Bartoloni, L., Blouin, J.-L., Pan, Y., Gehrig, C., Maiti, A.K., Scamuffa, N., Rossier, C., Jorissen, M., Armengot, M., Meeks, M., et al. (2002). Mutations in the DNAH11 (axonemal heavy chain dynein type 11) gene cause one form of situs inversus totalis and most likely primary ciliary dyskinesia. Proc. Natl. Acad. Sci. U. S. A. *99*, 10282–10286.

Basten, S.G., and Giles, R.H. (2013). Functional aspects of primary cilia in signaling, cell cycle and tumorigenesis. Cilia *2*, 6.

Baye, L.M., Patrinostro, X., Swaminathan, S., Beck, J.S., Zhang, Y., Stone, E.M., Sheffield, V.C., and Slusarski, D.C. (2011). The N-terminal region of centrosomal protein 290 (CEP290) restores vision in a zebrafish model of human blindness. Hum. Mol. Genet. *20*, 1467–1477.

Beisson, J., and Jerka-Dziadosz, M. (1999). Polarities of the centriolar structure: morphogenetic consequences. Biol. Cell Auspices Eur. Cell Biol. Organ. *91*, 367–378.

Benmerah, A. (2013). The ciliary pocket. Curr. Opin. Cell Biol. *25*, 78–84.

Berbari, N.F., Johnson, A.D., Lewis, J.S., Askwith, C.C., and Mykytyn, K. (2008a). Identification of Ciliary Localization Sequences within the Third Intracellular Loop of G Protein-coupled Receptors. Mol. Biol. Cell *19*, 1540–1547.

Berbari, N.F., Lewis, J.S., Bishop, G.A., Askwith, C.C., and Mykytyn, K. (2008b). Bardet-Biedl syndrome proteins are required for the localization of G protein-coupled receptors to primary cilia. Proc. Natl. Acad. Sci. U. S. A. *105*, 4242–4246.

Besschetnova, T.Y., Kolpakova-Hart, E., Guan, Y., Zhou, J., Olsen, B.R., and Shah, J.V. (2010). Identification of signaling pathways regulating primary cilium length and flow-mediated adaptation. Curr. Biol. CB *20*, 182–187.

Bettencourt-Dias, M., and Glover, D.M. (2007). Centrosome biogenesis and function: centrosomics brings new understanding. Nat. Rev. Mol. Cell Biol. *8*, 451–463.

Bhardwaj, G., Murdoch, B., Wu, D., Baker, D.P., Williams, K.P., Chadwick, K., Ling, L.E., Karanu, F.N., and Bhatia, M. (2001). Sonic hedgehog induces the proliferation of primitive human hematopoietic cells via BMP regulation. Nat. Immunol. *2*, 172–180.

Binder, L.I., Dentler, W.L., and Rosenbaum, J.L. (1975). Assembly of chick brain tubulin onto flagellar microtubules from Chlamydomonas and sea urchin sperm. Proc. Natl. Acad. Sci. U. S. A. *72*, 1122–1126.

Blacque, O.E., Cevik, S., and Kaplan, O.I. (2008). Intraflagellar transport: from molecular characterisation to mechanism. Front. Biosci. J. Virtual Libr. *13*, 2633–2652.

Boekhoff, I., Tareilus, E., Strotmann, J., and Breer, H. (1990). Rapid activation of alternative second messenger pathways in olfactory cilia from rats by different odorants. EMBO J. *9*, 2453–2458.

Brancati, F., Barrano, G., Silhavy, J.L., Marsh, S.E., Travaglini, L., Bielas, S.L., Amorini, M., Zablocka, D., Kayserili, H., Al-Gazali, L., et al. (2007). CEP290 mutations are frequently identified in the oculo-renal form of Joubert syndrome-related disorders. Am. J. Hum. Genet. *81*, 104–113.

Brancati, F., Dallapiccola, B., and Valente, E.M. (2010). Joubert Syndrome and related disorders. Orphanet J. Rare Dis. *5*, 20.

Calvert, P.D., Schiesser, W.E., and Pugh, E.N. (2010). Diffusion of a soluble protein, photoactivatable GFP, through a sensory cilium. J. Gen. Physiol. *135*, 173–196.

Carlén, B., and Stenram, U. (2005). Primary ciliary dyskinesia: a review. Ultrastruct. Pathol. *29*, 217–220.

Carter, S.D., and Sjögren, C. (2012). The SMC complexes, DNA and chromosome topology: right or knot? Crit. Rev. Biochem. Mol. Biol. *47*, 1–16.

Cavalier-Smith, T. (2010). Origin of the cell nucleus, mitosis and sex: roles of intracellular coevolution. Biol. Direct *5*, 7.

Cevik, S., Hori, Y., Kaplan, O.I., Kida, K., Toivenon, T., Foley-Fisher, C., Cottell, D., Katada, T., Kontani, K., and Blacque, O.E. (2010). Joubert syndrome Arl13b functions at ciliary membranes and stabilizes protein transport in Caenorhabditis elegans. J. Cell Biol. *188*, 953–969.

Chang, B., Khanna, H., Hawes, N., Jimeno, D., He, S., Lillo, C., Parapuram, S.K., Cheng, H., Scott, A., Hurd, R.E., et al. (2006). In-frame deletion in a novel centrosomal/ciliary protein CEP290/NPHP6 perturbs its interaction with RPGR and results in early-onset retinal degeneration in the rd16 mouse. Hum. Mol. Genet. *15*, 1847–1857.

Chang, Y.-F., Chan, W.-K., Imam, J.S., and Wilkinson, M.F. (2007). Alternatively spliced T-cell receptor transcripts are up-regulated in response to disruption of either splicing elements or reading frame. J. Biol. Chem. *282*, 29738–29747.

Chapman, E.R., An, S., Barton, N., and Jahn, R. (1994). SNAP-25, a t-SNARE which binds to both syntaxin and synaptobrevin via domains that may form coiled coils. J. Biol. Chem. *269*, 27427–27432.

Chen, C.-P. (2007). Meckel syndrome: genetics, perinatal findings, and differential diagnosis. Taiwan. J. Obstet. Gynecol. *46*, 9–14.

Chen, D., and Shou, C. (2001). Molecular cloning of a tumor-associated antigen recognized by monoclonal antibody 3H11. Biochem. Biophys. Res. Commun. *280*, 99–103.

Chen, C.H., Matthews, T.J., McDanal, C.B., Bolognesi, D.P., and Greenberg, M.L. (1995). A molecular clasp in the human immunodeficiency virus (HIV) type 1 TM protein determines the anti-HIV activity of gp41 derivatives: implication for viral fusion. J. Virol. *69*, 3771–3777.

Chen, Z., Indjeian, V.B., McManus, M., Wang, L., and Dynlacht, B.D. (2002). CP110, a cell cycle-dependent CDK substrate, regulates centrosome duplication in human cells. Dev. Cell *3*, 339–350.

Chung, D.C., and Traboulsi, E.I. (2009). Leber congenital amaurosis: clinical correlations with genotypes, gene therapy trials update, and future directions. J. AAPOS Off. Publ. Am. Assoc. Pediatr. Ophthalmol. Strabismus Am. Assoc. Pediatr. Ophthalmol. Strabismus *13*, 587–592.

Cideciyan, A.V., Rachel, R.A., Aleman, T.S., Swider, M., Schwartz, S.B., Sumaroka, A., Roman, A.J., Stone, E.M., Jacobson, S.G., and Swaroop, A. (2011). Cone photoreceptors are the main targets for gene therapy of NPHP5 (IQCB1) or NPHP6 (CEP290) blindness: generation of an all-cone Nphp6 hypomorph mouse that mimics the human retinal ciliopathy. Hum. Mol. Genet. *20*, 1411–1423.

Cole, D.G., Diener, D.R., Himelblau, A.L., Beech, P.L., Fuster, J.C., and Rosenbaum, J.L. (1998). Chlamydomonas kinesin-II-dependent intraflagellar transport (IFT): IFT particles contain proteins required for ciliary assembly in Caenorhabditis elegans sensory neurons. J. Cell Biol. *141*, 993–1008.

Collin, R.W., den Hollander, A.I., van der Velde-Visser, S.D., Bennicelli, J., Bennett, J., and Cremers, F.P. (2012). Antisense Oligonucleotide (AON)-based Therapy for Leber Congenital Amaurosis Caused by a Frequent Mutation in CEP290. Mol. Ther. Nucleic Acids *1*, e14.

Coppieters, F., Lefever, S., Leroy, B.P., and De Baere, E. (2010). CEP290, a gene with many faces: mutation overview and presentation of CEP290base. Hum. Mutat. *31*, 1097–1108.

Corbit, K.C., Aanstad, P., Singla, V., Norman, A.R., Stainier, D.Y.R., and Reiter, J.F. (2005). Vertebrate Smoothened functions at the primary cilium. Nature *437*, 1018–1021.

Corbit, K.C., Shyer, A.E., Dowdle, W.E., Gaulden, J., Singla, V., Chen, M.-H., Chuang, P.-T., and Reiter, J.F. (2008). Kif3a constrains beta-catenin-dependent Wnt signalling through dual ciliary and non-ciliary mechanisms. Nat. Cell Biol. *10*, 70–76.

Cornell, R.B., and Taneva, S.G. (2006). Amphipathic helices as mediators of the membrane interaction of amphitropic proteins, and as modulators of bilayer physical properties. Curr. Protein Pept. Sci. *7*, 539–552.

Craige, B., Tsao, C.-C., Diener, D.R., Hou, Y., Lechtreck, K.-F., Rosenbaum, J.L., and Witman, G.B. (2010). CEP290 tethers flagellar transition zone microtubules to the membrane and regulates flagellar protein content. J. Cell Biol. *190*, 927–940.

Czarnecki, P.G., and Shah, J.V. (2012). The ciliary transition zone: from morphology and molecules to medicine. Trends Cell Biol. *22*, 201–210.

D'Angelo, A., and Franco, B. (2009). The dynamic cilium in human diseases. Pathogenetics *2*, 3.

D'Angiolella, V., Donato, V., Vijayakumar, S., Saraf, A., Florens, L., Washburn, M.P., Dynlacht, B., and Pagano, M. (2010). SCF(Cyclin F) controls centrosome homeostasis and mitotic fidelity through CP110 degradation. Nature *466*, 138–142.

Dahl, H.A. (1963). Fine structure of cilia in rat cerebral cortex. Z. Für Zellforsch. Mikrosk. Anat. *60*, 369–386.

Dammermann, A., and Merdes, A. (2002). Assembly of centrosomal proteins and microtubule organization depends on PCM-1. J. Cell Biol. *159*, 255–266.

Davenport, J.R., Watts, A.J., Roper, V.C., Croyle, M.J., van Groen, T., Wyss, J.M., Nagy, T.R., Kesterson, R.A., and Yoder, B.K. (2007). Disruption of intraflagellar transport in adult mice leads to obesity and slow-onset cystic kidney disease. Curr. Biol. CB *17*, 1586–1594.

Deane, J.A., Cole, D.G., Seeley, E.S., Diener, D.R., and Rosenbaum, J.L. (2001). Localization of intraflagellar transport protein IFT52 identifies basal body transitional fibers as the docking site for IFT particles. Curr. Biol. CB *11*, 1586–1590.

Deretic, D., Huber, L.A., Ransom, N., Mancini, M., Simons, K., and Papermaster, D.S. (1995). rab8 in retinal photoreceptors may participate in rhodopsin transport and in rod outer segment disk morphogenesis. J. Cell Sci. *108 (Pt 1)*, 215–224.

Dingemans, K.P. (1969). THE RELATION BETWEEN CILIA AND MITOSES IN THE MOUSE ADENOHYPOPHYSIS. J. Cell Biol. *43*, 361–367.

Dishinger, J.F., Kee, H.L., Jenkins, P.M., Fan, S., Hurd, T.W., Hammond, J.W., Truong, Y.N.-T., Margolis, B., Martens, J.R., and Verhey, K.J. (2010). Ciliary entry of the kinesin-2 motor KIF17 is regulated by importin-β2 and RanGTP. Nat. Cell Biol. *12*, 703–710.

Doherty, D., Parisi, M.A., Finn, L.S., Gunay-Aygun, M., Al-Mateen, M., Bates, D., Clericuzio, C., Demir, H., Dorschner, M., van Essen, A.J., et al. (2010). Mutations in 3 genes (MKS3, CC2D2A and RPGRIP1L) cause COACH syndrome (Joubert syndrome with congenital hepatic fibrosis). J. Med. Genet. *47*, 8–21.

Drivas, T.G., Holzbaur, E.L.F., and Bennett, J. (2013). Disruption of CEP290 microtubule/membrane-binding domains causes retinal degeneration. J. Clin. Invest.

Elias, R.V., Sezate, S.S., Cao, W., and McGinnis, J.F. (2004). Temporal kinetics of the light/dark translocation and compartmentation of arrestin and alpha-transducin in mouse photoreceptor cells. Mol. Vis. *10*, 672–681.

Eliasson, R., Mossberg, B., Camner, P., and Afzelius, B.A. (1977). The immotile-cilia syndrome. A congenital ciliary abnormality as an etiologic factor in chronic airway infections and male sterility. N. Engl. J. Med. *297*, 1–6.

Engel, B.D., Ishikawa, H., Wemmer, K.A., Geimer, S., Wakabayashi, K., Hirono, M., Craige, B., Pazour, G.J., Witman, G.B., Kamiya, R., et al. (2012). The role of retrograde intraflagellar transport in flagellar assembly, maintenance, and function. J. Cell Biol. *199*, 151–167.

Farkas, M.H., Grant, G.R., White, J.A., Sousa, M.E., Consugar, M.B., and Pierce, E.A. (2013). Transcriptome analyses of the human retina identify unprecedented transcript diversity and 3.5 Mb of novel transcribed sequence via significant alternative splicing and novel genes. BMC Genomics *14*, 486.

Fawcett, D.W., and Porter, K.R. (1954). A study of the fine structure of ciliated epithelia. J. Morphol. *94*, 221–281.

Ferrari, S., Di Iorio, E., Barbaro, V., Ponzin, D., Sorrentino, F.S., and Parmeggiani, F. (2011). Retinitis pigmentosa: genes and disease mechanisms. Curr. Genomics *12*, 238–249.

Feuillan, P.P., Ng, D., Han, J.C., Sapp, J.C., Wetsch, K., Spaulding, E., Zheng, Y.C., Caruso, R.C., Brooks, B.P., Johnston, J.J., et al. (2011). Patients with Bardet-Biedl syndrome have hyperleptinemia suggestive of leptin resistance. J. Clin. Endocrinol. Metab. *96*, E528–535.

Finetti, F., Paccani, S.R., Rosenbaum, J., and Baldari, C.T. (2011). Intraflagellar transport: a new player at the immune synapse. Trends Immunol. *32*, 139–145.

Fischer, E., Legue, E., Doyen, A., Nato, F., Nicolas, J.-F., Torres, V., Yaniv, M., and Pontoglio, M. (2006). Defective planar cell polarity in polycystic kidney disease. Nat. Genet. *38*, 21–23.

Fliegauf, M., Benzing, T., and Omran, H. (2007). When cilia go bad: cilia defects and ciliopathies. Nat. Rev. Mol. Cell Biol. *8*, 880–893.

Fonte, V.G., Searls, R.L., and Hilfer, S.R. (1971). The relationship of cilia with cell division and differentiation. J. Cell Biol. *49*, 226–229.

Geerts, W.J.C., Vocking, K., Schoonen, N., Haarbosch, L., van Donselaar, E.G., Regan-Klapisz, E., and Post, J.A. (2011). Cobblestone HUVECs: a human model system for studying primary ciliogenesis. J. Struct. Biol. *176*, 350–359.

Geng, L., Okuhara, D., Yu, Z., Tian, X., Cai, Y., Shibazaki, S., and Somlo, S. (2006). Polycystin-2 traffics to cilia independently of polycystin-1 by using an N-terminal RVxP motif. J. Cell Sci. *119*, 1383–1395.

Gerard, X., Perrault, I., Hanein, S., Silva, E., Bigot, K., Defoort-Delhemmes, S., Rio, M., Munnich, A., Scherman, D., Kaplan, J., et al. (2012). AON-mediated Exon Skipping Restores Ciliation in Fibroblasts Harboring the Common Leber Congenital Amaurosis CEP290 Mutation. Mol. Ther. Nucleic Acids *1*, e29.

Gerdes, J.M., Liu, Y., Zaghloul, N.A., Leitch, C.C., Lawson, S.S., Kato, M., Beachy, P.A., Beales, P.L., DeMartino, G.N., Fisher, S., et al. (2007). Disruption of the basal body compromises proteasomal function and perturbs intracellular Wnt response. Nat. Genet. *39*, 1350–1360.

Gilula, N.B., and Satir, P. (1972). The ciliary necklace. A ciliary membrane specialization. J. Cell Biol. *53*, 494–509.

Di Gioia, S.A., Letteboer, S.J.F., Kostic, C., Bandah-Rozenfeld, D., Hetterschijt, L., Sharon, D., Arsenijevic, Y., Roepman, R., and Rivolta, C. (2012). FAM161A, associated with retinitis pigmentosa, is a component of the cilia-basal body complex and interacts with proteins involved in ciliopathies. Hum. Mol. Genet. *21*, 5174–5184.

Girard, D., and Petrovsky, N. (2011). Alström syndrome: insights into the pathogenesis of metabolic disorders. Nat. Rev. Endocrinol. *7*, 77–88.

Goetz, S.C., Liem, K.F., Jr, and Anderson, K.V. (2012). The spinocerebellar ataxia-associated gene Tau tubulin kinase 2 controls the initiation of ciliogenesis. Cell *151*, 847–858.

Gönczy, P. (2012). Towards a molecular architecture of centriole assembly. Nat. Rev. Mol. Cell Biol. *13*, 425–435.

Gorden, N.T., Arts, H.H., Parisi, M.A., Coene, K.L.M., Letteboer, S.J.F., van Beersum, S.E.C., Mans, D.A., Hikida, A., Eckert, M., Knutzen, D., et al. (2008). CC2D2A is mutated in Joubert syndrome and interacts with the ciliopathy-associated basal body protein CEP290. Am. J. Hum. Genet. *83*, 559–571.

Gordon, M.D., and Nusse, R. (2006). Wnt signaling: multiple pathways, multiple receptors, and multiple transcription factors. J. Biol. Chem. *281*, 22429–22433.

Goto, H., Inoko, A., and Inagaki, M. (2013). Cell cycle progression by the repression of primary cilia formation in proliferating cells. Cell. Mol. Life Sci. CMLS.

Grillo, M.A., and Palay, S.L. (1963). CILIATED SCHWANN CELLS IN THE AUTONOMIC NERVOUS SYSTEM OF THE ADULT RAT. J. Cell Biol. *16*, 430–436.

Guo, D.-F., and Rahmouni, K. (2011). Molecular basis of the obesity associated with Bardet-Biedl syndrome. Trends Endocrinol. Metab. TEM *22*, 286–293.

Guo, J., Jin, G., Meng, L., Ma, H., Nie, D., Wu, J., Yuan, L., and Shou, C. (2004). Subcellular localization of tumor-associated antigen 3H11Ag. Biochem. Biophys. Res. Commun. *324*, 922–930.

Guo, J., Yang, Z., Song, W., Chen, Q., Wang, F., Zhang, Q., and Zhu, X. (2006). Nudel Contributes to Microtubule Anchoring at the Mother Centriole and Is Involved in Both Dynein-dependent and -independent Centrosomal Protein Assembly. Mol. Biol. Cell *17*, 680–689.

Gustke, N., Trinczek, B., Biernat, J., Mandelkow, E.M., and Mandelkow, E. (1994). Domains of tau protein and interactions with microtubules. Biochemistry (Mosc.) *33*, 9511–9522.

Halbritter, J., Diaz, K., Chaki, M., Porath, J.D., Tarrier, B., Fu, C., Innis, J.L., Allen, S.J., Lyons, R.H., Stefanidis, C.J., et al. (2012). High-throughput mutation analysis in patients with a nephronophthisis-associated ciliopathy applying multiplexed barcoded array-based PCR amplification and next-generation sequencing. J. Med. Genet. *49*, 756–767.

Hammond, J.W., Blasius, T.L., Soppina, V., Cai, D., and Verhey, K.J. (2010). Autoinhibition of the kinesin-2 motor KIF17 via dual intramolecular mechanisms. J. Cell Biol. *189*, 1013–1025.

Han, Y.-G., Spassky, N., Romaguera-Ros, M., Garcia-Verdugo, J.-M., Aguilar, A., Schneider-Maunoury, S., and Alvarez-Buylla, A. (2008). Hedgehog signaling and primary cilia are required for the formation of adult neural stem cells. Nat. Neurosci. *11*, 277–284.

Han, Y.-G., Kim, H.J., Dlugosz, A.A., Ellison, D.W., Gilbertson, R.J., and Alvarez-Buylla, A. (2009). Dual and opposing roles of primary cilia in medulloblastoma development. Nat. Med. *15*, 1062–1065.

Haycraft, C.J., Banizs, B., Aydin-Son, Y., Zhang, Q., Michaud, E.J., and Yoder, B.K. (2005). Gli2 and Gli3 Localize to Cilia and Require the Intraflagellar Transport Protein Polaris for Processing and Function. PLoS Genet *1*, e53.

He, B., and Guo, W. (2009). The exocyst complex in polarized exocytosis. Curr. Opin. Cell Biol. *21*, 537–542.

Hearn, T., Spalluto, C., Phillips, V.J., Renforth, G.L., Copin, N., Hanley, N.A., and Wilson, D.I. (2005). Subcellular localization of ALMS1 supports involvement of centrosome and basal body dysfunction in the pathogenesis of obesity, insulin resistance, and type 2 diabetes. Diabetes *54*, 1581–1587.

Helou, J., Otto, E.A., Attanasio, M., Allen, S.J., Parisi, M.A., Glass, I., Utsch, B., Hashmi, S., Fazzi, E., Omran, H., et al. (2007). Mutation analysis of NPHP6/CEP290 in patients with Joubert syndrome and Senior-Løken syndrome. J. Med. Genet. *44*, 657–663.

Hildebrandt, F., Attanasio, M., and Otto, E. (2009). Nephronophthisis: disease mechanisms of a ciliopathy. J. Am. Soc. Nephrol. JASN *20*, 23–35.

Den Hollander, A.I., Koenekoop, R.K., Yzer, S., Lopez, I., Arends, M.L., Voesenek, K.E.J., Zonneveld, M.N., Strom, T.M., Meitinger, T., Brunner, H.G., et al. (2006). Mutations in the CEP290 (NPHP6) gene are a frequent cause of Leber congenital amaurosis. Am. J. Hum. Genet. *79*, 556–561.

Den Hollander, A.I., Roepman, R., Koenekoop, R.K., and Cremers, F.P.M. (2008). Leber congenital amaurosis: genes, proteins and disease mechanisms. Prog. Retin. Eye Res. *27*, 391–419.

Hsiao, Y.-C., Tong, Z.J., Westfall, J.E., Ault, J.G., Page-McCaw, P.S., and Ferland, R.J. (2009). Ahi1, whose human ortholog is mutated in Joubert syndrome, is required for Rab8a localization, ciliogenesis and vesicle trafficking. Hum. Mol. Genet. *18*, 3926–3941.

Hsiao, Y.-C., Tuz, K., and Ferland, R.J. (2012). Trafficking in and to the primary cilium. Cilia *1*, 4.

Hu, Q., and Nelson, W.J. (2011). Ciliary diffusion barrier: the gatekeeper for the primary cilium compartment. Cytoskelet. Hoboken NJ *68*, 313–324.

Hu, Q., Milenkovic, L., Jin, H., Scott, M.P., Nachury, M.V., Spiliotis, E.T., and Nelson, W.J. (2010). A Septin Diffusion Barrier at the Base of the Primary Cilium Maintains Ciliary Membrane Protein Distribution. Science *329*, 436–439.

Huangfu, D., Liu, A., Rakeman, A.S., Murcia, N.S., Niswander, L., and Anderson, K.V. (2003). Hedgehog signalling in the mouse requires intraflagellar transport proteins. Nature *426*, 83–87.

Ishikawa, H., and Marshall, W.F. (2011). Ciliogenesis: building the cell's antenna. Nat. Rev. Mol. Cell Biol. *12*, 222–234.

Iwanaga, T., Miki, T., and Takahashi-Iwanaga, H. (2011). Restricted expression of somatostatin receptor 3 to primary cilia in the pancreatic islets and adenohypophysis of mice. Biomed. Res. Tokyo Jpn. *32*, 73–81.

Jenkins, P.M., Hurd, T.W., Zhang, L., McEwen, D.P., Brown, R.L., Margolis, B., Verhey, K.J., and Martens, J.R. (2006). Ciliary targeting of olfactory CNG channels requires the CNGB1b subunit and the kinesin-2 motor protein, KIF17. Curr. Biol. CB *16*, 1211–1216.

Jin, H., White, S.R., Shida, T., Schulz, S., Aguiar, M., Gygi, S.P., Bazan, J.F., and Nachury, M.V. (2010). The conserved Bardet-Biedl syndrome proteins assemble a coat that traffics membrane proteins to cilia. Cell *141*, 1208–1219.

Kaplan, O.I., Molla-Herman, A., Cevik, S., Ghossoub, R., Kida, K., Kimura, Y., Jenkins, P., Martens, J.R., Setou, M., Benmerah, A., et al. (2010). The AP-1 clathrin adaptor facilitates cilium formation and functions with RAB-8 in C. elegans ciliary membrane transport. J. Cell Sci. *123*, 3966–3977.

Kartagener, O.D.M. (1933). Zur Pathogenese der Bronchiektasien. Beiträge Zur Klin. Tuberk. Spezifischen Tuberk.-Forsch. *83*, 489–501.

Kee, H.L., Dishinger, J.F., Blasius, T.L., Liu, C.-J., Margolis, B., and Verhey, K.J. (2012). A size-exclusion permeability barrier and nucleoporins characterize a ciliary pore complex that regulates transport into cilia. Nat. Cell Biol. *14*, 431–437.

Kevany, B.M., and Palczewski, K. (2010). Phagocytosis of retinal rod and cone photoreceptors. Physiol. Bethesda Md *25*, 8–15.

Kikkawa, M., Okada, Y., and Hirokawa, N. (2000). 15 A resolution model of the monomeric kinesin motor, KIF1A. Cell *100*, 241–252.

Kim, J., Krishnaswami, S.R., and Gleeson, J.G. (2008). CEP290 interacts with the centriolar satellite component PCM-1 and is required for Rab8 localization to the primary cilium. Hum. Mol. Genet. *17*, 3796–3805.

Kishimoto, N., Cao, Y., Park, A., and Sun, Z. (2008). Cystic kidney gene seahorse regulates cilia-mediated processes and Wnt pathways. Dev. Cell *14*, 954–961.

Klee, C.B. (1988). Ca2+-dependent phospholipid- (and membrane-) binding proteins. Biochemistry (Mosc.) *27*, 6645–6653.

Kobayashi, T., and Dynlacht, B.D. (2011). Regulating the transition from centriole to basal body. J. Cell Biol. *193*, 435–444.

Komiya, Y., and Habas, R. (2008). Wnt signal transduction pathways. Organogenesis *4*, 68–75.

Kong, J., Kim, S.-R., Binley, K., Pata, I., Doi, K., Mannik, J., Zernant-Rajang, J., Kan, O., Iqball, S., Naylor, S., et al. (2008). Correction of the disease phenotype in the mouse model of Stargardt disease by lentiviral gene therapy. Gene Ther. *15*, 1311–1320.

Koppanati, B.M., Li, J., Reay, D.P., Wang, B., Daood, M., Zheng, H., Xiao, X., Watchko, J.F., and Clemens, P.R. (2010). Improvement of the mdx mouse dystrophic phenotype by systemic in utero AAV8 delivery of a minidystrophin gene. Gene Ther. *17*, 1355–1362.

Kozminski, K.G., Johnson, K.A., Forscher, P., and Rosenbaum, J.L. (1993). A motility in the eukaryotic flagellum unrelated to flagellar beating. Proc. Natl. Acad. Sci. U. S. A. *90*, 5519–5523.

Kozminski, K.G., Beech, P.L., and Rosenbaum, J.L. (1995). The Chlamydomonas kinesin-like protein FLA10 is involved in motility associated with the flagellar membrane. J. Cell Biol. *131*, 1517–1527.

Kubo, A., Sasaki, H., Yuba-Kubo, A., Tsukita, S., and Shiina, N. (1999). Centriolar Satellites Molecular Characterization, Atp-Dependent Movement toward Centrioles and Possible Involvement in Ciliogenesis. J. Cell Biol. *147*, 969–980.

Kuehni, C.E., Frischer, T., Strippoli, M.-P.F., Maurer, E., Bush, A., Nielsen, K.G., Escribano, A., Lucas, J.S.A., Yiallouros, P., Omran, H., et al. (2010). Factors influencing age at diagnosis of primary ciliary dyskinesia in European children. Eur. Respir. J. *36*, 1248–1258.

Lancaster, M.A., and Gleeson, J.G. (2009). The primary cilium as a cellular signaling center: lessons from disease. Curr. Opin. Genet. Dev. *19*, 220–229.

Langmann, T., Di Gioia, S.A., Rau, I., Stöhr, H., Maksimovic, N.S., Corbo, J.C., Renner, A.B., Zrenner, E., Kumaramanickavel, G., Karlstetter, M., et al. (2010). Nonsense mutations in

FAM161A cause RP28-associated recessive retinitis pigmentosa. Am. J. Hum. Genet. *87*, 376–381.

Leitch, C.C., Zaghloul, N.A., Davis, E.E., Stoetzel, C., Diaz-Font, A., Rix, S., Alfadhel, M., Al-Fadhel, M., Lewis, R.A., Eyaid, W., et al. (2008). Hypomorphic mutations in syndromic encephalocele genes are associated with Bardet-Biedl syndrome. Nat. Genet. *40*, 443–448.

Li, Y., Wei, Q., Zhang, Y., Ling, K., and Hu, J. (2010). The small GTPases ARL-13 and ARL-3 coordinate intraflagellar transport and ciliogenesis. J. Cell Biol. *189*, 1039–1051.

Littink, K.W., Pott, J.-W.R., Collin, R.W.J., Kroes, H.Y., Verheij, J.B.G.M., Blokland, E.A.W., de Castro Miró, M., Hoyng, C.B., Klaver, C.C.W., Koenekoop, R.K., et al. (2010). A novel nonsense mutation in CEP290 induces exon skipping and leads to a relatively mild retinal phenotype. Invest. Ophthalmol. Vis. Sci. *51*, 3646–3652.

Louvi, A., and Grove, E.A. (2011). Cilia in the CNS: The Quiet Organelle Claims Center Stage. Neuron *69*, 1046–1060.

Lum, L., and Beachy, P.A. (2004). The Hedgehog Response Network: Sensors, Switches, and Routers. Science *304*, 1755–1759.

Luyten, A., Su, X., Gondela, S., Chen, Y., Rompani, S., Takakura, A., and Zhou, J. (2010). Aberrant Regulation of Planar Cell Polarity in Polycystic Kidney Disease. J. Am. Soc. Nephrol. JASN *21*, 1521–1532.

MacDonald, B.T., Tamai, K., and He, X. (2009). Wnt/β-Catenin Signaling: Components, Mechanisms, and Diseases. Dev. Cell *17*, 9–26.

Maguire, A.M., High, K.A., Auricchio, A., Wright, J.F., Pierce, E.A., Testa, F., Mingozzi, F., Bennicelli, J.L., Ying, G., Rossi, S., et al. (2009). Age-dependent effects of RPE65 gene therapy for Leber's congenital amaurosis: a phase 1 dose-escalation trial. Lancet *374*, 1597–1605.

Mahjoub, M.R. (2013). The importance of a single primary cilium. Organogenesis *9*, 61–69.

Maquat, L.E. (2004). Nonsense-mediated mRNA decay: splicing, translation and mRNP dynamics. Nat. Rev. Mol. Cell Biol. *5*, 89–99.

Marion, V., Stoetzel, C., Schlicht, D., Messaddeq, N., Koch, M., Flori, E., Danse, J.M., Mandel, J.-L., and Dollfus, H. (2009). Transient ciliogenesis involving Bardet-Biedl syndrome proteins is a fundamental characteristic of adipogenic differentiation. Proc. Natl. Acad. Sci. *106*, 1820–1825.

Marion, V., Mockel, A., De Melo, C., Obringer, C., Claussmann, A., Simon, A., Messaddeq, N., Durand, M., Dupuis, L., Loeffler, J.-P., et al. (2012). BBS-induced ciliary defect enhances adipogenesis, causing paradoxical higher-insulin sensitivity, glucose usage, and decreased inflammatory response. Cell Metab. *16*, 363–377.

Masland, R.H. (2001). The fundamental plan of the retina. Nat. Neurosci. *4*, 877–886.

Mason, J.M., and Arndt, K.M. (2004). Coiled coil domains: stability, specificity, and biological implications. Chembiochem Eur. J. Chem. Biol. *5*, 170–176.

Mazelova, J., Ransom, N., Astuto-Gribble, L., Wilson, M.C., and Deretic, D. (2009). Syntaxin 3 and SNAP-25 pairing, regulated by omega-3 docosahexaenoic acid, controls the delivery of rhodopsin for the biogenesis of cilia-derived sensory organelles, the rod outer segments. J. Cell Sci. *122*, 2003–2013.

McAteer, J.A., Dougherty, G.S., Gardner, K.D., Jr, and Evan, A.P. (1986). Scanning electron microscopy of kidney cells in culture: surface features of polarized epithelia. Scan. Electron Microsc. 1135–1150.

McEwen, D.P., Koenekoop, R.K., Khanna, H., Jenkins, P.M., Lopez, I., Swaroop, A., and Martens, J.R. (2007). Hypomorphic CEP290/NPHP6 mutations result in anosmia caused by the selective loss of G proteins in cilia of olfactory sensory neurons. Proc. Natl. Acad. Sci. *104*, 15917–15922.

Melby, T.E., Ciampaglio, C.N., Briscoe, G., and Erickson, H.P. (1998). The symmetrical structure of structural maintenance of chromosomes (SMC) and MukB proteins: long, antiparallel coiled coils, folded at a flexible hinge. J. Cell Biol. *142*, 1595–1604.

Menotti-Raymond, M., David, V.A., Schäffer, A.A., Stephens, R., Wells, D., Kumar-Singh, R., O'Brien, S.J., and Narfström, K. (2007). Mutation in CEP290 discovered for cat model of human retinal degeneration. J. Hered. *98*, 211–220.

Miyamoto, T., Porazinski, S., Wang, H., Borovina, A., Ciruna, B., Shimizu, A., Kajii, T., Kikuchi, A., Furutani-Seiki, M., and Matsuura, S. (2011). Insufficiency of BUBR1, a mitotic spindle checkpoint regulator, causes impaired ciliogenesis in vertebrates. Hum. Mol. Genet. *20*, 2058–2070.

Moen, R.J., Johnsrud, D.O., Thomas, D.D., and Titus, M.A. (2011). Characterization of a myosin VII MyTH/FERM domain. J. Mol. Biol. *413*, 17–23.

Molla-Herman, A., Ghossoub, R., Blisnick, T., Meunier, A., Serres, C., Silbermann, F., Emmerson, C., Romeo, K., Bourdoncle, P., Schmitt, A., et al. (2010). The ciliary pocket: an endocytic membrane domain at the base of primary and motile cilia. J. Cell Sci. *123*, 1785–1795.

Moradi, P., Davies, W.L., Mackay, D.S., Cheetham, M.E., and Moore, A.T. (2011). Focus on molecules: centrosomal protein 290 (CEP290). Exp. Eye Res. *92*, 316–317.

Mougou-Zerelli, S., Thomas, S., Szenker, E., Audollent, S., Elkhartoufi, N., Babarit, C., Romano, S., Salomon, R., Amiel, J., Esculpavit, C., et al. (2009). CC2D2A mutations in Meckel and Joubert syndromes indicate a genotype-phenotype correlation. Hum. Mutat. *30*, 1574–1582.

Mu, F.T., Callaghan, J.M., Steele-Mortimer, O., Stenmark, H., Parton, R.G., Campbell, P.L., McCluskey, J., Yeo, J.P., Tock, E.P., and Toh, B.H. (1995). EEA1, an early endosome-associated protein. EEA1 is a conserved alpha-helical peripheral membrane protein flanked by cysteine "fingers" and contains a calmodulin-binding IQ motif. J. Biol. Chem. *270*, 13503–13511.

Murga-Zamalloa, C.A., Atkins, S.J., Peranen, J., Swaroop, A., and Khanna, H. (2010). Interaction of retinitis pigmentosa GTPase regulator (RPGR) with RAB8A GTPase: implications for cilia dysfunction and photoreceptor degeneration. Hum. Mol. Genet. *19*, 3591–3598.

Murga-Zamalloa, C.A., Ghosh, A.K., Patil, S.B., Reed, N.A., Chan, L.S., Davuluri, S., Peränen, J., Hurd, T.W., Rachel, R.A., and Khanna, H. (2011). Accumulation of the Raf-1 kinase inhibitory protein (Rkip) is associated with Cep290-mediated photoreceptor degeneration in ciliopathies. J. Biol. Chem. *286*, 28276–28286.

Mustafi, D., Engel, A.H., and Palczewski, K. (2009). Structure of cone photoreceptors. Prog. Retin. Eye Res. *28*, 289–302.

Nagase, T., Ishikawa, K., Nakajima, D., Ohira, M., Seki, N., Miyajima, N., Tanaka, A., Kotani, H., Nomura, N., and Ohara, O. (1997). Prediction of the coding sequences of unidentified human genes. VII. The complete sequences of 100 new cDNA clones from brain which can code for large proteins in vitro. DNA Res. Int. J. Rapid Publ. Reports Genes Genomes *4*, 141–150.

Najafi, M., Maza, N.A., and Calvert, P.D. (2012). Steric volume exclusion sets soluble protein concentrations in photoreceptor sensory cilia. Proc. Natl. Acad. Sci. *109*, 203–208.

Nauli, S.M., Alenghat, F.J., Luo, Y., Williams, E., Vassilev, P., Li, X., Elia, A.E.H., Lu, W., Brown, E.M., Quinn, S.J., et al. (2003). Polycystins 1 and 2 mediate mechanosensation in the primary cilium of kidney cells. Nat. Genet. *33*, 129–137.

Nishio, S., Tian, X., Gallagher, A.R., Yu, Z., Patel, V., Igarashi, P., and Somlo, S. (2010). Loss of Oriented Cell Division Does not Initiate Cyst Formation. J. Am. Soc. Nephrol. *21*, 295–302.

Noor, A., Windpassinger, C., Patel, M., Stachowiak, B., Mikhailov, A., Azam, M., Irfan, M., Siddiqui, Z.K., Naeem, F., Paterson, A.D., et al. (2008). CC2D2A, encoding a coiled-coil and C2 domain protein, causes autosomal-recessive mental retardation with retinitis pigmentosa. Am. J. Hum. Genet. *82*, 1011–1018.

Oh, E.C., and Katsanis, N. (2012). Cilia in vertebrate development and disease. Dev. Camb. Engl. *139*, 443–448.

Olbrich, H., Häffner, K., Kispert, A., Völkel, A., Volz, A., Sasmaz, G., Reinhardt, R., Hennig, S., Lehrach, H., Konietzko, N., et al. (2002). Mutations in DNAH5 cause primary ciliary dyskinesia and randomization of left-right asymmetry. Nat. Genet. *30*, 143–144.

Otto, E.A., Loeys, B., Khanna, H., Hellemans, J., Sudbrak, R., Fan, S., Muerb, U., O'Toole, J.F., Helou, J., Attanasio, M., et al. (2005). Nephrocystin-5, a ciliary IQ domain protein, is mutated in Senior-Loken syndrome and interacts with RPGR and calmodulin. Nat. Genet. *37*, 282–288.

Otto, E.A., Ramaswami, G., Janssen, S., Chaki, M., Allen, S.J., Zhou, W., Airik, R., Hurd, T.W., Ghosh, A.K., Wolf, M.T., et al. (2011). Mutation analysis of 18 nephronophthisis associated ciliopathy disease genes using a DNA pooling and next generation sequencing strategy. J. Med. Genet. *48*, 105–116.

Ou, G., Koga, M., Blacque, O.E., Murayama, T., Ohshima, Y., Schafer, J.C., Li, C., Yoder, B.K., Leroux, M.R., and Scholey, J.M. (2007). Sensory Ciliogenesis in Caenorhabditis elegans: Assignment of IFT Components into Distinct Modules Based on Transport and Phenotypic Profiles. Mol. Biol. Cell *18*, 1554–1569.

Ounjai, P., Kim, K.D., Liu, H., Dong, M., Tauscher, A.N., Witkowska, H.E., and Downing, K.H. (2013). Architectural Insights into a Ciliary Partition. Curr. Biol. *23*, 339–344.

Paintrand, M., Moudjou, M., Delacroix, H., and Bornens, M. (1992). Centrosome organization and centriole architecture: their sensitivity to divalent cations. J. Struct. Biol. *108*, 107–128.

Papon, J.F., Perrault, I., Coste, A., Louis, B., Gérard, X., Hanein, S., Fares-Taie, L., Gerber, S., Defoort-Dhellemmes, S., Vojtek, A.M., et al. (2010). Abnormal respiratory cilia in non-syndromic Leber congenital amaurosis with CEP290 mutations. J. Med. Genet. *47*, 829–834.

Pazour, G.J., Wilkerson, C.G., and Witman, G.B. (1998). A dynein light chain is essential for the retrograde particle movement of intraflagellar transport (IFT). J. Cell Biol. *141*, 979–992.

Pazour, G.J., Dickert, B.L., and Witman, G.B. (1999). The DHC1b (DHC2) isoform of cytoplasmic dynein is required for flagellar assembly. J. Cell Biol. *144*, 473–481.

Pazour, G.J., Dickert, B.L., Vucica, Y., Seeley, E.S., Rosenbaum, J.L., Witman, G.B., and Cole, D.G. (2000). Chlamydomonas IFT88 and its mouse homologue, polycystic kidney disease gene tg737, are required for assembly of cilia and flagella. J. Cell Biol. *151*, 709–718.

Pazour, G.J., San Agustin, J.T., Follit, J.A., Rosenbaum, J.L., and Witman, G.B. (2002). Polycystin-2 localizes to kidney cilia and the ciliary level is elevated in orpk mice with polycystic kidney disease. Curr. Biol. CB *12*, R378–380.

Pedersen, L.B., and Rosenbaum, J.L. (2008). Intraflagellar transport (IFT) role in ciliary assembly, resorption and signalling. Curr. Top. Dev. Biol. *85*, 23–61.

Pennarun, G., Escudier, E., Chapelin, C., Bridoux, A.M., Cacheux, V., Roger, G., Clément, A., Goossens, M., Amselem, S., and Duriez, B. (1999). Loss-of-function mutations in a human gene related to Chlamydomonas reinhardtii dynein IC78 result in primary ciliary dyskinesia. Am. J. Hum. Genet. *65*, 1508–1519.

Perrault, I., Delphin, N., Hanein, S., Gerber, S., Dufier, J.-L., Roche, O., Defoort-Dhellemmes, S., Dollfus, H., Fazzi, E., Munnich, A., et al. (2007). Spectrum of NPHP6/CEP290 mutations in Leber congenital amaurosis and delineation of the associated phenotype. Hum. Mutat. *28*, 416.

Piperno, G., Mead, K., and Henderson, S. (1996). Inner dynein arms but not outer dynein arms require the activity of kinesin homologue protein KHP1(FLA10) to reach the distal part of flagella in Chlamydomonas. J. Cell Biol. *133*, 371–379.

Poole, C.A., Flint, M.H., and Beaumont, B.W. (1985). Analysis of the morphology and function of primary cilia in connective tissues: a cellular cybernetic probe? Cell Motil. *5*, 175–193.

Praetorius, H.A., and Spring, K.R. (2001). Bending the MDCK cell primary cilium increases intracellular calcium. J. Membr. Biol. *184*, 71–79.

Puisac, B., Teresa-Rodrigo, M.E., Arnedo, M., Gil-Rodríguez, M.C., Pérez-Cerdá, C., Ribes, A., Pié, A., Bueno, G., Gómez-Puertas, P., and Pié, J. (2013). Analysis of aberrant splicing and nonsense-mediated decay of the stop codon mutations c.109G>T and c.504_505delCT in 7 patients with HMG-CoA lyase deficiency. Mol. Genet. Metab. *108*, 232–240.

Quintyne, N.J., and Schroer, T.A. (2002). Distinct cell cycle–dependent roles for dynactin and dynein at centrosomes. J. Cell Biol. *159*, 245–254.

Rao, T.P., and Kühl, M. (2010). An Updated Overview on Wnt Signaling Pathways A Prelude for More. Circ. Res. *106*, 1798–1806.

Van Reeuwijk, J., Arts, H.H., and Roepman, R. (2011). Scrutinizing ciliopathies by unraveling ciliary interaction networks. Hum. Mol. Genet. *20*, R149–157.

Reiter, J.F., Blacque, O.E., and Leroux, M.R. (2012). The base of the cilium: roles for transition fibres and the transition zone in ciliary formation, maintenance and compartmentalization. EMBO Rep. *13*, 608–618.

Ringo, D.L. (1967). FLAGELLAR MOTION AND FINE STRUCTURE OF THE FLAGELLAR APPARATUS IN CHLAMYDOMONAS. J. Cell Biol. *33*, 543–571.

De Robertis, E. (1956). MORPHOGENESIS OF THE RETINAL RODS. J. Biophys. Biochem. Cytol. *2*, 209–218.

Rohatgi, R., Milenkovic, L., and Scott, M.P. (2007). Patched1 Regulates Hedgehog Signaling at the Primary Cilium. Science *317*, 372–376.

Röhlich, P. (1975). The sensory cilium of retinal rods is analogous to the transitional zone of motile cilia. Cell Tissue Res. *161*, 421–430.

Romano, S., Milan, G., Veronese, C., Collin, G.B., Marshall, J.D., Centobene, C., Favaretto, F., Dal Pra, C., Scarda, A., Leandri, S., et al. (2008). Regulation of Alström syndrome gene expression during adipogenesis and its relationship with fat cell insulin sensitivity. Int. J. Mol. Med. *21*, 731–736.

Ronquillo, C.C., Bernstein, P.S., and Baehr, W. (2012). Senior-Løken syndrome: a syndromic form of retinal dystrophy associated with nephronophthisis. Vision Res. *75*, 88–97.

Rosenbaum, J.L., and Child, F.M. (1967). Flagellar regeneration in protozoan flagellates. J. Cell Biol. *34*, 345–364.

Ross, A.J., May-Simera, H., Eichers, E.R., Kai, M., Hill, J., Jagger, D.J., Leitch, C.C., Chapple, J.P., Munro, P.M., Fisher, S., et al. (2005). Disruption of Bardet-Biedl syndrome ciliary proteins perturbs planar cell polarity in vertebrates. Nat. Genet. *37*, 1135–1140.

Ruiz i Altaba, A., Palma, V., and Dahmane, N. (2002). Hedgehog–GLI signaling and the growth of the brain. Nat. Rev. Neurosci. *3*, 24–33.

Satir, P., Mitchell, D.R., and Jékely, G. (2008). How did the cilium evolve? Curr. Top. Dev. Biol. *85*, 63–82.

Sato, T., Mushiake, S., Kato, Y., Sato, K., Sato, M., Takeda, N., Ozono, K., Miki, K., Kubo, Y., Tsuji, A., et al. (2007). The Rab8 GTPase regulates apical protein localization in intestinal cells. Nature *448*, 366–369.

Sayer, J.A., Otto, E.A., O'Toole, J.F., Nurnberg, G., Kennedy, M.A., Becker, C., Hennies, H.C., Helou, J., Attanasio, M., Fausett, B.V., et al. (2006). The centrosomal protein nephrocystin-6 is mutated in Joubert syndrome and activates transcription factor ATF4. Nat. Genet. *38*, 674–681.

Schäfer, T., Pütz, M., Lienkamp, S., Ganner, A., Bergbreiter, A., Ramachandran, H., Gieloff, V., Gerner, M., Mattonet, C., Czarnecki, P.G., et al. (2008). Genetic and physical interaction between the NPHP5 and NPHP6 gene products. Hum. Mol. Genet. *17*, 3655–3662.

Schwaiger, I., Sattler, C., Hostetter, D.R., and Rief, M. (2002). The myosin coiled-coil is a truly elastic protein structure. Nat. Mater. *1*, 232–235.

Seaman, M.N., Sowerby, P.J., and Robinson, M.S. (1996). Cytosolic and membrane-associated proteins involved in the recruitment of AP-1 adaptors onto the trans-Golgi network. J. Biol. Chem. *271*, 25446–25451.

Shou, C., Li, C., and Meng, L. (1997). [Construction, expression and activity of a single chain antibody to gastric cancer cells]. Zhonghua Yi Xue Za Zhi *77*, 434–438.

Signor, D., Wedaman, K.P., Orozco, J.T., Dwyer, N.D., Bargmann, C.I., Rose, L.S., and Scholey, J.M. (1999). Role of a class DHC1b dynein in retrograde transport of IFT motors and IFT raft particles along cilia, but not dendrites, in chemosensory neurons of living Caenorhabditis elegans. J. Cell Biol. *147*, 519–530.

Sillibourne, J.E., Hurbain, I., Grand-Perret, T., Goud, B., Tran, P., and Bornens, M. (2013). Primary ciliogenesis requires the distal appendage component Cep123. Biol. Open *2*, 535–545.

Simons, M., Gloy, J., Ganner, A., Bullerkotte, A., Bashkurov, M., Krönig, C., Schermer, B., Benzing, T., Cabello, O.A., Jenny, A., et al. (2005). Inversin, the gene product mutated in nephronophthisis type II, functions as a molecular switch between Wnt signaling pathways. Nat. Genet. *37*, 537–543.

Smith, W.J., Nassar, N., Bretscher, A., Cerione, R.A., and Karplus, P.A. (2003). Structure of the active N-terminal domain of Ezrin. Conformational and mobility changes identify keystone interactions. J. Biol. Chem. *278*, 4949–4956.

Song, X., Yang, J., Hirbawi, J., Ye, S., Perera, H.D., Goksoy, E., Dwivedi, P., Plow, E.F., Zhang, R., and Qin, J. (2012). A novel membrane-dependent on/off switch mechanism of talin FERM domain at sites of cell adhesion. Cell Res. *22*, 1533–1545.

Sorokin, S. (1962). Centrioles and the Formation of Rudimentary Cilia by Fibroblasts and Smooth Muscle Cells. J. Cell Biol. *15*, 363–377.

Sorokin, S.P. (1968). Reconstructions of Centriole Formation and Ciliogenesis in Mammalian Lungs. J. Cell Sci. *3*, 207–230.

Spektor, A., Tsang, W.Y., Khoo, D., and Dynlacht, B.D. (2007). Cep97 and CP110 suppress a cilia assembly program. Cell *130*, 678–690.

Stephan, A., Vaughan, S., Shaw, M.K., Gull, K., and McKean, P.G. (2007). An essential quality control mechanism at the eukaryotic basal body prior to intraflagellar transport. Traffic Cph. Den. *8*, 1323–1330.

Stone, E.M., Cideciyan, A.V., Aleman, T.S., Scheetz, T.E., Sumaroka, A., Ehlinger, M.A., Schwartz, S.B., Fishman, G.A., Traboulsi, E.I., Lam, B.L., et al. (2011). Variations in NPHP5 in patients with nonsyndromic leber congenital amaurosis and Senior-Loken syndrome. Arch. Ophthalmol. *129*, 81–87.

Stowe, T.R., Wilkinson, C.J., Iqbal, A., and Stearns, T. (2012). The centriolar satellite proteins Cep72 and Cep290 interact and are required for recruitment of BBS proteins to the cilium. Mol. Biol. Cell *23*, 3322–3335.

Sturgess, J.M., Chao, J., Wong, J., Aspin, N., and Turner, J.A. (1979). Cilia with defective radial spokes: a cause of human respiratory disease. N. Engl. J. Med. *300*, 53–56.

Szymanska, K., and Johnson, C.A. (2012). The transition zone: an essential functional compartment of cilia. Cilia *1*, 10.

Tal, J. (2000). Adeno-associated virus-based vectors in gene therapy. J. Biomed. Sci. *7*, 279–291.

Tallila, J., Jakkula, E., Peltonen, L., Salonen, R., and Kestilä, M. (2008). Identification of CC2D2A as a Meckel syndrome gene adds an important piece to the ciliopathy puzzle. Am. J. Hum. Genet. *82*, 1361–1367.

Tobin, J.L., and Beales, P.L. (2007). Bardet-Biedl syndrome: beyond the cilium. Pediatr. Nephrol. Berl. Ger. *22*, 926–936.

Torikata, C. (1988). The ciliary necklace--a transmission electron microscopic study using tannic acid-containing fixation. J. Ultrastruct. Mol. Struct. Res. *101*, 210–214.

Torres, V.E., and Harris, P.C. (2006). Mechanisms of Disease: autosomal dominant and recessive polycystic kidney diseases. Nat. Clin. Pract. Nephrol. *2*, 40–55; quiz 55.

Tsang, W.Y., Bossard, C., Khanna, H., Peränen, J., Swaroop, A., Malhotra, V., and Dynlacht, B.D. (2008). CP110 suppresses primary cilia formation through its interaction with CEP290, a protein deficient in human ciliary disease. Dev. Cell *15*, 187–197.

Valente, E.M., Silhavy, J.L., Brancati, F., Barrano, G., Krishnaswami, S.R., Castori, M., Lancaster, M.A., Boltshauser, E., Boccone, L., Al-Gazali, L., et al. (2006). Mutations in CEP290, which encodes a centrosomal protein, cause pleiotropic forms of Joubert syndrome. Nat. Genet. *38*, 623–625.

Vermeulen, K., Van Bockstaele, D.R., and Berneman, Z.N. (2003). The cell cycle: a review of regulation, deregulation and therapeutic targets in cancer. Cell Prolif. *36*, 131–149.

Vuoristo, M.M., Pappas, J.G., Jansen, V., and Ala-Kokko, L. (2004). A stop codon mutation in COL11A2 induces exon skipping and leads to non-ocular Stickler syndrome. Am. J. Med. Genet. A. *130A*, 160–164.

Wang, J., Chang, Y.F., Hamilton, J.I., and Wilkinson, M.F. (2002). Nonsense-associated altered splicing: a frame-dependent response distinct from nonsense-mediated decay. Mol. Cell *10*, 951–957.

Wang, W.-J., Tay, H.G., Soni, R., Perumal, G.S., Goll, M.G., Macaluso, F.P., Asara, J.M., Amack, J.D., and Tsou, M.-F.B. (2013). CEP162 is an axoneme-recognition protein promoting ciliary transition zone assembly at the cilia base. Nat. Cell Biol. *15*, 591–601.

Wang, Y., McMahon, A.P., and Allen, B.L. (2007). Shifting paradigms in Hedgehog signaling. Curr. Opin. Cell Biol. *19*, 159–165.

Ward, H.H., Brown-Glaberman, U., Wang, J., Morita, Y., Alper, S.L., Bedrick, E.J., Gattone, V.H., Deretic, D., and Wandinger-Ness, A. (2011). A conserved signal and GTPase complex are required for the ciliary transport of polycystin-1. Mol. Biol. Cell *22*, 3289–3305.

Waters, A.M., and Beales, P.L. (2011). Ciliopathies: an expanding disease spectrum. Pediatr. Nephrol. Berl. Ger. *26*, 1039–1056.

Weber, K.L., Sokac, A.M., Berg, J.S., Cheney, R.E., and Bement, W.M. (2004). A microtubule-binding myosin required for nuclear anchoring and spindle assembly. Nature *431*, 325–329.

Wei, Q., Zhang, Y., Li, Y., Zhang, Q., Ling, K., and Hu, J. (2012). The BBSome controls IFT assembly and turnaround in cilia. Nat. Cell Biol. *14*, 950–957.

Westlake, C.J., Baye, L.M., Nachury, M.V., Wright, K.J., Ervin, K.E., Phu, L., Chalouni, C., Beck, J.S., Kirkpatrick, D.S., Slusarski, D.C., et al. (2011). Primary cilia membrane assembly is initiated by Rab11 and transport protein particle II (TRAPPII) complex-dependent trafficking of Rabin8 to the centrosome. Proc. Natl. Acad. Sci. *108*, 2759–2764.

Williams, C.L., Li, C., Kida, K., Inglis, P.N., Mohan, S., Semenec, L., Bialas, N.J., Stupay, R.M., Chen, N., Blacque, O.E., et al. (2011). MKS and NPHP modules cooperate to establish basal

body/transition zone membrane associations and ciliary gate function during ciliogenesis. J. Cell Biol. *192*, 1023–1041.

Wiszniewski, W., Lewis, R.A., Stockton, D.W., Peng, J., Mardon, G., Chen, R., and Lupski, J.R. (2011). Potential involvement of more than one locus in trait manifestation for individuals with Leber congenital amaurosis. Hum. Genet. *129*, 319–327.

Wong, S.Y., Seol, A.D., So, P.-L., Ermilov, A.N., Bichakjian, C.K., Epstein, E.H., Jr, Dlugosz, A.A., and Reiter, J.F. (2009). Primary cilia can both mediate and suppress Hedgehog pathway-dependent tumorigenesis. Nat. Med. *15*, 1055–1061.

Wright, K.J., Baye, L.M., Olivier-Mason, A., Mukhopadhyay, S., Sang, L., Kwong, M., Wang, W., Pretorius, P.R., Sheffield, V.C., Sengupta, P., et al. (2011). An ARL3–UNC119–RP2 GTPase cycle targets myristoylated NPHP3 to the primary cilium. Genes Dev. *25*, 2347–2360.

Wu, Z., Yang, H., and Colosi, P. (2010). Effect of Genome Size on AAV Vector Packaging. Mol. Ther. *18*, 80–86.

Ye, J., and Koumenis, C. (2009). ATF4, an ER stress and hypoxia-inducible transcription factor and its potential role in hypoxia tolerance and tumorigenesis. Curr. Mol. Med. *9*, 411–416.

Yzer, S., Hollander, A.I. den, Lopez, I., Pott, J.-W.R., de Faber, J.T.H.N., Cremers, F.P.M., Koenekoop, R.K., and van den Born, L.I. (2012). Ocular and extra-ocular features of patients with Leber congenital amaurosis and mutations in CEP290. Mol. Vis. *18*, 412–425.

Zach, F., Grassmann, F., Langmann, T., Sorusch, N., Wolfrum, U., and Stöhr, H. (2012). The retinitis pigmentosa 28 protein FAM161A is a novel ciliary protein involved in intermolecular protein interaction and microtubule association. Hum. Mol. Genet. *21*, 4573–4586.

Zhang, Q., Seo, S., Bugge, K., Stone, E.M., and Sheffield, V.C. (2012). BBS proteins interact genetically with the IFT pathway to influence SHH-related phenotypes. Hum. Mol. Genet. *21*, 1945–1953.

Zhang, Q., Nishimura, D., Vogel, T., Shao, J., Swiderski, R., Yin, T., Searby, C., Carter, C.S., Kim, G., Bugge, K., et al. (2013). BBS7 is required for BBSome formation and its absence in mice results in Bardet-Biedl syndrome phenotypes and selective abnormalities in membrane protein trafficking. J. Cell Sci. *126*, 2372–2380.

Zhang, T., Kee, W.H., Seow, K.T., Fung, W., and Cao, X. (2000). The coiled-coil domain of Stat3 is essential for its SH2 domain-mediated receptor binding and subsequent activation induced by epidermal growth factor and interleukin-6. Mol. Cell. Biol. *20*, 7132–7139.

Zhao, C., and Malicki, J. (2011). Nephrocystins and MKS proteins interact with IFT particle and facilitate transport of selected ciliary cargos. EMBO J. *30*, 2532–2544.

Zhao, Y., Hong, D.-H., Pawlyk, B., Yue, G., Adamian, M., Grynberg, M., Godzik, A., and Li, T. (2003). The retinitis pigmentosa GTPase regulator (RPGR)- interacting protein: subserving RPGR function and participating in disk morphogenesis. Proc. Natl. Acad. Sci. U. S. A. *100*, 3965–3970.

Zhu, D., Shi, S., Wang, H., and Liao, K. (2009). Growth arrest induces primary-cilium formation and sensitizes IGF-1-receptor signaling during differentiation induction of 3T3-L1 preadipocytes. J. Cell Sci. *122*, 2760–2768.

Zimmermann, K.W. (1898). Beiträge zur Kenntniss einiger Drüsen und Epithelien. Arch. Für Mikrosk. Anat. *52*, 552–706.